# RADIOISOTOPE FUELED PULSED POWER GENERATION SYSTEM FOR PROPULSION AND ELECTRICAL POWER FOR DEEP SPACE MISSIONS

A Dissertation

Presented in Partial Fulfillment of the Requirements for the

Degree of Doctor of Philosophy

with a

Major in Mechanical Engineering

in the

College of Graduate Studies

University of Idaho

by

Troy Howe

Major Professor: John Crepeau, Ph.D.

Committee Members: Ralph Budwig, Ph.D.; Ragunath Kanakala, Ph.D;
Mary Lou Dunzik-Gougar, Ph.D.

Department Administrator: Steve Beyerlein, Ph.D.

August, 2015

**Authorization to Submit Dissertation**

This dissertation of Troy Howe, submitted for the degree of Doctor of Philosophy with a major in Mechanical Engineering and titled "Radioisotope Fueled Pulsed Power Generation System for Propulsion and Electrical Power For Deep Space Missions," has been reviewed in final form. Permission, as indicated by the signatures and dates given below, is now granted to submit final copies to the College of Graduate Studies for approval.

| | | |
|---|---|---|
| Major Professor | _____Date_____ | |
| | Dr. John Crepeau | |
| Committee Members | _____Date_____ | |
| | Dr. Ralph Budwig | |
| | _____Date_____ | |
| | Dr. Ragunath Kanakala | |
| | _____Date_____ | |
| | Dr. Mary Lou Dunzik-Gougar | |
| Department Administrator | _____Date_____ | |
| | Dr. Steve Beyerlein | |

**Abstract**

Space exploration missions to the moon, Mars, and other celestial bodies have allowed for great scientific leaps to enhance our knowledge of the universe; yet the astronomical cost of these missions limits their utility to only a few select agencies. Reducing the cost of exploratory space travel will give rise to a new era of exploration, where private investors, universities, and world governments can send satellites to far off planets and gather important data. By using radioisotope power sources and thermal storage devices a duty cycle can be introduced to extract large amounts of energy in short amounts of time, allowing for efficient space travel. This duty cycle would be comprised of a period of power generation and a period of recharging. The same device can also provide electrical power for subsystems such as communications, drills, lasers, or other components that can provide valuable scientific information.

This project examines the use of multiple radioisotope sources combined with a thermal capacitor using Phase Change Materials (PCMs), which can collect energy over a period of time. The radioisotope fuel provides heat that is stored in the PCM core, and that stored heat serves as the heat source for a Brayton power cycle when operating. The result of this design culminates in a variety of possible spacecraft with their own varying costs, transit times, and objectives. Among the most promising are missions to Mars, which cost less than $18M, missions that can provide power to satellite constellations for decades, or missions that can deliver large, sized payloads similar to the "Opportunity" rover (185kg) to Mars for less than $55M. All of these options can be made available to a much wider range of customer with commercially available satellite launches from earth. The true cost of such progress lies in the sometimes substantial increase in transit times for these missions.

The results of this project showed that pulsed power systems enable a more customizable spacecraft that can effectively exchange cost for time, and make space exploration missions available to those who before could not afford to send equipment beyond the confines of Earth.

**Acknowledgements**

I would like to thank Dr. John Crepeau for all his help with this project. His guidance and advice has always been a great source of value for my work.

I would also like to thank the Center for Space Nuclear Research for their interest in this project. Without their support this project would not have had the resources necessary to investigate this concept.

A portion of this work was funded by a NASA Innovative and Advanced Concepts (NIAC) grant to explore the possibility of exploring the solar system with pulsed power radioisotope systems. Without their contribution this work would not have been possible.

## Dedication

Dedicated to Mom and Dad, who always provided a constant source of wisdom and encouragement, and are my greatest role models.

## Table of Contents

**List of Figures**

# CHAPTER 1: Introduction

## 1.1 Space Exploration Overview

Space exploration is a necessary step in the evolution of humanity in the sense that it pushes scientific and technological boundaries beyond what is normally achieved by man and towards ideas previously thought impossible. A method of making space exploration more readily available to mankind by reducing the exorbitant cost will allow for more scientists, engineers, entrepreneurs, and universities to learn from the nearby astral bodies and accelerate this advancement.

Small, unmanned satellites have the capability to gather scientific data from all manner of celestial bodies in the solar system, thanks to the advancements made to electronics and computer technology in recent years. All that is required to allow for a vast exodus into the solar system is a compact, inexpensive source of power and propulsion. With the use of high energy radioisotope fuel and an innovative use of thermal storage, a small device can provide very high power levels for short amounts of time, increase system efficiency, provide power, and allow for highly efficient propulsion to a craft.

The major issue to overcome with space travel is the high cost associated with each mission. Radioisotope power sources are incredibly expensive due to the fuel costs. A recent estimate on the cost of plutonium rated it at $4-8 million per kilogram [1][2]. While in its oxide form, PuO2 produces slightly over 400 watts of thermal power per kg of mass [3], which makes the dollar per watt cost of current radioisotope systems very high.

Launch costs are the other major factor in cost calculations, the current cost to launch a payload in to low earth orbit varies from $4,500-29,000 per kilogram [4][5]. Because of this, it is very desirable to have a low mass system in space exploration. Additionally, for systems that propel themselves out of earth's orbit, a lower mass equates to less propellant taken to space. Even though it is easier to move in space where the earth's gravity is not a factor, often times ship propellant can compose 70-80% of a ship's mass. This can be seen clearly later in the mission trajectory chapter.

Because of the concerns to increase power output and decrease system mass, the terms "specific power" and "specific mass" are often used. Specific power refers to how much electrical

power (in watts) a device can generate per kilogram of mass it has. For example, a Sunpower 327 solar panel on earth can generate 327 watts of electrical power, and has a mass of 18.6 kg [6]. This equates to a specific power of 17.58 W/kg. The inverse of specific power is specific mass, which describes how much mass is required to provide a kilowatt of electrical power. Specific mass is often denoted with the character alpha ($\alpha$). For the same terrestrial solar panel, the specific mass is equal to the mass of 18.6 kg divided by the power output (in kilowatts) of 0.327 kW. This results in a specific mass, or $\alpha$ value, of 56.88 kg/kW. Having a low specific mass (or high specific power) generally results in better propulsion and less expensive systems.

Both metrics are valid methods of rating space power systems, but it is important to differentiate between them to avoid confusion. This paper will use specific mass whenever possible, and a goal of the project will be to minimize the specific mass of the system.

The last major issue to be addressed is the communications systems of deep space systems. Currently, the Voyager 1 spacecraft is greater than 19.5 billion km away from earth, and the Voyager 2 greater than 16.1 billion [7]. Although these crafts are significantly farther away than any other man-made object, it can be seen that the huge distances involved with space travel can introduce difficulties with sending or receiving communications. Due to this, a system of satellite dishes called the Deep Space Network (DSN) has been constructed on earth for the purpose of receiving signals from missions in space. Often times, a deep space probe must schedule time with the DSN to transmit its signals back to earth. Thus, having a high powered communication system that can transmit data quickly will ensure that there is enough time on the DSN to gather all the necessary data the probe has acquired.

The space travel issues that this project will address will be the large costs involved with current missions that arise from launching large payloads that are necessary for large scale missions. By reducing the mass of the subsystems, such as communications and power, smaller missions can be performed and the overall cost reduced. This allows for many missions to be performed for the same price as one current mission, and other entities with limited budgets to participate in space exploration. For comparison, examples of other space exploration missions are shown below.

### 1.1.1 Philae Lander

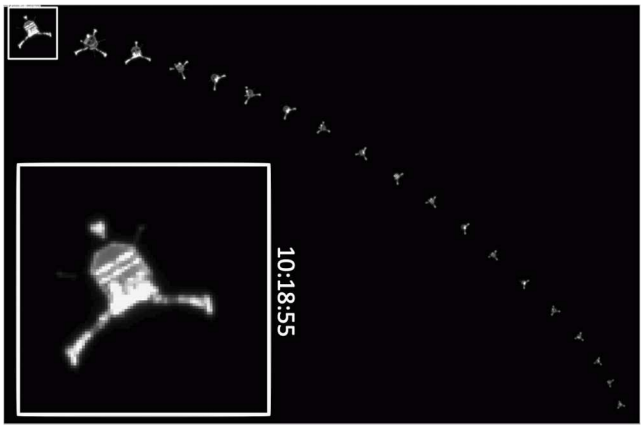


Figure 1: Rosetta spacecraft time lapse travel path [8]

Recently, the European Space Agency sent a mission to a comet that was passing close to earth in an attempt to land a small lander on the surface of the comet [8]. The Rosetta craft took a ten year journey to intercept the comet by using multiple earth flybys. When it arrived at its destination, it dropped a small lander, named Philae, which attempted to attach to the surface of the comet through the use of harpoon like hooks. Unfortunately, one of the hooks did not attach properly and the lander ended up stuck in a shadow. Because it was entirely dependent on solar power, the batteries soon drained and the mission essentially ended.

Lessons such as the Rosetta mission are valuable in space exploration because it shows that care must be taken to prepare for unexpected circumstances. The dependence on solar power for this mission inevitably caused the lander to run out of power. The inclusion of a radioisotope power source could have provided enough power for the craft, not only for the term of the intended mission but during times when the comet had traveled too far from the sun to use solar power at all. Sadly, current radioisotope power sources are much too heavy and expensive for use in small probes such as Philae.

### 1.1.2 Juno

Another relatively recent mission is the Juno mission to Jupiter. This craft also utilizes solar photovoltaic power systems for use in powering instruments. Jupiter's orbit is so far away from the sun though, that it sees roughly 1/25$^{th}$ the sunlight intensity than that of earth [9].

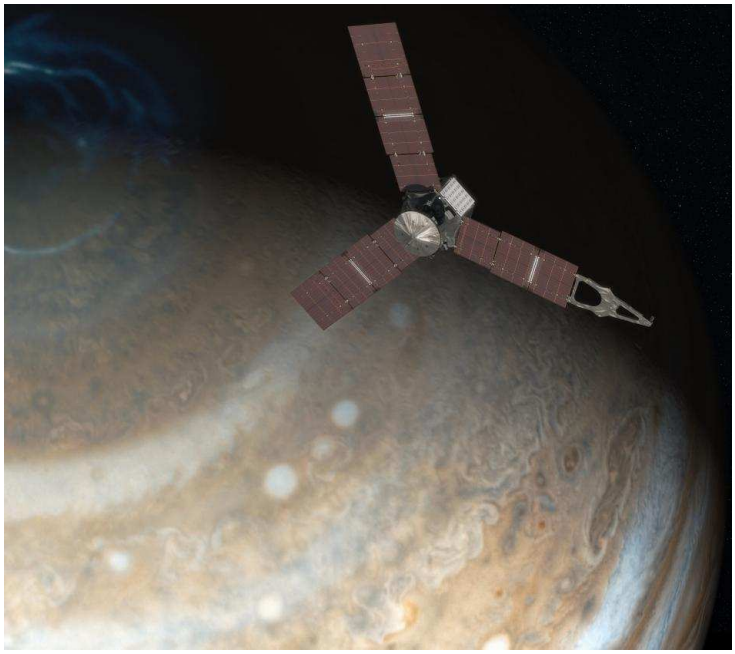

Figure 2: Juno concept illustration [9]

This makes the necessary photovoltaic arrays extremely large and massive. Current commercially available photovoltaics have a specific mass of ~56.9 kg/kW, and existing radioisotope power systems have a specific mass of ~350kg/kW [4][5]. However, with 1/25$^{th}$ of the power input to the photovoltaic array, their specific mass increases to over 1400 kg/kW. This makes the power system aboard the Juno incredibly heavy and inefficient. Even existing RPS systems would improve upon the current design, but the cost for current radioisotope systems makes the mission more expensive.

As stated above, the estimated cost for 1 kg of pure plutonium-238 can be up to $8 million. The Multi-Mission Radioisotope Power Generator (MMRTG) system currently used for radioisotope power uses 4.8 kg of PuO2, or 4.23 kg of pure Pu 238 [5]. At $8 million/kg this equates to a cost of $33.84 million for the fuel alone. On a per-kilowatt of electricity basis, the MMRTG produces .125 kW of electrical power, resulting in a cost per kW of $270 million/kWe.

Launch costs are often the next highest source of expense, with the cost to launch per kg being up to $29,000/kg [10]. For the solar power system described above, the specific mass is roughly 1,400 kg/kWe. At $29,000/kg, this equates to $40.6 million/kWe to launch the power system. When comparing costs to the radioisotope system, it is not surprising that current missions prefer to use solar power when available.

Although plutonium is the most common radioisotope heat source used, there are alternatives, which can be used to decrease the cost. Many of these alternatives have their own strengths and weaknesses that are discussed in more detail in later chapters. With the use of some of these less expensive materials, radioisotope power can decrease the cost for spacecraft that are even within the range of solar power. Another method to reduce the cost is the introduction of a duty cycle, which can also greatly reduce the cost/kWe.

### 1.1.3 New Horizons

The New Horizons mission was launched in 2006 in an attempt to deliver a satellite to Pluto for scientific data acquisition; it used a Star48 solid rocket motor for the 3$^{rd}$ stage of its launch, which propelled it at incredible speeds away from earth [11]. The latest version, Star48BV, has an ISP of 292.1 seconds, a mass of 2164.5 kg, and a propellant mass of 2010.0 kg [12]. With the mass of the New Horizons satellite being 478 kg, that makes the total wet mass of the 3$^{rd}$ stage 2642.5 kg

with a propellant mass fraction of 0.761. In other words, the entire craft used to escape from earth's orbit was ~76% propellant.

The mission itself takes the craft close to Jupiter and on to Pluto, where it will gather data with its many scientific instruments. However, there is no breaking system on the craft and so it will eventually fly past Pluto and out of the solar system. This is an impressive technological feat, but severely limits the amount of time available to gather data. Designing a mission that includes orbiting a distant planet is difficult because it requires the craft to bring propellant with it to enter the planet's orbit. High propellant mass fractions contribute to high costs that are associated with transporting large amounts of breaking propellant, and so often a flyby is the preferred method for deep space exploration.

### 1.1.4 Europa/Ceres Missions

Missions to Europe and Ceres are also missions that are gaining interest in the space exploration community; NASA Ames research center has been in contact with researchers at Idaho National Labs to contribute information on radioisotope power sources for proposals for missions to both destinations. In February of 2015 there was also a workshop hosted by NASA Ames specifically dedicated to ideas regarding finding life in a Europa plume [13].

The plume to which the mission refers is an event on frozen celestial bodies with a thick icy shell and a section of liquid water underneath. Europa, one of Jupiter's moons, is a good example of this type of body. As the moon is subject to stresses caused by the moon's rotation and local gravitational pulls, the icy crust tends to crack and eject a plume of liquid water high above the surface. A properly timed probe may be able to explore this plume of ejected water and look for life in the liquid ocean below the crust, without having to drill or pass through the ice layer. This type of mission is quite different than a flyby, because the plumes are unpredictable and a probe would need to be in orbit for extended periods of time to encounter one.

## 1.2 Cubesat History

"Cubesats" are a relatively new concept in satellite technology, which takes advantage of the advancements in electronics and technology to create much smaller electric devices. These units are on the order of a 10cm cube, and contain microprocessors, cameras, GPS units, and other devices for data gathering [14]. One of the first cubesats was called the "PhoneSat," which was built

from a smart phone. It became apparent that the capabilities of a modern cell phone were enough to take pictures, send data, and perform basic satellite tasks, and so it was launched in to orbit to show that small satellites were viable [15]. Recent advancements in cubesat technology include improved imaging capabilities, advanced propulsion and control systems, GIS mapping, GPS, and data transfer.


Figure 3: Example of a cubesat – the PhoneSat [16]

Due to their small size, the cost to launch a cubesat is much smaller than that of a normal satellite; their masses often range from 1-10kg [14]. This makes the terrestrial satellite industry more available to entrepreneurs, small businesses, and universities. Unfortunately, available power sources for such small devices are often limited to solar panels. This provides sufficient power for orbit around earth, but as these small cubesats attempt to increase their distance from the sun their power decreases significantly. Smaller, lighter, and less expensive power sources would help to make the cubesat revolution available to those who are interested in other planets, asteroids, or deep space missions.

### 1.3 Propulsion systems

As mentioned earlier, the propellant systems of a spacecraft can contribute greatly to the cost. Escaping gravitational wells or just imparting momentum onto the ship can take huge masses of propellant, and each kilogram of propellant that must be used later has to also be propelled with the craft at the start of the mission. The fraction of the total mass that a craft needs is based on the Ideal Rocket Equation as seen below [17].

$$\frac{M_{final}}{M_{initial}} = e^{\frac{-\Delta V}{V_{exit}}} \quad (1)$$

Where $M_{final}$ = The mass of the ship after achieving the required $\Delta V$, $M_{initial}$ = The initial mass of the ship, with full propellant, $\Delta V$ = The change in velocity necessary to achieve the desired orbital change, and $V_{exit}$ = The exit speed of the propellant from the nozzle.

As the ideal rocket equation shows, the variables $\Delta V$ and $V_{exit}$ are of utmost importance when determining the amount of propellant required.

The value $\Delta V$ is a parameter that describes the necessary change in velocity to perform a specific orbital maneuver. For example, in order to increase the orbital radius of a craft in a standard circular orbit, it must fire a burst of propellant out in order to move forward. The craft will then travel in the opposite direction of the propellant flow. Conservation of momentum dictates that the momentum imparted into the propellant will be equal and opposite in direction to the resulting momentum of the craft, as seen below [18].

$$M_{propellant}V_{exit} = -M_{ship}V_{ship} \tag{2}$$

Where $M_{propellant}$ = Mass of the propellant exiting the ship, $V_{exit}$ = Velocity of the exiting propellant, $M_{ship}$ = Mass of the ship and remaining propellant, and $V_{ship}$ = Resulting velocity of the ship.

From this it can be seen that for a given mass of a ship, a faster exit velocity or more massive propellant will result in more momentum being imparted to the ship, and thus a faster ship velocity. The mass of the propellant can be based on the mass flow rate, or often based on the atomic mass of the particles making up the propellant. For a reference frame based on the original ship position, the change in ship velocity is equal to the $\Delta V$. However, because the ship may be in orbit, it may need multiple changes in velocity to perform a specific maneuver. In the example above, if a ship attempts to move from one circular orbit to another with a longer orbital radius, it must burn once at the perigee of its orbit, and again at the apogee in order to make the orbit circular. Each burn will require a certain $\Delta V$, but the sum of both $\Delta V$'s necessary to achieve the maneuver will be what dictates the necessary propellant.

The exit velocity of the propellant is also a very important aspect, and is often represented with the metric of Specific Impulse (ISP), given in seconds (s). The relationship between ISP and exit velocity is given below [19].

$$ISP = V_{exit}/9.81 \quad (3)$$

A higher ISP directly results in a higher exit velocity, which translates to a smaller mass fraction of propellant. However, often times the higher ISP is achieved by using smaller particles for fuel, or a decreased mass flow rate. This reduces the momentum imparted to the ship by the propellant. It is often difficult to have a high ISP and a high change in momentum, especially for systems with a set power level.

### 1.3.1 Chemical Rockets

Chemical rockets work by combusting two materials together and releasing energy stored in chemical bonds. As they combust, they produce a gas with a much larger volume than the original fuel. The increase in pressure pushes the gas out of the rocket nozzle, and the spacecraft is propelled forwards. Often times, the resulting molecules that form the propellant have a rather large atomic mass, and thus the mass flow rate of the propellant is quite high. This results in a large amount of thrust, but not necessarily a large ISP. Due to this, chemical rockets often have a high mass fraction of propellant, and are capable of escaping gravity wells, accelerating quickly, or imparting large $\Delta V$ values quickly.


Figure 4: Minotaur IV chemical rocket [48]

Because of the high mass fraction of chemical rockets, they are costly to bring along on a mission from a mass standpoint. Each kg of propellant that is required at the end of the mission, for stopping, entering orbit, or other maneuvers, must be taken in to account at the beginning of the mission. This drives many chemical rockets to be used in “flyby” missions, where the spacecraft travels through the solar system passing by objects of interest and then continues on into deep space. Examples of these missions are the Voyager missions or New Horizons.

If a Cubesat was properly equipped with a long term power source, small chemical rockets could be used to launch the satellite on a flyby mission. However, because solar power only works near the sun, current Cubesats would quickly run out of power if launched on a flyby mission with chemical rockets.

### 1.3.2 Nuclear Rockets

Nuclear rocket systems run on the idea of a hot reactor core heating a propellant and exhausting it out the back of the nozzle, thus providing thrust. In contrast to chemical rockets, nuclear rockets can use almost any fluid as propellant because it is not required to form a chemical reaction. Instead, it merely expands as it heats up. This gives the propellants a more diverse range of possibilities. Nuclear rockets also have an abundance of energy in their fuel, which allows them to burn for longer durations than chemical rockets. However, they must have a reactor large enough to maintain criticality, and this often makes them rather large systems.

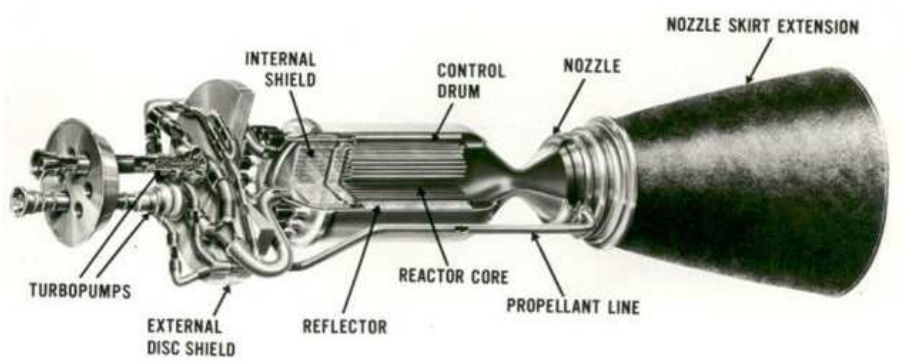


Figure 5: NTR diagram [111]

In 1955, Los Alamos National Laboratory began research on project “Rover,” which was a program designed to create a nuclear thermal rocket for space flight. Their work paved the way for NASA’s project NERVA, which was another nuclear thermal rocket program starting in 1961 [20]. Both of these projects used uranium loaded carbon fuel elements to form the reactor. Through these rods were small flow channels that would have cold propellant forced through them. As the propellant heated in the flow channel, it would expand and be pushed out the nozzle. The NERVA program flow channels were used in the design of this project as a starting point for flow channel sizing.

**Figure 6: Graphite NERVA fuel element (left) and new, tungsten based fuel element (right). Image courtesy of the Center for Space Nuclear Research**

Another important aspect of the old NTR programs was the effects of propellant temperature and atomic mass on ISP. They found that the ISP of hydrogen propellant at 2550 K was 850 s. Yet they found that when the atomic mass of the propellant increased, the ISP decreased by the ratio of the square roots of the molecular hydrogen mass over the new mass. Also, when the temperature increased the ISP increased by the ratio of the ratio square roots of the new temperature over the old. This gave rise to the approximation below [21].

$$ISP = \frac{\sqrt{T_{new}}}{\sqrt{2550}} * \frac{\sqrt{2}}{\sqrt{M_{new}}} * 850 \quad (4)$$

Where $T_{new}$ = The exit temperature of the new propellant and $M_{new}$ = Atomic mass of the new propellant.

With this approximation, the performance of other propellants could be estimated. For example a heavier element, such as helium would have an atomic mass of 4. At the same temperature of 2550 K, the ISP would decrease to 601s. However, because the mass of the propellant has increased, the thrust would increase as well. This would result in a higher mass fraction but larger thrust values.

### 1.3.3 Cold Gas Thrusters

Cold gas thrusters are a method of propulsion wherein compressed gas is released through a nozzle without any sort of heating involved. Due to the relatively high density of the cold gas, this results in a very low ISP, but high thrust. Cold gas thrusters are often used for minor corrections, such as dodging debris or changing spacecraft orientation. They may be taken as an extreme case of the tradeoff between ISP and rapid $\Delta V$ gain, in the sense that a ship that quickly jettisons a large fraction of its mass will notice an extremely rapid change in direction.

Figure 7: Cold gas thruster [22]

### 1.3.4 Electric Propulsion

Electric thrusters are devices which use high voltages to propel ionized atoms at incredibly high speeds as a propellant method [23]. Types of electric thrusters include ion thrusters and Hall Effect thrusters. Electric thrusters have a very high ISP, on the order of thousands of seconds, because the exit speed is so high. However, the mass flow rate is relatively small, so they do not produce much thrust. Electric thrusters are useful for long term missions where their high ISP equates to a small propellant mass fraction and they are able to function for long periods of time.

Figure 8: Hall Effect thruster image (left) and while operating (right) [23]

Unfortunately, electric thrusters need a source of electric power, and that aspect is often overlooked in their design. Batteries tend to run out of energy quickly, nuclear reactor systems have huge masses that won't be moved by small thrust levels. Radioisotope power provides too low of power levels, and chemical power tends to run out of fuel quickly. One of the only viable power methods for electric thrusters is solar power, and even then it has to be very close to the sun. If

there was a low mass power source that could provide large power levels then electric thrusters would be very useful for long term deep space missions.

### 1.4 Radioisotope Systems

Non-critical assemblies using naturally decaying materials are referred to as radioisotope power systems (RPS's). They have the benefit of huge specific energy levels that are associated with nuclear systems, but they release that energy over a very long period of time. This makes their specific power often relatively low. Plutonium Dioxide ($PuO_2$), for example, is a favorite material for radioisotope power systems because of its low amount of damaging radiation, high power density, and long life. It produces roughly 400 watts of thermal power per kilogram at the beginning of its lifetime, and is reduced to 200 watts after 87.7 years [5]. This thermal power can be converted to electrical power in order to provide power to systems for extremely long missions.

The most current model of the RPS is known as the Multi-Mission Radioisotope Thermoelectric Generator (MMRTG), shown to the right. It is powered by $PuO_2$ loaded General Purpose Heat Source (GPHS) units, which provide thermal energy. That heat is converted to electrical energy through the use of thermoelectric converters. The system efficiency is roughly 6-7%, it has a mass of 45 kg, and produces 110-125 W of electric power [5]. The MMRTG differs from previous RTG models due to the fact that it is totally sealed and can function either in the vacuum of space or in the atmosphere of a planet, making it a viable power source for many types of missions.

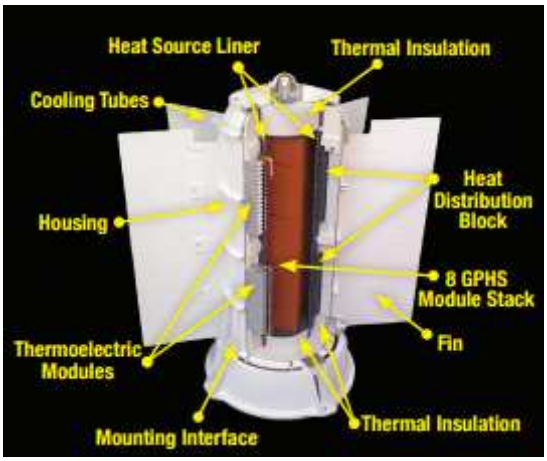


Figure 9: MMRTG diagram [24]

Other RPS designs include the Advanced Stirling Radioisotope Generator (ASRG), Radioisotope Thermo-Photovoltaics (RTPV), or decay batteries. The ASRG system uses the same GPHS unit as a power source, but instead of using thermoelectric conversion it uses a Stirling engine. This has caused some difficulties during testing due the fact that it has moving parts and may have trouble stopping and starting [25]. RTPV systems function by converting the radiated light from a high temperature heat source through the use of photovoltaic cells [26]. This method has a high

theoretical efficiency, but has not yet been effectively demonstrated as a possible power source. Decay batteries, such as beta batteries, use the charged particle decay products from a radioisotope to create a voltage, and thus power. Beta batteries collect emitted electrons at a junction, which then flow towards the positive side of the circuit. Unfortunately, the power levels in these systems are relatively small, and they are somewhat inefficient overall [27].

Reliability and cost are the major factors in RPS systems, because they are often designed for long term missions and it is important that they function autonomously for extended periods of time. Additionally, their fuel source is often extremely expensive, as most systems use plutonium based heat sources. Plutonium is attractive from an RPS standpoint because it is mostly an alpha emitter, and its decay products can be shielded relatively easily. Isotopes that emit neutrons or gamma rays are much less desirable because they require large amounts of shielding to protect components from radiation damage.

### 1.5 Need for High Power Systems

Having a system on board that could provide high power levels would allow for the use of many components not normally available for spacecraft. As mentioned before, high power levels can provide for faster communication rates, and thus less time on the DSN. It also provides better communication capabilities and can reduce noise or provide gain. Additionally, high power systems can allow for capabilities such as laser induced breakdown spectroscopy, Raman spectroscopy, or other scientific experiments that can benefit from larger systems.

Recently, the Curiosity rover on Mars discovered evidence of water by drilling into a rock and analyzing the materials it found [28]. The act of drilling and analyzing samples are two things that can use high powered systems to increase productivity. Minimizing the masses of the power systems used to run these devices is integral in decreasing overall costs and allowing for advanced capabilities.

### 1.6 Power Cycles

Having a traditional power cycle in space, such as a Brayton or Rankine cycle, can introduce many complications but is still a viable option if enough care is taken ahead of time. One of the major issues is the inability to effectively reject the waste heat of the system. Unlike on earth, there are no sources of water to use as coolant, or even flowing air available. Instead, the only method of

rejecting heat from the system is through radiative heat transfer to space. This method is largely dependent on the temperature of the radiating surface, as seen by the Stephan Boltzmann equation below [29].

$$Q = \varepsilon \vartheta A(T^4 - T_0^4) \quad (5)$$

Where Q = power emitted, $\varepsilon$ = emissivity, $\vartheta$= Planck's constant (5.67x10^-8), T= surface temperature, and $T_0$= ambient temperature.

If the temperature of the radiating body is low, the surface area must be very large; this naturally increases the mass of the radiator as more material is used. If the radiating temperature is high, the power cycle efficiency drops because the system is not extracting all the power it can from the working fluid. While this is still an issue for radioisotope systems, they often produce much smaller power levels and their radiator mass is relatively small.

Another issue with traditional power cycles is the issue of moving parts and working fluids. Turbines may need maintenance after a certain number of operating hours, and that cannot be easily performed in deep space. Fluid flow, specifically two phase flow in a Rankine cycle, is very difficult to manage due to the lack of gravity. Liquids in space tend to form spheres and do not form separated areas from their gaseous portions, due to a lack of gravity. This makes designing two phase systems difficult. Some possible methods of countering this issue could be with induced rotation or wicking systems such as heat pipe.

The final consideration for these systems is the overall size and cost. Radioisotope power systems are often limited in their components to the heat source, converter, and rejection system. Traditional systems, however, may have pumps, compressors, and turbines as part of their cycles. These extra components add mass, which makes them viable mostly for very large scale power generation and high cost missions.

### 1.7 Need for Low Cost Systems

It is important to reduce the overall cost for space exploration in order to facilitate mission availability for a wider range of interested parties. Cubesats have shown that if the cost can be sufficiently reduced, there is a market for space technologies. Additionally, with the influx of users, the technology levels of the area will naturally increase; improving capabilities for detection, measurement, instrumentation, and even space travel itself. Universities, independent companies,

and even more government missions could all contribute to the advancement of modern technology. With this potential for advancement eventually achieved, human exploration of the solar system, deep space resource mining, and eventually exploration out of the solar system might be achieved.

### 1.8 Recent Advancements

A large amount of research has been done in the area of space power generation, as the operation of power systems in space introduce a variety of challenges. Among these challenges are the technological development of propulsion systems, small satellites, and thermal core design. Improvements to thermal management and energy storage are also of utmost importance, as is addressing the issues of traditional power generation systems in space.

Recent advancements in the area of electric propulsion have increased the capabilities of efficient space travel systems. The NASA NEXT ion thruster is one of the most advanced electric thrusters, and has been analyzed in depth by Quarta and Mengali [30]. Their findings showed that an optimal trajectory to Mars would take 489.6 days using a solar powered system. However, it would required a power plant capable of providing a maximum of 10 kWe on a near continuous duty cycle. This results in a very large and expensive mission.

Researchers at Ad Astra Rocket Company have developed a variable ISP electric thruster called the VASIMR, which operates at very high power levels but provides excellent performance characteristics [31]. It is possible that the VASIMR will improve the capabilities of electric space travel, but because it is in a relatively early development phase and is being developed privately, it was not considered for use in this project.

Additionally, the introduction of small, affordable satellites has allowed for a variety of scientific topics to be addressed in increased numbers. Woellert et. al. have shown that the market for cubesats expands the realm of space travel by allowing other, less developed countries to participate [32]. With the reduced costs, countries such as Malaysia, South Africa, and Egypt have been able to make great advances to their space programs [33]. Students from US universities have also been able to explore space. For the years of 2000-2005, over 35 student built satellites were launched in the US [34], providing educational and research experience to those who would previously not have had the budget to perform these experiments.

Cubesats perform well with electric thrusters due to their small sizes and small mass allowances for fuel. Because of this, they are largely powered by solar arrays [35][36]. Some others use alternative methods such as solar sails, as proposed by Lappas et. al. [37]. Even with these capabilities, many small satellites are still confined to areas near the sun.

Using a hot core to run thermal rockets is a method that has been explored for decades. The most common method is to use a nuclear reactor for a nuclear thermal rocket, but other thermal cores have been investigated as well. Many terrestrial reactors also use Brayton cycles powered by hot cores. Forsberg, et. al., for example, have looked at a reactor powered Brayton cycle system that uses a molten salt flowing through a hot reactor core [38]. Although the molten salt for this application is different than the proposed design, it does include valuable information on the power cycle and thermal performance of core-based systems.

Even though many terrestrial Brayton cycles use air as a working fluid, Tournier and El-Genk [39] have documented the relevant properties of different noble gasses. For expanded gas properties, specifically xenon, Sifner and Klomar [40] explored and documented a wealth of thermodynamic properties in regards to state points at different temperatures and pressures.

Thermal storage mechanisms have also been looked at recently, most heavily in the area of solar power storage on earth. However, the technologies investigated could easily be adapted to space applications. Many of these applications for thermal storage examine the use of low temperature materials such as paraffin wax and resin, such as explored by Aadmi et. al. [41]. Their exploration in to heterogeneous PCM systems helped to show the changes in effective heat transfer coefficients of materials that are varying in composition as well as phase.

Work by Sahan et. al. [42] helped to show that introducing alternate materials into a PCM may affect the heat transfer rate, even if the dopant is not a PCM itself. Adding nano-particles in solid form can also change the bulk heat transfer rate. Research by Siahpush, O'Brien, and Crepeau [43] into porous foam additives has also shown that the thermal conductivity can be artificially enhanced by introducing a conductive material into the PCM. In their case, a metallic foam provided heat transfer pathways through the material.

Chen and Wolcott [44] examined the difficulties encountered with PCMs leaking through their housing, and concluded that certain PCMs may in fact seep into their containers and exit the

system. However, their experiments dealt largely with plastic housing materials that do not benefit from the welded housing proposed in this project.

Higher temperature PCMs are in development for direct power conversion, similar to the ideas proposed in this project. Liu et. al. [45] have examined the properties of high temperature salts (up to 600 $^{o}$C), and their ability to cycle through multiple uses. An important finding of their was the fact that even though the phase change occurs at a single temperature, the bulk temperature of the system varies slightly during the process. This is due in part to the heating rate and the buildup of thermal energy in the system when the heat transfer rate of the material is not high enough to dissipate the incoming energy.

Other PCMs, including organic materials, salts, and metals, have been explored by Su, Darkwa, and Kokogiannakis [46]. They found that molecular PCMs may provide benefits in regards to thermal storage capabilities, but often the heat transfer rates were greatly reduced, and some organic PCMs had issues with flammability. The elemental PCMs, however, were more predictable. Problems with low thermal conductivity were also encountered by Bruno et. al. [47] in their experiments with PCMs.

From the information gathered in these areas, it can be seen that the synergy of these technologies can allow for a cost effective and efficient method of deep space exploration. Adapting existing technologies in the power generation field to ground breaking technologies in satellite development will allow for much more research to be done on distant celestial bodies by a much wider range of researchers.

## CHAPTER 2: Overview of Pulsed Power/Propulsion System

The goal of this design project was to create a propulsion system that could take a small Cubesat payload from low earth orbit to any planet in the solar system for a fraction of the cost of normal methods. This would be done by introducing a duty cycle to the propulsion system that would allow it to propel the craft only once per day. During the down time, the system would gather thermal energy from a radioisotope heat source. The reduced power levels would in turn reduce the amount of costly radioisotope fuel required. Storing the energy over a period of time and releasing the energy quickly provides high power levels, which in turn equates to a more efficient system. By using phase change materials (PCMs), the thermal energy can be efficiently stored in a two phase solution, thereby reducing entropic losses and ensuring effective thermal storage.

Figure 10: Artist concept of pulsed power and propulsion system, courtesy of Center for Space Nuclear Research

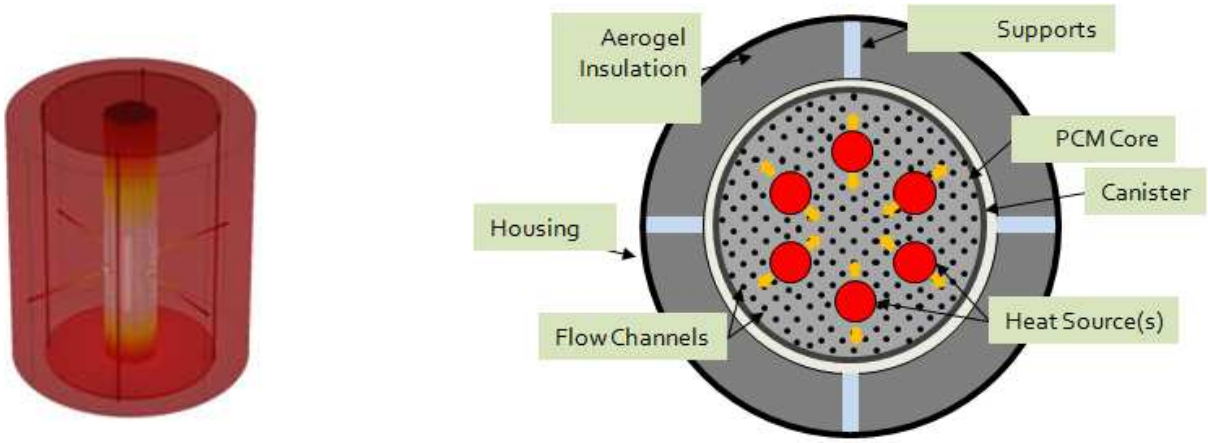


Figure 11: Core example (left) and top-down cutaway view of core components (right). The core occupies the center cylinder of the concept shown in figure 10. Possible configurations may include varying numbers of flow channels, sizes, and number of heat sources.

This project was funded in part by a NASA Innovative and Advanced Concepts (NIAC) phase I grant to deliver a small payload of cubesats to Saturn's moon Enceladus. The NIAC project included determining a set of parameters that were used as baseline points upon which permutations were performed to classify different systems. A default burn time of six minutes was used, as well as a repetition rate of one burn per day. An electric power level of 25 kW was also determined based on desired communication rates from Enceladus. The project was then continued without NASA support to investigate different burn times, repetition rates, propulsion methods, and fuel types, as well as further investigation into aspects already touched upon by the phase I NIAC.

The fuel source used is one of many possible radioisotopes that can provide decay heat. The incredibly large energy density is optimal for long term missions that may be far away from the sun. Some possible isotopes are listed in the table below.

Table 1. Characteristics of radioisotopes in their pure elemental forms

| Element | Specific Power (W/kg) | Half Life (years) | Benefits | Issues |
|---|---|---|---|---|
| Am241 | 111 | 432.7 | low amount of hazardous radiation | low specific power |
| Pu238 | 500 | 87.7 | good balance of power density and low radiation | limited supply |
| Cm244 | 2500 | 18.1 | very high power density | very high neutron flux generated |
| Sr90 | 2309 (incl. Y90) | 28.8 | high power density | daughter (Y-90) emits >2 MeV beta, causing Bremsstrahlung radiation. Very soluble in water |

As the table shows, each possible radioisotope fuel has its own benefits and complications that must be addressed. Americium has a relatively low power density, so more material is required. Plutonium is quite costly due to its limited supply. Curium and strontium both have decay

products that are difficult to shield against, so more shielding is required. Bremsstrahlung radiation from strontium occurs when the high energy beta emission is slowed by other particles and generates a gamma ray with energy equivalent to the energy lost from the electron. There are of course other options for radioisotope materials, but these four have shown themselves to be the most promising.

The inclusion of PCMs in as a thermal capacitor in the system is one of the major factors in keeping the mass down and the $\alpha$ value high. A thermal capacitor allows for the radioisotope heat to be collected over a period of time and extracted at a much faster rate than the radioisotope itself can provide. This equates to much higher power levels during the "blow down," or the period when the working fluid is extracting the heat from the core. That fluid can then either operate a power cycle or be used for direct propulsion. The PCM allows for the capacitor to maintain a constant temperature during the blow down, increasing the efficiency of the turbine and components compared to a sensible heat system that will cool over the heat extraction period.

When generating electrical power, the cycle is closed and the working fluid is reused during the blow down. In order to return to its initial state, the waste heat must be rejected. In space, this can be difficult because the only heat rejection method is through radiation, as discussed earlier. In the case of high power systems, the radiators must be very large to reject the large amount of waste heat generated. However, for pulsed power systems there is an extended period of time where the power cycle is not functioning. If the radiators could be rejecting heat during this time as well, they would need to radiate the waste heat at a much lower rate than the rate at which the cycle was producing power.

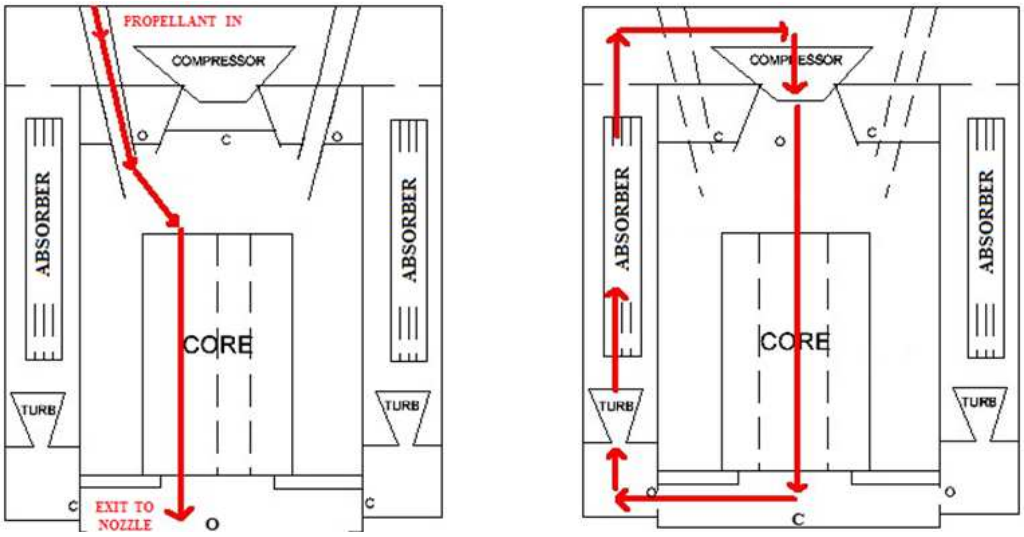


Figure 12: Working fluid pathways for thermal propulsion mode (left) and power generation mode (right)

To achieve this, another thermal capacitor is used for the waste heat. It is beneficial for this capacitor to be a PCM as well in order to keep the input to the compressor constant and radiate at a constant temperature. If, for example, the absorber was allowed to cool as it rejected heat, the rate of heat rejection would decrease drastically as seen in equation 5. But if the system was undergoing a phase change, it could reject heat without decreasing in temperature, thus keeping the rejection rate high.

## 2.1 Requirements: Size, Mass, Power

The craft is designed to fit inside the payload bay of a Minotaur IV launch vehicle. This vehicle was selected because of its frequent use in deep space launches. Although the Minotaur V was used for the New Horizons mission, the only difference between it and the Minotaur IV is the inclusion of the Star solid rocket motors. Because that motor is not necessary, the Minotaur IV was selected [48].

The Minotaur IV is capable of launching a 1000 kg payload to an altitude of 600 km using the lowest performing system. The lowest orbital height of low earth orbit is around 300 km. Given that the goal of this design is to be inclusive of all missions even under non-ideal conditions, a 1000 kg system launch to 300 km should be easily achievable, and the target goal for the system.

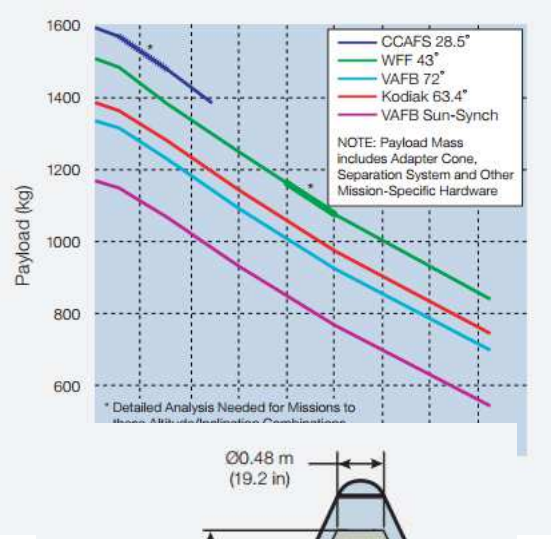


Fig

## 2.2 Launch Envelope

The available launch envelope on a Minotaur IV launch vehicle is roughly 23 cubic meters, with specific dimensions provided in the figure to the right. This volume is much larger than the size of the core and instruments, but may become a limiting factor for some propellant tanks. For thermal propellants with very low densities, the tanks

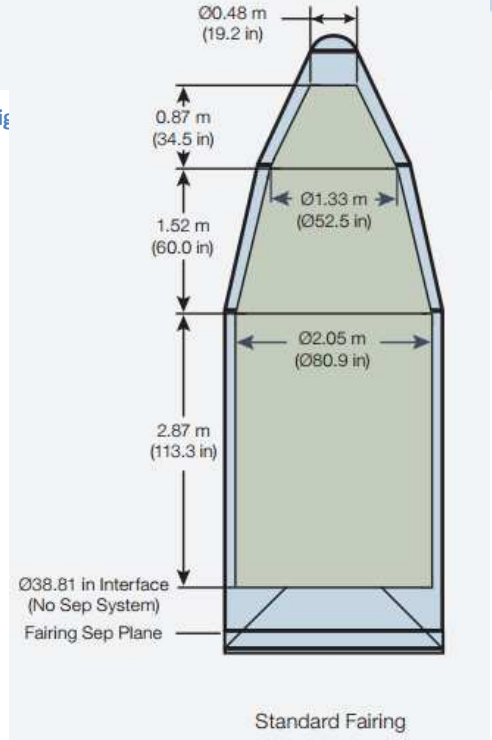

are often very large even though the ISP may be quite high and the mass quite low.

### 2.3 Launch Cost

According to the Air Force, a standard launch cost for one Minotaur IV launch is $50M [40]. With the total possible payload being 1735 kg, that equates to ~$29,000/kg. However, many missions "ride share" with other satellites attempting to enter earth's orbit or travel on to other missions. If there is unused volume and mass available, the cost of the launch can be split between multiple satellites [49] [50]. This can decrease the cost in some cases to ~$10,000/kg if the payload is small enough [51], and numbers as low as $4,500 have been claimed by NASA [52]. Because the baseline propulsion system is designed to take up the majority of the available mass, the larger value of $29,000/kg is used for cost estimates. If the volume of the system will not be limiting, then the mass fraction may decrease the cost accordingly. Therefore, the goal will be to minimize mass and volume, and being at least below 1000 kg and 23 $m^3$.

Figure 14: Minotaur payload size [48]

### 2.4 Power Levels

A study done by the Center for Space Nuclear Research in 2014 showed that for a 6 minute communication window, a data rate of 1 Mb/s would require 25 kW of electrical power to communicate from Saturn's orbit [52]. Current electric thrusters, such as the NEXT ion thruster or the Aerojet BPT 2000 thruster require 6.9 kW and 2.2 kW of power, respectively [53][54]. This sets the scale for the desired power output to be in the range of kW, and ideally 25 kW or above. With a power level in excess of the thruster requirements, multiple thrusters can be used and a redundancy available in case one fails. Based on this information, the desired power level and time was decided to be 25 kW of electrical power for a 6 minute burn.

### 2.5 Topics to Address

The major topics related to the development of the system are introduced below and explored in further depth in subsequent chapters.

#### 2.5.1 Design of Core

The design of the PCM core is important in determining the cost, heat up times, and mass of the spacecraft. Ideally, the core would be small, provide high power levels, require low times

between burns, and be inexpensive. However, high power levels often mean more expensive radioisotopes, or higher masses for shielding. Rapid burn times often increase the mass of the absorber, and small sizes may result in increased costs or low power. All of these aspects must be properly balanced and their effects on one another explored.

The materials used in the core must be evaluated for their thermodynamic properties; the insulation must be effective but light, the PCM must have high energy density, and the whole system must be able to withstand high temperatures. Many materials were examined in order to achieve the required capabilities and still keep masses low.

### 2.5.2 Power Cycle

The development of the power cycle is important because it will determine the requirements of the system to generate the necessary electrical power levels, as well as determine the absorber size, core size, and mass flow rate. While the core development process dictates the time required to recharge the system, the power cycle will determine the blow down characteristics. The power cycle is the main driving force behind the communications and power production capabilities, as well as the size of the mechanical portions of the spacecraft. The electricity generated can also charge attached batteries for Cubesat uses during recharge times.

### 2.5.3 Propulsion

Thermal propulsion is an option for effective extraction of thermal heat and conversion into motion of the craft. The spacecraft would be equipped with a tank of propellant, such as hydrogen, that it would use during times when thermal propulsion was required. The thermal mode would be useful for escaping from earth's gravity early in the mission, and then the propellant tanks would be jettisoned. This method imparts larger $\Delta V$ values per burn, but requires large amounts of propellant. Additionally, the inclusion of this system would require some method of switching between electric and thermal modes. This can be done with a valve system or with a manifold, with each possibility having its own pro's and con's.

### 2.5.4 Orbital Mechanics/Trajectory

The mission architecture must also be defined in order to ensure that the craft can make it to the destination, what propellant is needed, and what times are involved in doing so. The mission design is kept general as to eliminate the need for launch windows, this means losing any benefits

from gravity assists or time specific launches. Instead, a worst-case scenario is used to show the transit times.

Propulsion modes are also compared in regards to cost and time; thermal, electric, and chemical systems can all be used at certain times and it is important to explore the benefits and consequences of each method. In the event that different propulsion methods are used, the issues of switching between them must also be addressed. Additionally, catastrophic failure may be an issue with chemical systems. While thermal and electric systems may break and stop working, a chemical system has a greater chance of exploding and distributing radioactive material. Calculations are also done in regards to $\Delta V$ budgets and trajectories in both terrestrial and heliocentric orbits.

### 2.5.5 Switching Mechanism

Some possibilities for a switching mechanism include magnetic switches or mechanical arms that can open or close valves, or simply a manifold that allows different working fluids to flow through different flow channels. All of these systems will have to withstand the high temperatures of operation, as well as very long mission times and repeated use. They must also insure that they can form tight seals and avoid leakage when closed.

### 2.5.6 Experimental Demonstration

In order to show the proof of concept, an experimental system was constructed using a PCM to heat air in a Brayton cycle. The goal of this experiment was to show the plateau in power generation formed by the inclusion of a PCM, as well as the repeatability in running the system.

# CHAPTER 3: Core Development

## 3.1 Overview

The thermal capacitor core is a new and innovative concept in space travel that takes advantage of current thermal storage mechanisms. Introducing a duty cycle to the system allows for huge power to weight ratios and the operation of high power levels. One of the first aspects to address in the core is the use of latent heat of fusion versus sensible heating systems.

Sensible heat can be very useful because it is usually a large amount of energy per unit mass. Materials can also remain in their normal state as they are heated or cooled, so there is not a problem with melting, boiling, or solids becoming fluid. It is less attractive in the sense that the temperature varies as the material cools. This makes heat transfer more complicated, as a working fluid may extract heat from a hot core very well at the beginning of the blow down, but less effectively as the core cools. Additionally, the temperature of the working fluid may change as the temperature of the core changes. This makes the input to the turbine different over the course of the blow down, and makes components hard to size.

Temperature changes in the gas can be avoided to some degree by making the flow channels long enough to allow for the output side of the core to never decrease in temperature. An example of the working fluid temperature profile can be seen below in figure [22] to illustrate the concept of a sufficiently sized flow channel.

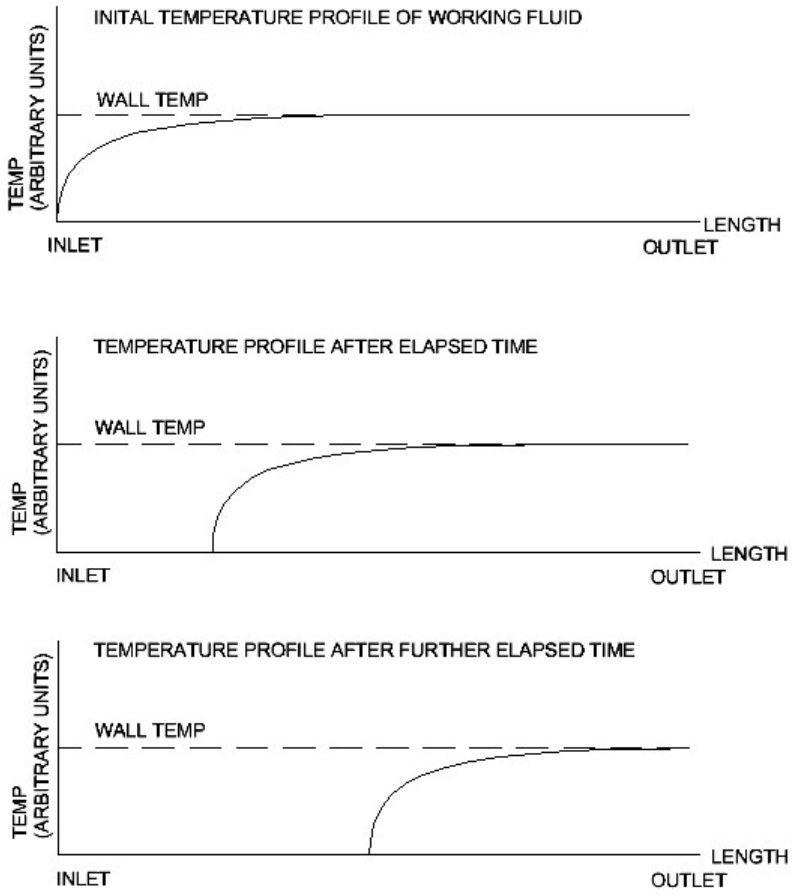


**Figure 15: Illustration of temperature of an example working fluid in heat exchanger. The left side of the hypothetical channel cools as the blow down process extracts heat.**

As the figure shows, the temperature may stay relatively constant as heat is extracted so long as there is sufficient length to reach temperature. If the blow down continues past the bottom graph, the exit temperature of the fluid will begin to drop. Although this allows the exit temperature to remain somewhat level, it introduces thermal and cycling stresses in the core and the housing due to the changing temperature of the front of the core. Additionally, the length of the core will be much longer than that of a core that did not have the inlet side cooled in temperature.

The absorption of the latent heat of fusion is a phenomenon that occurs when a solid object melts, and stays at the same temperature while in a two-phase state. It can continue to absorb energy, and increase the fraction of the liquid state, but the temperature of the mixture stays constant. This allows the system to absorb or release energy without changing temperature and can simplify modeling and calculations. In some cases, the cooling of the PCM can still develop a

temperature profile axially, so it is important to make sure the heat transfer properties of the PCM are sufficient to keep the temperature along the flow channel relatively constant. However, a PCM also introduces liquids into the system, which can cause changes in pressures and leakage issues. Most materials expand when they enter a liquid state and are able to freely flow to fill the available volume. Water, silicon, and some other materials expand when they freeze and can develop large stress concentrations as they press against their container. It is important to take these effects in to account when designing a PCM system that uses latent heat to avoid cracks or leaks.

PCMs have been a possible solution for energy storage in other applications as well, particularly solar power. Because solar energy is generally available only during the day, many researchers are attempting to store the sun's energy for use later. Some ideas include compressed air, pumped water, or PCMs [56]. The latter is a viable solution because the change in internal energy of a PCM does not create significant irreversible increases in entropy; the material can be melted and frozen over and over again without major losses. PCMs also have rather high latent heat of fusion values. Silicon has a latent heat of fusion of 1800 kJ/kg, Beryllium has 1356 kJ/kg, and lithium hydride has 2582 kJ/kg [56] [57] [58]. By contrast, the specific heat of silicon metal is 0.71 kJ/kg*K. The latent heat of silicon then contains as much energy as silicon metal changing over 2500 degrees K.

Because of the leveled temperature and high thermal capacity it was decided that a PCM core would be ideal for the design of this system. Keeping masses low and outputs predictable and robust are of utmost importance in space travel systems.

## 3.2 Phase Change Materials

It is important to compare different types of materials in order to ensure the proper PCM is selected for the core design. Major elemental contenders include silicon, boron, germanium, and beryllium. Molten salts were also investigated based on research by NASA into thermal energy storage for space applications. Aspects of these material options are discussed below.

### 3.2.1 Silicon

Silicon has a very high melting temperature of 1683 K, which can be useful for some aspects and quite detrimental for others. For a thermal propulsion system the high temperature would provide an increased ISP, and thus lower overall propellant mass. However, the high temperature

also would require more insulation or result in more heat losses. It would also require very specialized materials to be able to withstand the high temperatures. Additionally, silicon expands when freezing, which can create issues with stresses in the core housing. After hundreds or thousands of cycles, frozen silicon may eventually crack the housing. Although it has a very high latent heat of fusion value of 1800 kJ/kg, Silicon was ultimately eliminated as the optimal option for this device due to the complications of the expanding frozen state [57].

### 3.2.2 Boron

Boron has an even higher melting temperature than silicon at 2348 K, which makes it almost impossible to use in this capacity. Again, for a thermal system the ISP would be phenomenal, especially with the latent heat value of 2090 kJ/kg, but managing the material at that temperature would require a very advanced design [59].

### 3.2.3 Germanium

Germanium is an option for lower temperature systems; it has a melting temperature of only 1216 K. This makes it more manageable than some other options, but less effective for thermal propulsion. For electrical power generation however, that temperature is more than sufficient. Many Brayton power cycles prefer to run at a hot temperature of near 1000 K [60] [61][62]. Germanium has a latent heat of fusion of 465 kJ/kg [60].

### 3.2.4 Beryllium

Beryllium has another relatively high melting temperature of 1551 K, and a high heat of fusion of 1387 kJ/kg. Although it seems like it may be a feasible alternative that does not expand when frozen, it is a very dangerous material to work with. Beryllium can have fatal effects on a person's respiratory system if inhaled, and so it is rarely machined. This would significantly add to the cost, as well as introduce a very dangerous aspect to the manufacturing, handling, and possible mission abort of the system and so it was disqualified as a possible PCM [63].

### 3.2.5 Molten Salts

Salts are compounds that may have different melting temperatures, heat of fusion values, or thermodynamic aspects than the elements from which they are formed. Often, their melting temperatures are below 1125 K, and heat of fusion values below 2600 kJ/kg [56]. This makes their

use less than ideal for thermal propulsion, but very plausible for power generation. As an example, Hydrogen propellant heated by Silicon to 1683 K would have an ISP of 690 s, while at 1125 K it would be only 564 s. This would increase the mass of propellant by roughly 17%, according to equation 1. Table 2 below shows a comparison of different molten salts.

Table 2. List of molten salt PCMs

| MATERIAL | MELTING TEMPERATURE (K) | HEAT OF FUSION (KJ/KG) |
|---|---|---|
| KF | 1125 | 454 |
| $Na_2Co_3$ | 1125 | 279 |
| Ca | 1123 | 221 |
| LiF | 1121 | 1044 |
| $LiBO_2$ | 1108 | 698 |
| $75NaF+25MgF_2$ | 1105 | 649 |
| $62.5NaF+22.5MgF_2+15KF$ | 1082 | 607 |
| NaCl | 1074 | 484 |
| CaI | 1057 | 1425 |
| $CaCl_2$ | 1046 | 256 |
| KCl | 1043 | 372 |
| $67LiF+33MgF_2$ | 1019 | 97 |
| $65NaF+23CaF_2+12MgF_2$ | 1018 | 574 |
| $Na_2B4O_7$ | 1013 | 523 |
| $Li_2CO_3$ | 998 | 605 |
| $MgCl_2$ | 988 | 454 |
| 60KF+40NaF | 983 | 479 |
| LiH | 956 | 2582 |
| Al | 933 | 388 |
| 60LiF+40NaF | 925 | 816 |
| Mg | 923 | 372 |
| $46LiF+44NaF+10MgF_2$ | 905 | 858 |
| $52LiF+35NaF+13CaF_2$ | 888 | 640 |
| LiCl | 883 | 470 |
| 52NaCl+48NiCl | 843 | 558 |
| $Ca(NO_3)_2$ | 834 | 130 |
| 73LiCl+27NaCl | 825 | 430 |
| 48KF+51LiF | 773 | 328 |
| 49KF+51LiF | 765 | 461 |
| $80Li_2CO_2+20K_2CO_3$ | 763 | 377 |
| LiOH | 743 | 930 |
| 11.5NaF+42KF+46.5LiF | 727 | 442 |
| 80LiOH+20LiF | 700 | 1163 |
| KOH | 673 | 140 |
| LiCl+KCl | 623 | 255 |
| $KNO_3$ | 613 | 128 |

As the table shows, lithium hydride is a very attractive material due to its operational temperature of 956 K and its energy capacitance of 2582 kJ/kg. For a power cycle that would run around 1000 K, this material is almost ideal. Silicon and LiH were the two major PCMs addressed in this study. The silicon in the event that a high temperature thermal system would be used, and LiH in the event that the system would be completely electric.

### 3.3 High Temperature vs Low Temperature

As discussed earlier, the melting temperature of the PCM will dictate the operating temperature and have an effect on the performance of the thermal propulsion and power generation modes. Additionally, the losses through the insulation and mounting will increase with higher temperatures unless extra insulation is added. If the same insulation is used, the overall system efficiency will drop as more heat is lost from the core for higher temperature materials. This will also translate to longer heat up times, because less of the radioisotope heat is being transferred to the PCM core. However, the decrease in fuel mass is so large that extra insulation or reduction in performance will likely be outweighed by the reduction in launch costs.

As an example, a 1000 kg craft that would use hydrogen to escape earth's gravity might use 452 kg of propellant at a temperature of 956K, corresponding to the melting temperature of LiH. At 1683K, the melting temperature of Si, it would only require 365 kg, saving 87 kg of mass and roughly $2.5M, at $29,000/kg.

### 3.4 Radioisotope Selection

The production of heat by the radioisotope in question is of utmost importance, as it will determine the mass required as well as the cost of the fuel source. In order to calculate the power generated by a radioisotope, the following formula is used [27].

$$P = \frac{C*E*N_A*\lambda}{M} \tag{6}$$

Where P = Power generated in w/g, C = conversion constant from MeV/s to W: $1.6*10^{-13}$, E = Energy per decay in MeV, $N_A$ = Avogadro's Number: $6.022*10^{23}$, λ = Radioisotope decay constant. and M = Atomic mass of isotope.

Plutonium-238 is a favorite for radioisotope power sources because of its high power density and lack of dangerous radiation effects. It is primarily an alpha particle emitter, which is a

charged particle and has a very small penetration depth. It does also emit a relatively small gamma ray that can be hazardous if not properly shielded. Because of the small amount of shielding needed and the high power density, plutonium-238 has been used for years in radioisotope thermoelectric generators of all kinds.

Unfortunately, plutonium-238 has to be made from a reactor, and is often done at a very slow rate. There is a limited amount available at any given time, and unless the production rate is increased the cost of plutonium is likely to remain very high. Costs for plutonium-238 can vary wildly with time, and because all plutonium must technically be owned by the Department of Energy, it is difficult to determine the exact cost. However, reports of $4M/kg [55] to $8M/kg [56] have been released, and efforts by the Center for Space Nuclear Research have provided plans to produce new Pu for as little as $1.6M/kg [64]. For the purpose of this project, the highest reported value of $8M/kg will be used as a worst-case scenario. For plutonium dioxide, which is the preferred form of Pu for radioisotope power production, the power density is decreased from 500 W/kg to 400 W/kg. This places the cost per kg at $7.05M/kg, and a cost per watt of thermal power at $16,000/W.

Americium 241 is another option for power production, and is also often used in an oxide state. AmO2 has a lower power density than PuO2, but is even easier to shield against and has an even longer half life. It is also more readily available than PuO2. Because of the lower power, more material is needed, which can contribute to launch costs. Current prices for Am are around $1.5M/kg [65]. With the power density of AmO2 being near 100 W/kg, the price per watt equates to $15,000/W, but the contribution to the launch cost would be roughly 4x that of PuO2.

Curium 244 has a very high power density of 2500 W/kg, and it also more readily available than Pu. This would allow for a slightly cheaper launch as well as a reduced overall cost. Unfortunately, the major radiation method of Cm is to spontaneously fission, which creates a large neutron flux. Neutrons require a large amount of low density shielding to slow and eventually stop them, so the core would require a large volume of foam, water, or other hydrogen rich material to shield sensitive components [66]. Oak Ridge National Lab has listed the price for Cm 244 as $185/mg, or $185M/kg ($740,000/W) [67]. While it is likely that this price would be reduced for scales larger than 1mg, the exorbitant cost may eliminate curium as a possible power source all together.

Strontium 90 is a possible power source that was used in the Systems for Nuclear Auxiliary Power (SNAP) program in the 1960's [68]. It provides 2,309 W/kg, and has a cost of $100,000/kg, or $107/W [69]. However, it is very soluble in water and will create a very dangerous situation if the mission is aborted over the ocean or any amount of Sr90 is somehow lost to the atmosphere. For this reason, it is often used in a form of strontium titanate, SrTiO3, which is insoluble. This reduces its power density, but without this modification it is difficult to gain launch approval. In this form, the power density is decreased to 916 W/kg.

The primary decay method for Sr90 is to release a high energy electron, which results in a yttrium 90 isotope that also beta decays into stable zirconium 90. The half life of yttrium 90 is only 64 hours, so the decay from the Y90 can also be used to in the calculations of the thermal power released. The beta particle from Sr90 and Y90 is easily shielded, but when an electron's momentum is changed it releases a photon to maintain conservation of momentum. The energy of that photon is proportional to the energy lost by the electron, so a ~0.5 MeV photon from Sr90 that is completely stopped in one collision will result in a high energy ~0.5 MeV gamma ray. This can be difficult to shield against, as gamma ray shielding is often very dense material like lead or heavy metals. Y90 discharges an even stronger 2.28 MeV beta particle, which occurs quickly after the Sr90 decays.

To properly shield Sr90, the emitted beta particles should be gradually slowed with a low Z material in order to generate multiple, low energy photons as opposed to a single, high energy photon. The PCM core will assist in this aspect, but it is still possible that the beta particles will hit a heavy nucleus and create a strong gamma ray.

In order to make sure the shielding for Sr90 and Y90 is sufficient to protect sensitive electronics and scientific devices, shielding calculations can be done using the attenuating properties of the material, geometry of the system, and allowable radiation dose.

For Sr90, each beta decay has the possibility of creating a 0.546 MeV gamma ray. A lead shield has a coefficient of 1.875 $cm^{-1}$ for 0.546 MeV gamma rays [27]. The daughter product, Y90, also has the potential to create 2.28 MeV gamma rays. The attenuation coefficient for lead and 2.28 MeV rays is .525 $cm^{-1}$ [27].

The main concern in the radiation dose seen by sensitive payloads is caused by the Y90 Bremsstrahlung radiation. In a worst-case scenario, the beta particles would interact with a heavy

nucleus and rapidly change direction. This would create a 2.28 MeV gamma ray. In the event that not all of the beta particle's energy was lost in the interaction, it would continue on a path that created a larger number of lower energy photons. Although this would cause a distribution of gamma ray energies, for the purposes of estimating shielding requirements the high energy gamma calculations will suffice.

Additionally, the acceptable dose to the payload depends on the payload itself. Human dose limits are well established, and can serve as a baseline for acceptable radiation levels. Again, if certain components are particularly sensitive or robust they must be addressed on an individual basis. According to the DOE Handbook of Radiological Worker Training, the exposure limit of a radiation worker is 5 rem/year [70]. This will be the maximum amount allowed for the payload of the propulsion system as well.

In order to find the exposure, three major factors are taken in to account: the distance from the source, the effectiveness of the shielding, and the tendency of the payload to absorb the radiation. The distance from the source is important because the radiation naturally spreads in all directions. If the source is treated as a point source, the dependence on distance is given by equation [27] below.

$$\varphi = \frac{S}{4*\pi*r^2} \tag{7}$$

Where $\varphi$ = Photon flux, S = Source activity, and r = Distance from source.

At a certain distance from the source, shielding is placed. The flux at distance "r" then attempts to pass through the shielding, and the transmittance is reduced according to equation [27].

$$\varphi = \varphi_0 e^{-\mu x} \tag{8}$$

Where $\varphi$ = Photon flux exiting shielding, $\varphi_0$ = Photon flux entering shielding, $\mu$ = Attenuation coefficient, and x = Thickness of shielding.

From this flux exiting the shielding, the Kerma can be calculated. The Kerma is the amount of energy the radiation is depositing into the object of interest, and is given by equation [27].

$$K = 1.602\ x\ 10^{-10} * E * \left(\frac{\mu}{\rho}\right) * \varphi \tag{9}$$

Where K = Kerma, E = Energy of the photon, $\mu$ = Absorption coefficient, $\rho$ = Density of target, and $\varphi$ = Particle flux.

Kerma is often reported in units of "Grays," which is equivalent to 1 J/kg. Exposure limits are often given in Sieverts or Rem, which take in to account the susceptibility of the target to types of radiation by introducing a quality factor. Parts of the body that are very sensitive to radiation have a higher multiplication factor. For the sake of generalization, in this instance the quality factor is equal to 1. This makes 1 Gray equal to 1 Sievert, or .01 Rem.

For this model, the gamma rays start at a point source 0.5 meters away from a lead shield. The shield attenuates the gamma rays by an amount dependant on the shield thickness, and the remaining rays interact with a water based target, similar to a human being. The initial activity of the source is $6.8*10^{15}$ decays per second, and the allowable exposure limit is 5 Rem/year.

Based on these inputs, the thickness of a lead shield would have to be 34.08 cm to get the exposure down to the necessary levels. At 11.35 $g/cm^3$, a shield the diameter of the core (21 cm) would have a mass of 133.97 kg. The extra shielding mass makes Sr90 a rather unattractive fuel source, but may still be used for small systems that cannot afford $PuO_2$ fuel.

However, it may be beneficial to investigate the effect of the LiH core as a shielding mechanism, as well as include proper Bremsstrahlung energy distributions to improve upon these assumptions. For systems that are particularly resistant to gamma irradiation, strontium-90 may yet be a viable candidate; however, analysis of shielding effects of the complex geometry and unusual materials are beyond the scope of this study.

Work has recently been done for nuclear rocket applications in the area of matrix encapsulation of radioactive materials. In previous nuclear rocket designs, the uranium of the core was trapped in a graphite matrix, creating fuel rods. Sometimes the cladding on these rods would chip away, resulting in radioactive exhaust. Due to this, research into other methods of encapsulation has given rise to a high temperature tungsten based matrix to hold the material. When it is coupled with a radioactive oxide, it is referred to as a cermet (ceramic-metal) material. cermet fuel rods have very high strength and are very adept at keeping the encapsulated material within the rod. This makes the danger of radioactive exhaust or distribution during failure much smaller than the old graphite rods. Unfortunately, the heavy tungsten atoms often create more

Bremsstrahlung radiation. Despite this, the tungsten cermet is the preferred method of encapsulation for this project, largely for its robustness and universality.

Another shortcoming of radioisotope power is the decrease in total power output over time. Although radioisotopes are much longer lived than other sources of energy, when the long mission lengths are taken in to account the decay of the source becomes non-trivial. The power output of the source will begin to drop immediately after the isotope is formed, and there are two methods to account for this in design; either oversize the system so the core always has enough power to recharge over the same interval, or take in to account the slowing of the charge times. Because the charge times directly affect the transit times, it was decided that the system should be overcharged to the point that it can reach its destination before the core begins to extend its charging times. Therefore, the power production needed was found in order to maintain a specific repetition rate, and sized accordingly to be in excess at the beginning of the mission.

As an example, a 60 MJ core requires 1104 W of thermal power to charge in time to fire once per day. A cermet fuel rod with 3 kg of $PuO_2$ would produce 1200 W at the beginning of the mission. The graph below shows the cutoff point where the required power and produced power meet. For transit times to the left of this point, there will be no delay, but for times longer than that, the craft will begin to slow. For this example, the cutoff time is ~10 years.

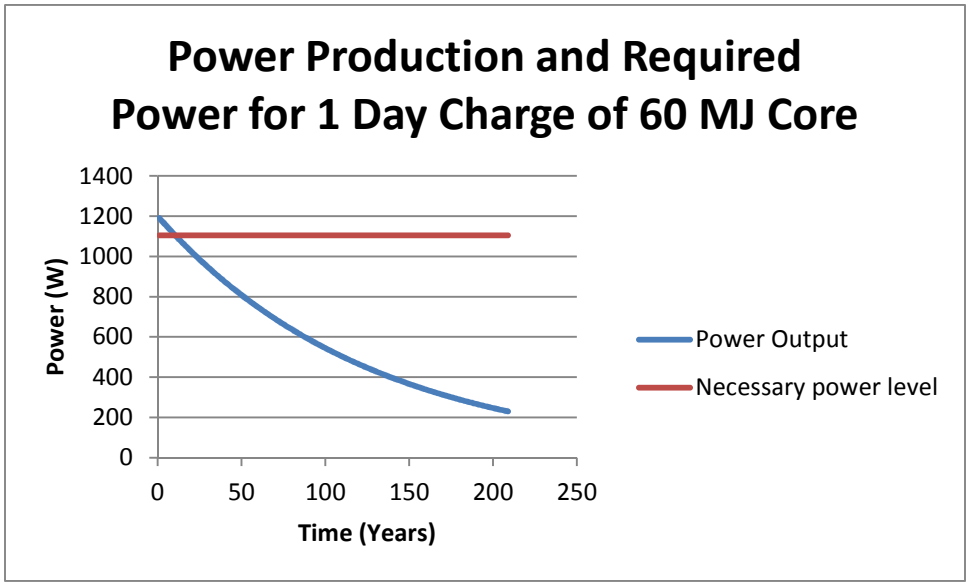


Figure 16: Decay of power production and power requirements

The figure above shows how the amount of power produced above the minimum can often be a small fraction of the total lifetime of the isotope. Although the system may keep functioning for decades, it must make its transit relatively quickly.

### 3.5 Core Materials

The heat source includes a number of components that work together to form a thermal system which is referred to as the "core." This core is comprised of a solid cermet rod loaded with radioisotope fuel imbedded in a thermal capacitor, which is all surrounded by insulation and supported by a structural assembly. When selecting materials for the core, it is important to consider two major factors: material strength and heat transfer capabilities. Material strength is important because launches can induce vibrations and forces many times that of earth's gravity. At high temperatures, many materials will lose their strength, and if they deform the system will not function properly. The heat transfer of materials is important because many different components will be operating at different temperatures. The core, for example, will stay at temperatures greater than or equal to 900 K throughout the mission duration. The satellites and scientific systems, however, will need to stay relatively cool. Many electrical components should not exceed 350K to work properly. Because of this, insulation and heat exchangers play an important part in the design of the system. Different types of insulation/structural materials can be seen below, each with their own strengths and weaknesses. Although other options for these materials exist, the four most promising options were found to be carbon aerogel, silica aerogel, zirconia, and pyrolytic graphite.

#### 3.5.1 Carbon Aerogel

Carbon aerogel is a relatively new material made of a very thin walled carbon matrix filled with a large fraction of void spaces. It has a very high operating temperature, high thermal resistivity, and a very low mass. However, it is not particularly strong and cannot be used as a supporting structure.

#### 3.5.2 Silica Aerogel

Silica aerogel is similar to carbon aerogel, but comprised of a silica foam instead of carbon. It is often lighter than its carbon counterpart, but melts around 1600K, so very high temperature operation is not feasible.

### 3.5.3 Zirconia

Zirconia also has a relatively low thermal conductivity, although not quite as low as aerogel. The major benefit of zirconia is its strength and ability to be used as a structural component. Although brittle and prone to chipping, properly treated zirconia can be quite strong. Unfortunately, it also contains oxygen, which at high temperatures tends to attach to other materials and cause oxidation. If zirconia was directly in contact with the metal housing of the core, it could cause embrittlement in the core and possibly cause a rupture.

### 3.5.4 Pyrolytic Graphite

Pyrolytic graphite is another carbon based material, but instead of using a matrix of void spaces to reduce heat transfer paths it relies on the flat structure of graphite. The graphite molecules are oriented in such a way that they line up and form very small layers. Along the horizontal paths of these layers, the heat transfer rate is actually quite high. But when trying to cross the layer boundaries, it acts as a very good insulator. If the graphite can be properly oriented to slow the heat transfer, it can act as a primary insulator that can safely contact the core, provide strength, and stop the majority of heat from escaping through the mounting system.

## 3.6 Geometry

The geometry of the core is designed so that the working fluid blows down through the axis of the craft and has its hottest point near the exit of the core. The actual core itself is comprised of a hollow cylindrical canister with small flow channels running axially down it. Alongside the flow channels, and inside is a radioisotope fuel rod to heat the system. Initial approximations of flow channels were 100-200 flow channels with a diameter of 2mm each, and a single fuel rod in the center of the system. Inside the canister is the mass of PCM material. The top and bottom of the canister are held tightly by Pyrolytic graphite caps with the thermally resistant direction pointing away from the core. Pyrolytic graphite feet are also in contact with the sides of the canister, with the resistive direction pointing radially away. The graphite components are held in place by a steel frame that keeps the whole system in compression. Filling in the remaining spaces is carbon aerogel, which helps to reduce heat losses from exposed surfaces in the form of thermal radiation. The end result is a cylindrical PCM core, surrounded by layers of insulation and held in compression by a metal frame.

The material of the canister will be required to withstand the high temperatures involved with the molten core. This temperature is dependent on the PCM used. For silicon, a refractory metal such as tungsten or tantalum is necessary. Tungsten is somewhat difficult to machine due to its high hardness value. Tantalum is much easier to machine, and will make fabrication of the canister much easier. Both tantalum and tungsten are also difficult to weld due to their high melting temperatures [81] [82]. Stainless steel may be used for lower temperature applications; however the long duration of the mission may give in to long term effects and warp flow channels or container dimensions. Without in depth analysis of the long term performance of different types of steels, their use is not recommended.

## CHAPTER 4: Modeling the Core

The modeling of the core was done in COMSOL, a finite element analysis program that has the capability to model heat transfer and structural aspects. In order to form a baseline model, the preliminary modeling was done with some assumptions made and with a minimum of non-critical components. It had a completely homogeneous core that was designed to mimic the PCM core as well as the housing. The flow channels were enlarged to reduce computation time, which made parametric sweeps feasible. The insulation was made up of 100% zirconia, which would be incredibly heavy in a real world application.

This model of the core allowed for the rapid change in parameters and a better understanding of the transient nature of the core. Total time to reach operating temperature, maximum temperature, melting times, and surface losses could all be found while simultaneously varying the geometry of the system. While the accuracy of this model was not particularly high, it did show the basic nature of the system.

Once flow channel lengths were determined and mass became more of an issue, the model was reconstructed to better reflect the system. The zirconia insulation was replaced with aerogel in areas where no structural support was required, and with Pyrolytic graphite in places where it was. The flow channels were also adjusted to be much smaller and much greater in number. The model operated as expected, although calculation times were greatly increased.

The support structure was then added to better show the heat transfer path of the escaped heat to the heat sink. The ends of the supports were set to a constant temperature of 300 K, simulating the housing of the spacecraft. This assumes that the craft is capable of rejecting any waste heat in order to reach this operating temperature. The final result of the baseline core can be seen below.

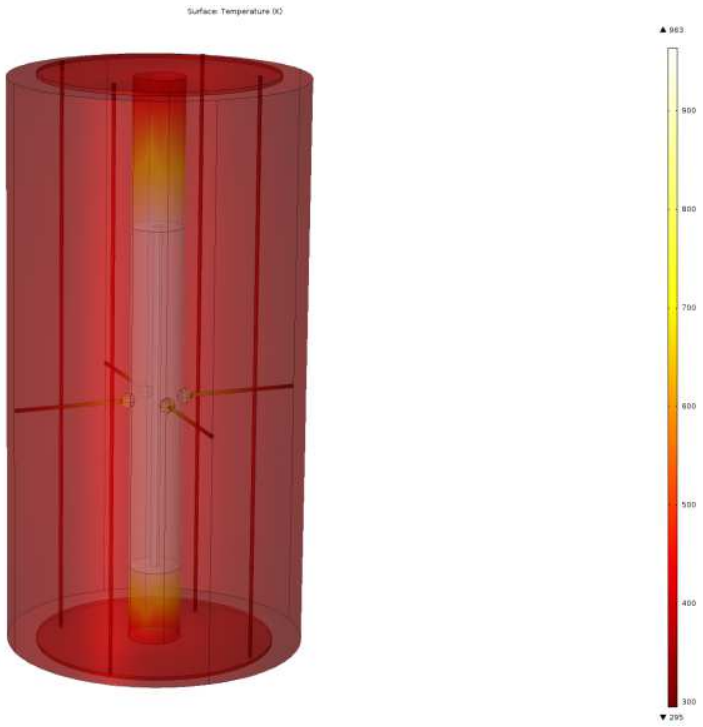


Figure 17: FEA model of hot core with structural supports (max temp 963K)

The main focus of the core model was to find the steady state heat generation rate at the melting temperature. When the core reached the melting temperature of the PCM, the amount of heat being generated by the fuel was recorded. It stands to reason, that at this temperature all of the heat being generated by the fuel is also escaping the system, as it is steady state. Therefore, if the temperature of the core stays the same but the heat generation is increased, it must be traveling into some sort of heat sink. In this case, the latent heat of fusion of the material is absorbing the excess heat. Once the core is completely melted, the temperature of the core will once again rise. To better illustrate this concept, refer to the diagram below.

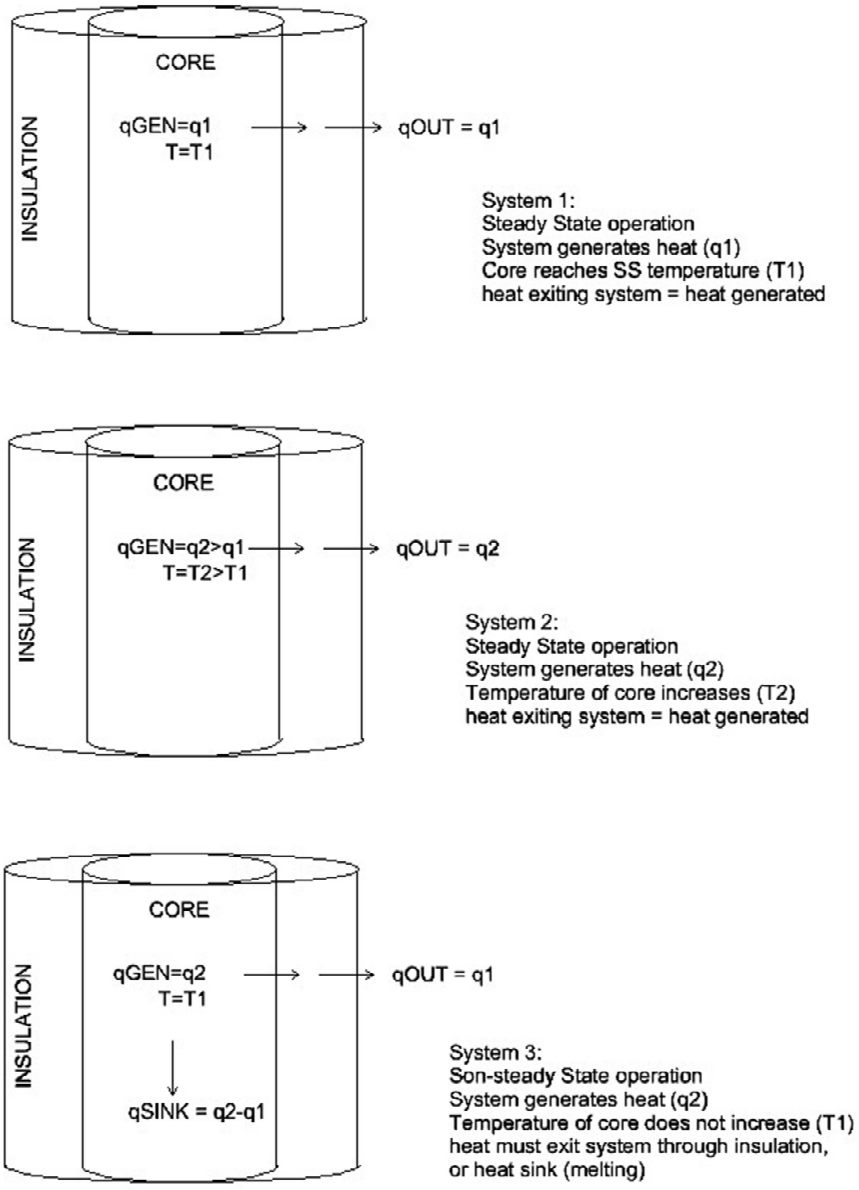


Figure 18: Diagram of heat loss mechanisms from the core

Based on this idea, the heat lost at temperature could be found, and the heat input to the core found. Along with the total energy needed to melt the entire core, the heat up time could be found. With the PCM core holding 30 MJ of thermal energy, it only took ~9 hours for the core to become completely liquid. Increasing the size of the core to 60 MJ allowed for a ~20 hour heat up time, which corresponded more closely to the planned rate of fire of once per day. Because the system is designed for high temperature use, there extra four hour buffer zone will not damage the system and will allow for a slight margin of error. This conclusion was then verified by FEA modeling as well, and found to be accurate.

The FEA modeling of the melting core was performed with a 2-dimensional system, complete with flow channels and a single solid fuel core. The temperature of the system was started at 960 K and allowed to heat up until it reached 965 K. At that point, the equation for heat capacity was altered to allow for the melting of the system. The model would require 2582 kJ/kg to further increase the temperature of the core. This simulated the melting of the core. This model did not take in to account the volumetric change of the melting core, and if small voids form they may detrimentally effect the performance of the system.

The computational results of the final model are below.

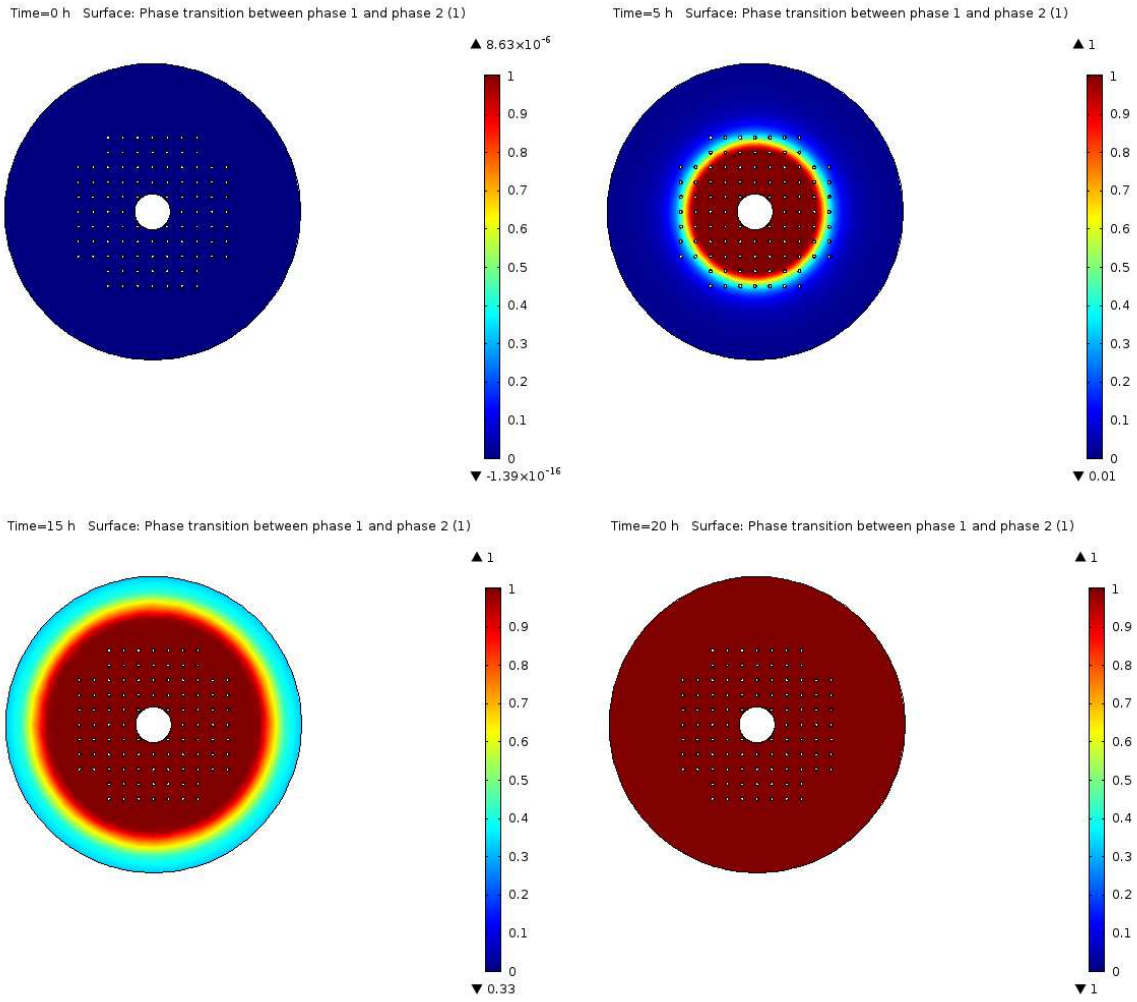


**Figure 19: Melting of PCM core due to center fuel rod. View is from the top.**

# CHAPTER 5: Power Cycle

## 5.1 Overview

The power cycle is designed to gather the heat from the radioisotope in the PCM core until it is completely molten, and then extract the stored heat with a working fluid to create electrical power. The power cycle was originally designed for one 6 minute burn per day, but based on the analysis of the LiH core, it was discovered that more core mass was needed to match the 1/day duty cycle. The power cycle was then designed to operate once per day for 12 minutes, using a 60 MJ capacitor. During the downtime, the core will recharge with thermal energy and the waste heat absorbers will dissipate the waste heat from the power cycle.

Rankine cycles, or steam cycles, operate by taking advantage of the huge change in volume of a working fluid as it changes from liquid to gas phases. The heat source in a Rankine cycle boils the fluid before it flows through a turbine, and as it expands through the turbine it begins to condense slightly. The remaining waste heat is then extracted by a cooling system and the fluid returns to its original state.

In zero gravity systems, the two phase flow of a Rankine cycle can introduce complications because the gas portions and liquid portions do not naturally separate based on their densities. This makes condensation difficult and can damage components if large amounts of liquid merge together and impact turbine blades.

The major problem Rankine cycles face in space is the fact that they need to reject a huge amount of waste heat to return the working fluid to liquid phase. This results in massive radiators, or in the case of pulsed power systems, increased absorber mass. By comparison, the major loss factor in a Brayton cycle is the compressor that uses a large fraction of the produced energy to prepare the gas for the heating chamber. Because heat rejection in space is such an obstacle, and two phase flow can cause issues, Rankine cycles are rarely considered for power space environments.

Because of the complications of two phase flow and the desire to keep radiator masses down, a Brayton cycle was selected as the preferred method of power generation. Brayton cycles use a gaseous working fluid only, which expands when heated. The expanded gas forces itself through the turbine to generate electricity.

Other possible power generation methods include thermoelectric conversion, thermo-photovoltaic conversion, or a Stirling cycle. Thermoelectric conversion is currently used for RTGs, but has a very low efficiency and a rather high mass. This is due to the system being comprised mostly of metallic parts, which in large quantities tend to become quite heavy. Thermo-photovoltaic conversion is usually most efficient at temperatures above 1500 K and would require the removal of the aerogel insulation to allow the radiated heat to escape. Neither the thermoelectric or thermo-photovoltaic conversion methods are designed to start and stop rapidly, so a pulsed 25 kW system would still require the full mass of a 25 kW continuous system. Stirling engines have reliability issues, and are often difficult to start. The inherent disadvantages of the Stirling engine can be seen in the now cancelled ASRG program by NASA and the fact that very few commercial power plants use Stirling engines.

## 5.2 Working Fluids

Selecting a working fluid for the power cycle is an important part of determining state points and performance. Some fluids to consider are hydrogen, xenon, helium, and carbon dioxide. A helium xenon mixture is often used as a working fluid. However, mixtures may leak at different rates over long missions due to different atom sizes, and so the elements were analyzed independently. Hydrogen is a common propellant for thermal rockets, which warranted its inclusion in possible working fluids. Carbon dioxide as a supercritical fluid is also used in more advanced power cycles based on unique aspects of its supercritical state. Air was eliminated as a possible fluid due to the presence of oxygen and the fact that it is comprised of many different types of elements.

### 5.2.1 $CO_2$

Supercritical $CO_2$ is a relatively new area of research for power cycles, because the fluid behaves in some ways like a liquid and in some ways like a gas. When heated, it experiences a very large change in volume, which can be very beneficial. However, the introduction of oxygen to the system can be very dangerous considering the high temperatures and threat of oxidation. Ellingham diagrams are useful in determining the state at which molecules prefer to exist at certain temperatures. The lowest line on the chart determines the most likely molecule to be formed. The lines above perform their conversion in the reverse direction from the arrow in order to maintain the proper balance. For tantalum, the metal prefers to oxidize at nearly all temperatures. This would not only mean that the canister containing the PCM was becoming more brittle, but that the

CO2 was losing Oxygen and becoming either C or CO. For Tungsten, the metal will oxidize at temperatures below 1000 K. At temperature above 1000K, CO2 is not the most stable form for the gas, and it will try to convert to CO. This would leave a free Oxygen atom available to possibly oxidize the exposed metal [77].

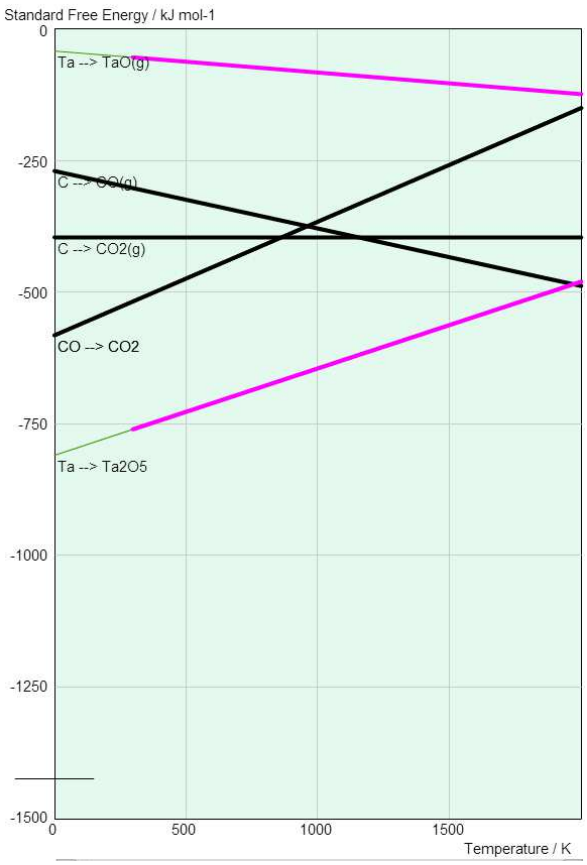


**Figure 20: Ellingham free energy diagram of tantalum VS CO2. $Ta_2O_5$, being the lowest line, is most likely to be formed at nearly all temperatures. [77]**

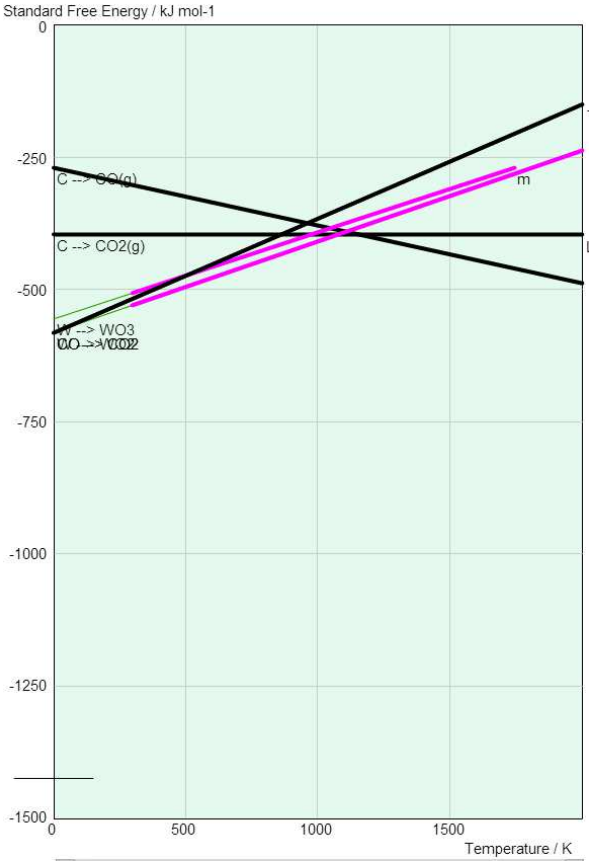


**Figure 21: Ellingham free energy diagram of tungsten VS CO2. The lowest line shows which compound is most likely to be formed at any temperature. [77]**

Because of the danger of oxidation and the fact that supercritical CO2 is not as established as a working fluid in zero gravity, it was eliminated as an option.

### 5.2.2 $H_2$

Hydrogen is a possibility for the working fluid, the major benefit for this would be that a system using thermal propulsion would probably use hydrogen as a propellant anyway. This would allow the thermal mode and electric mode to possibly share the same fluid. However, if the initial thermal tank was jettisoned after use, a separate tank would be necessary regardless.

Using Hydrogen would not introduce the oxidation problems present with $CO_2$, and if there was no oxygen present in the system the risk of combustion would be minimal. The state points of Hydrogen are also quite well known, and it would have the benefit of being a well established fluid.

One issue with Hydrogen would be the possibility of leaking over the course of a long duration mission. The small size of the hydrogen molecule is often difficult to stop from leaking out through seals over time, and the hydrogen reserves would deplete long missions. This would require the use of an increased reservoir size to make up for lost fluid during transit.

### 5.2.3 Xe

Xenon is another possible fluid, and without the high propensity to leak. The atom is much larger than hydrogen and is more easily contained. The electric thrusters are also designed to run on xenon fuel, so in some instances the tanks could be shared. Because the power cycle will be running the electrical systems, it makes sense to use the same fluid so excess fuel can be used to make up any losses for leaks. Unlike the hydrogen tanks in the thermal cycle, the xenon tanks will travel with the craft for the duration of the mission.

## 5.3 Final configuration

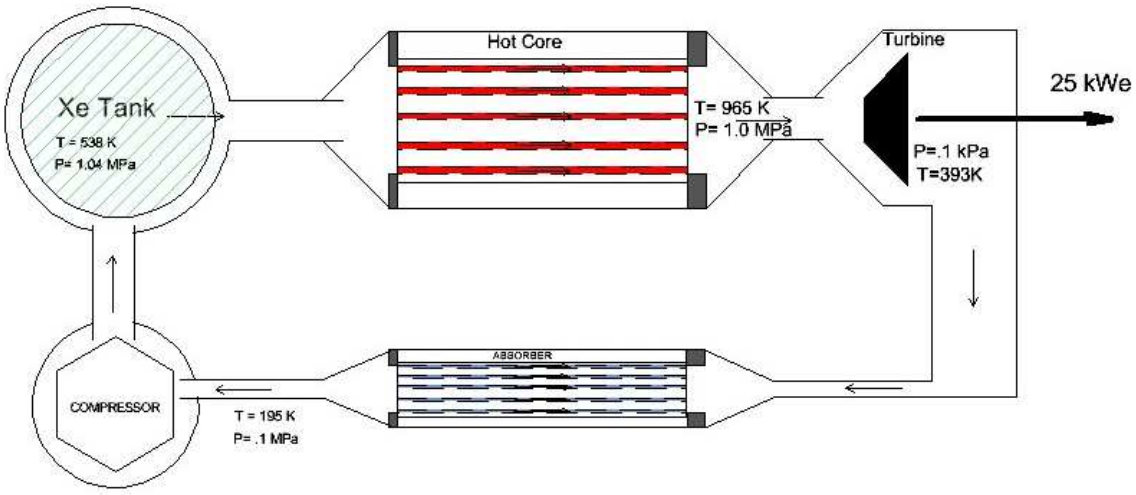


Figure 22: Final Brayton cycle diagram for power conversion

The PCM core is designed to be filled with lithium hydride (LiH), which has a high latent heat of fusion and a melting temperature of 965K. Research into common power cycles suggests that the pressure ratio between the high pressure and low pressure sides can vary, but generally speaking a

higher pressure ratio results in higher cycle efficiencies [71]. Conversely, a higher pressure ratio also usually increases the mass of the compressor, which is space applications can have a detrimental and costly effect [72]. Because of this, a compression ratio of 10:1 was used, which is within the range of existing devices [73].

The working fluid is pure xenon because Xe is also the fuel for the electric thruster, so lost fluid can be recovered. In many Brayton cycles, including some He to increase thermal conductivity if often done [74]. However, the mission may last >15 years [75], so leaking He through seals may be a problem due to its small molecular size. Hydrogen is removed from the list of possible fluids because of this as well. Pure xenon is also used in the electric propulsion system, so there will be a tank of compressed xenon on board that can be used to refill the fluid in the cycle if necessary. This makes pure xenon an ideal working fluid for this system.

The Initial and final pressures are based largely on the available data and the compression ratio of 10:1; resulting in a low pressure of 0.1MPa and a high pressure of 1.0Mpa. A common operating pressure for terrestrial systems is 2Mpa [76], so the 1.0Mpa max pressure should be within the bounds of a feasible system.

Efficiency and values for components were provided by turbine manufacturer CREARE Engineering [62].

Table 3. Brayton cycle efficiencies

| | |
|---|---|
| **Absorber pressure increase (assumed)** | 4 kPa |
| **Core pressure decrease (assumed)** | 4 kPa |
| **Compressor efficiency** | 0.85 |
| **Turbine efficiency** | 0.88 |
| **Alternator efficiency** | 0.98 |
| **Motor efficiency** | 0.98 |
| **Dc to AC** | 0.97 |
| **Ac to DC** | 0.97 |

The temperature into the compressor is determined by the waste heat absorbers. PCMs will be used here as well in order to level the power requirements of the compressor. If the absorbers were to operate over a range of temperatures, the compressor would require more power to compress the hot gas as the temperature increased. This would reduce the amount of net power produced by the system as the cycle ran, which would be detrimental to components. Using a frozen ammonia absorber limits the max temperature to 195K, which sets the compressor inlet state to 195 K and .1 Mpa. To achieve the desired electrical power output of 25 kWe, a mass flow rate of 1.33 kg/s must be maintained.

Values for xenon properties were taken from Sifner and Klomfar [78], and extrapolated/interpolated where necessary. The major source of error in this method is in the extrapolation from the maximum recorded temperature data of 800 K to the hot temperature of the system, 965 K. The values were calculated using a linear extrapolation of the existing data. Although the actual values of enthalpy and entropy may change slightly in a real situation, the variance is expected to be small enough that the system should still function as designed.

The optimization of the Brayton cycle was done by making calculations at different operating pressures and comparing the results. Pressure ratios of 5, 10, 15, and 20 were used while the hot and cold temperatures remained constant. By performing these permutations, it was seen that the pressure ratio of 10 provided the highest efficiency. One difference between this cycle and a more common coal or gas fueled cycle is the constant hot side temperature. In a combustion fueled cycle, the working fluid exits the compressor at a certain temperature, and is then heated by the combusting gas. If the fluid exits the compressor at a low temperature, the combustion heats it to the desired levels. If the fluid exits at a higher temperature (due to higher compression ratios), the combustion can still heat the fluid to even higher temperatures. With a core-driven cycle, higher compression ratios can be detrimental because the fluid can only be heated to the core temperature. If the fluid exits the compressor at a low temperature, it can extract a large amount of energy from the core, but if it exits at a high temperature the core cannot increase the temperature by as much. This drives the design of the cycle towards lower pressure ratios.

A T-S diagram of the system can be seen below.

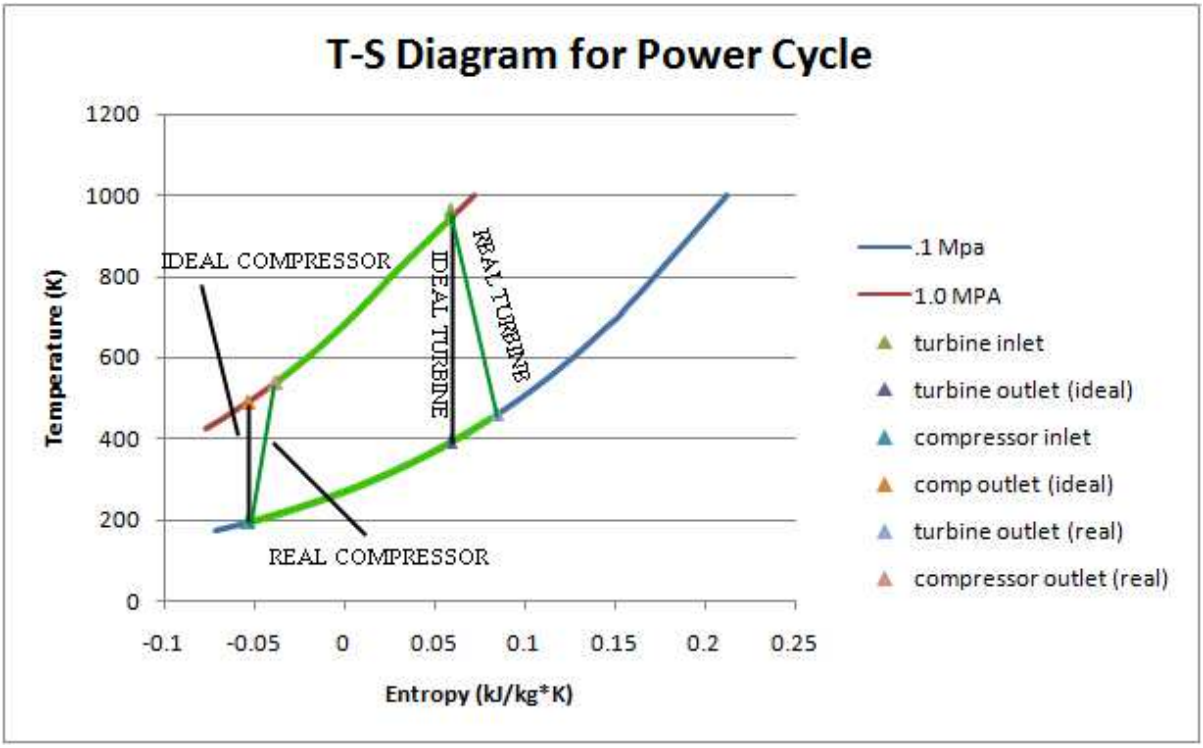


Figure 23: T-S diagram for Brayton cycle of pulsed power system

With the state points of the cycle determined, and the required power generation conditions met, the fluid analysis can be done on the flow of gas through the core.

# CHAPTER 6: Flow analysis

The dimensions of the core are important to the heat transfer capabilities, and the length of the flow channels must be long enough to effectively heat the working fluid. Based on a LiH core, the flow analysis of the working fluid through the core is as follows.

## 6.1 Diameter/Length Considerations

One of the major driving factors, as mentioned previously, is the size and geometry of the flow channels through which the working fluid flows to extract heat. As with most internal flow systems, a larger channel diameter often results in increased mass flow rates and decreased frictional losses. However, the ratio of surface area to volume also decreases, so the flow is less effective at removing heat from the walls of the core. In order to avoid a series of recalibrations, the flow channel geometry must be determined as early as possible.

One important aspect of the flow analysis whether or not the "lumped sum capacitance" model holds true. This model assumes that the heat transfer rate within the solid part of the material is much higher than the heat transfer rate of the fluid flow along the walls. Therefore, the temperature inside the solid area can be assumed to be relatively constant. This removes the need for complicated calculations regarding the temperature profile inside the material, and instead allows for an analysis focusing on the convective flow characteristics.

The lumped sum capacitance model is assumed to be valid in the cases where the Biot number is less than 1. The Biot number relates the heat transfer rate of the working fluid to the heat transfer rate of the solid material. If the material conducts heat much quicker than that gas, it can be assumed that the temperature profile within the solid is uniform. The Biot number is given below [79].

$$Bi = \frac{h*L}{k} \tag{10}$$

Where Bi = Biot number, h = Convective heat transfer coefficient. L = Characteristic length (in this case, diameter), k = conductive heat transfer coefficient of the solid material.

Because the diameter of the channel is one of the parameters that remains to be found, the Biot number should be checked to ensure that the lumped sum capacitance model holds true once the geometry is determined. For now, as assumed value can be used to see on what scale the Biot

number falls. The thermal conductivity of lithium hydride at the melting temperature is roughly 4.0 W/m*K [80]. The tantalum shell, however, has a thermal conductivity value of 57.5 W/m*K [81], but a very small thickness of 1mm. As the LiH is the limiting factor, it will be used to calculate the Biot number. Assuming the channel is on the order of .002 M wide, and the convective heat transfer is around 1400 W/M2*k (which will be shown later), the Biot number has a value near 0.7. Therefore the model should hold true, although it is somewhat close to the limiting value of 1.

With the characteristics of the power cycle determined in the previous section, state points can be used to calculate flow characteristics of the fluid.

The analysis of the flow through a flow channel is modeled by a considering only one flow channel and adapting the results to the array of flow channels (roughly 100) inside the core. The channel temperature is assumed to remain constant, which holds true if the Lumped Sum Capacitance model is valid, IE the Biot number must be < 1. The channel temperature and inlet temperature were determined by the state points found in the design of the power cycle in the previous chapter. The flow channel length will vary as the diameter changes in order to achieve the desired exit temperature.

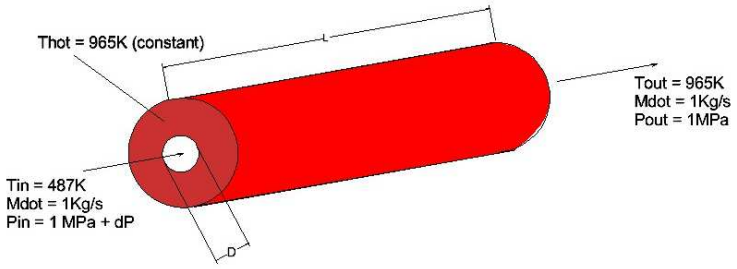


Figure 24: Single channel model

In order to determine the convective heat transfer coefficient for the channel, empirical correlations must be used. Many correlations exist based on the nature of the flow channel. Some are more accurate for laminar flow, some are accurate over small temperature changes, and some work best for very smooth surfaces. For this application, the channel was treated as a very smooth internal flow surface with fully developed turbulent flow and forced convection.

The Gnielinski correlation was used to find the average convective heat transfer coefficient, based on the parameters of the channel. With this correlated value and the total amount of energy

required to heat a volume of the working fluid from the cold to hot temperatures, the necessary surface area can be found. From that point, the values of length and diameter can be found.

The Gnielinski correlation in its simplest form is given by equation 11 [83], and is valid for situations when Re > 3,000 and .5 ≤ Pr ≤ 2,000. The Reynolds number is given in equation 12 [79].

$$Nu = \frac{\frac{f}{8}*(Re-1000)*Pr}{(1+12.7*\left(\frac{f}{8}\right)^{\frac{1}{2}}*Pr^{\frac{2}{3}}-1)} \quad (11)$$

Where f = Darcy Friction Factor, Re = Reynolds number, and Pr = Prandtl number. The surface of the flow channel was determined to have a relative roughness of .00125, resulting in a friction factor of .023 for 2mm flow channels.

$$Re = \rho * V * L/\mu \quad (12)$$

Where Re = Reynolds Number, L = Characteristic length (Diameter), $\mu$ = Viscosity, V = Velocity, and $\rho$ = fluid density.

The Prandtl number is given by equation 13 [79]:

$$Pr = \mu * Cp/k \quad (13)$$

Where Cp = Specific heat at constant pressure, $\mu$ = Viscosity, and $k$ = Thermal conductivity.

In order to find the thermodynamic properties of the fluid, a temperature value must be determined. For this, the Log Mean Temperature Difference (LMTD) is used. The LMTD value can be found by equation 14 below [79].

$$\Delta Tlm = \frac{\Delta To-\Delta Ti}{\ln(\frac{\Delta To}{\Delta Ti})} \quad (14)$$

Where $\Delta To = T_{hot}-T_{out}$ and $\Delta Ti = T_{hot}-T_{in}$.

Although the exit temperature of the gas will never reach the temperature of the wall in theory, reaching within 0.2% will be used as an acceptable approximation for reaching the full exit temperature. With this in mind, a LMTD of 86 degrees K is found, and the temperature used is 86 degrees below the hot temperature, or 879K.

With the mass flow remaining constant at 1kg/s, the maximum velocity of the gas can be found by using the thermodynamic properties of the gas at the exit condition. The density of Xe at 879K and 1Mpa is .0186 g/cm3, or 18.6 kg/m3, found by extrapolating data recorded from thermodynamic tables in citation [25]. With this information, the maximum velocity can be found by equation 15 below [79].

$$V = \frac{Mdot}{A*\rho} \tag{15}$$

Where Mdot = Mass flow rate in one channel, A = Cross sectional area, and $\rho$ = Fluid density.

For an assumed channel diameter of 2mm (based on NERVA program dimensions), the resulting maximum velocity is ~171 m/s. To determine if the flow is turbulent, the Reynolds number is used.

Xenon at 879K has a viscosity of 59.02 μ Pa/s [84]. By using the values of density and viscosity at the log mean temperature, a Reynolds number of 107,865 is found. Thus, the flow is well above the fully turbulent limit of 4,000.

The specific heat for Xe at 879K is found to be 152.3 j/kg*k by extrapolation [78]. The thermal conductivity was found to be .014 W/m*k at 879K, based on the assumption that the changes in pressure would be negligible. Based on these numbers, the Prandtl number is 0.64. Putting the values for Pr and Re into eq. 11 results in a Nusselt number of 261.5.

To find the average heat transfer coefficient for the flow channel the definition of the Nusselt number is used, as seen in equation 16 [79].

$$Nu = h * D/k \tag{16}$$

Where $h$ = Average heat transfer coefficient, D = Channel diameter, and $k$ = Thermal conductivity.

The equation is then re-arranged, and solved for $h$, resulting in an average heat transfer coefficient of 1836.3 w/m$^2$*k.

With this value for$h$, a total contact area can be found by using Newton's law of cooling with an average temperature value used for the flow. To find the average temperature value, the log mean temperature value is used, and can be found by using equation 14 above.

Newton's law of cooling can be seen below in equation 17 [79].

$$q = h * A * \Delta T \tag{17}$$

Where q = Heat rate, $h$ = Average heat transfer coefficient, A = Contact area, and $\Delta T$ = Temperature difference.

The total heat rate can be found for the fluid based on equation 18 [79]:

$$q = Mdot * Cp * \Delta T \tag{18}$$

Where Cp = Specific heat at constant pressure, Mdot = Mass flow rate in one channel, and $\Delta T$ = Temperature difference.

In this case, q is equal to 728 W. Therefore, by rearranging equation 17 the value of A is found to be 0.0046 square meters per flow channel. With the assumed diameter of 2mm, that sets the necessary length of the core to 0.731 meters. However, because this model assumes fully developed flow, there is a region where the flow must initially develop. To account for this change an entrance length of 100 times the channel diameter will be used for calculations to allow for flow development, resulting in a total core length of 0.831 m [85][86].

With the properties calculated, it is important to check that the original assumptions are still valid. For the cases of 100 flow channels of diameter of .002m, the Reynolds number 107,865, the Prandtl number is 0.64, and the Biot number is 0.718. All of these values are within the ranges of the correlations used, so their results remain valid.

It is also important to understand the possible variances in the configuration in the event that the system parameters change. To approximate the upper and lower bounds of this system, the hottest temperature and the coldest temperature state points can also be used to show the possible range of core lengths. If the hottest temperature is used, the core length decreases to 0.814 m. If the coldest temperature is used, the core length increases to 0.883 m. Therefore, if the temperature changes in a manner not expected, the core length may change by up to 8%.

### 6.2 Mach Number

When fluids travel faster than the speed of sound in the fluid then certain aspects are changed. The ratio of the fluid speed over the speed of sound in the medium is known as the Mach

number. Nozzles may switch from a converging design to a diverging design, diffusers are changed in an opposite manner, and some assumptions about heat transfer and fluid flow no longer hold true. Therefore, it is important to know the speed at which the fluid is traveling, and what the speed of sound in the fluid at that state is.

In this case, the fluid is traveling at high speed through the core at 171 m/s and the coldest temperature it will be traveling at is 487 K. The speed of sound in a medium is faster with higher temperatures, so the high speed and coldest temperature will provide the upper bound for the Mach number, which should remain less than 1 so stay subsonic.

The speed of sound in a gas is given by equation 19 [87].

$$c = \sqrt{\gamma * R * T} \tag{19}$$

Where c = Speed of sound in the medium, $\gamma$ = Ratio of specific heats, R = Specific gas constant, and T = Absolute temperature.

For xenon at 487 K, the speed of sound is calculated to be 936.6 m/s. With the maximum speed of the fluid being 171 m/s, the Mach number is found to be 0.183. Thus the flow is not supersonic and will behave predictably.

### 6.3 Final Dimensions

The final core will have a length of .831 meters, and each flow channel inside will have a diameter of .002 meters. There will be 100 total flow channels in the core, and the power cycle will produce 25 kW of electrical power when running. This system assumes the channel walls are very smooth and the Gnielinski correlation holds true. Varying the channel diameter while keeping the number of channels constant results in the charts below:

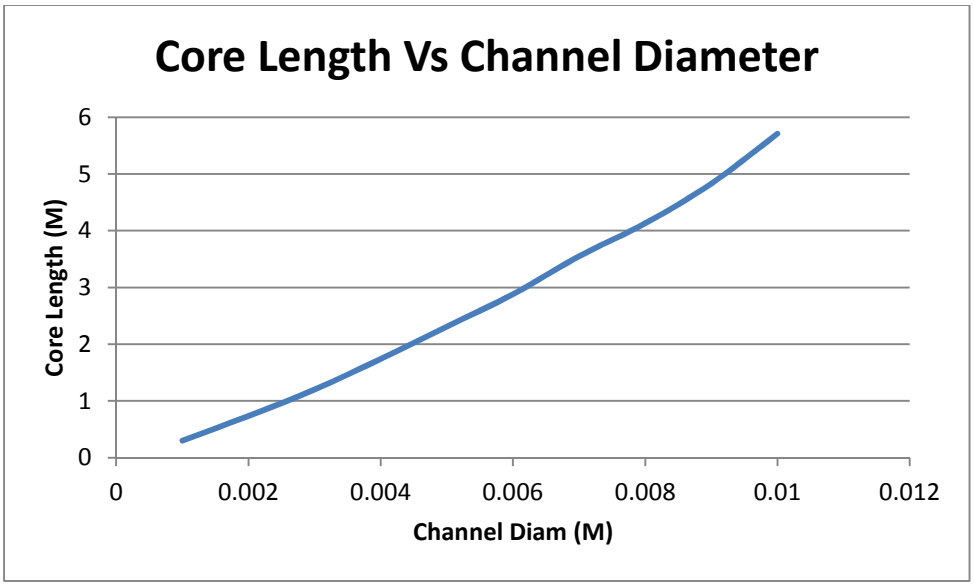


Figure 25: Length of the PCM core as a function of flow channel diameter through the core

Additionally, the number of flow channels may change the length of the core. While holding the channel diameter constant at 2mm, the length of the core changes according to the graph below.

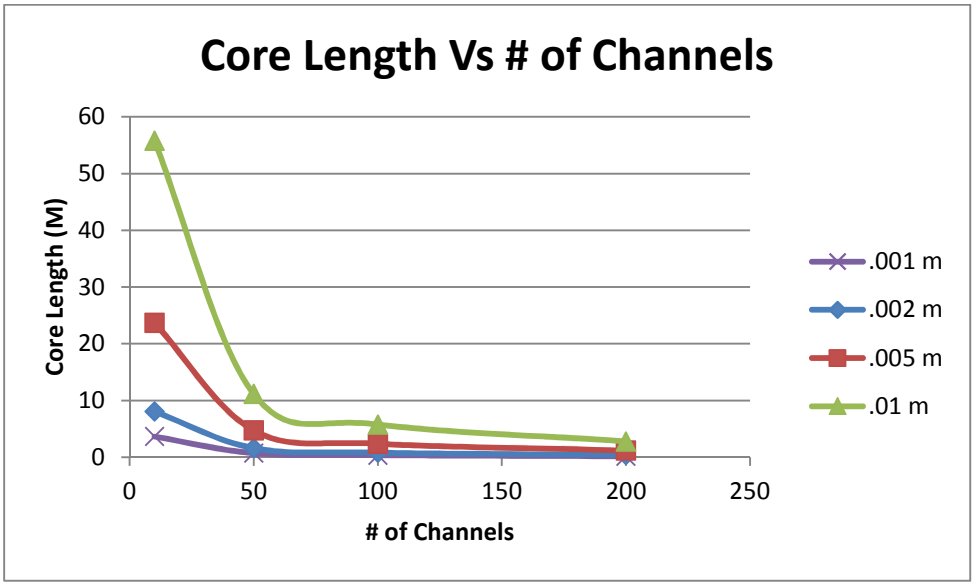


Figure 26: Core Length Vs total # of Channels at different channel diameters

These results suggest that smaller flow channels always reduce the core length, and more flow channels are better. However, head loss, high pressures, and shear stresses may become a

larger factor when dealing with very small flow channels, and so remaining at or above a diameter that has been shown effective in the NERVA program was determined to be reliable. Additionally, manufacturing numerous channels will be much more difficult as the diameters shrinks. Due to these factors, it is assumed that 100 channels of 2mm diameter channels is an acceptable configuration.

This process can be repeated for other PCMs, such as silicon, and other working fluids, such as He. Unfortunately, the different characteristics of the PCMs and working fluids make the power cycle difficult to standardize, and a new cycle must be built each time. Because of this, it is important to reduce the number of possible materials involved early on.

# CHAPTER 7: Absorbers

The waste heat absorber of the power cycle is an important aspect because it removes the need for large radiator systems, which often significantly add to the mass of a spacecraft. The absorber/radiator mass is dependent on two aspects: the amount of waste heat required to store and the desired repetition rate. Based on the latent heat of fusion of the material, the mass of the PCM material is relatively easy to calculate, as seen below in equation 20 [79].

$$m = \frac{Q}{h_f} \tag{20}$$

Where m = Mass of PCM in absorber, Q = Waste heat. and $h_f$ = Heat of fusion of PCM

The other aspect to the heat rejection system is the rate at which it can reject the heat by radiative means. This is dependent on the melting temperature of the PCM and the exposed surface area. For systems with low recharge times and low power, the surface area of the canister containing the absorber PCM may be sufficient to reject the heat before the next cycle starts. However, if that is not the case, radiative fins must be added to the absorber to increase the surface area. To determine the required total surface area, equation 5 can be used. It is worth noting that as the repetition rate increases to the point of a continuously running power cycle, the radiator size approaches the large size of a traditional space power system. This effectively removes the benefits gained from the pulsed power system. However, a reduced duty cycle also means that the ratio of input power to core material must be reduced, to allow for the core to take time to heat up. The reduction of input power will decrease the performance of the system simply because there is not as much power available.

## 7.1 Current Methods

There is a great deal of research being performed on radiator technologies, due to the fact that they take up so much mass and volume on space missions. Improvements to selective emission, material strength, and deployment strategies are just a few aspects that are involved with common radiators. Lockheed Martin has developed and deployed radiator systems for the International Space Station in earth's orbit [88]. Each radiator unit had a mass of 1120 kg, and an exposed surface area of 147.14 $M^2$, assuming both sides of the radiator were emitting to space. This equates to 7.61 $kg/M^2$; an important metric when dealing with radiators because it equates the mass cost involved to radiator capabilities. Although other radiator systems may vary from this

value, because it has been tried and proven effective the value of 7.61 kg/$M^2$ will be used for comparisons and calculations.

### 7.2 Absorber Design

The absorber system is required to reduce the temperature of the working fluid based on the design of the power cycle. Because of this, a PCM absorber provides benefits similarly to the PCM core of the power cycle. It keeps the temperature constant and can take advantage of the high heat of fusion of materials. Because of this, a PCM absorber was used instead of a solid version.

Frozen ammonia has a melting temperature of 195K, and a heat of fusion of 332.3 kJ/kg [89]. Although the heat of fusion is significantly smaller than other PCMs, it is one of the highest for materials near that temperature range. The low melting temperature is necessary for cooling the exhaust gas, even though it provide a slow heat rejection rate though radiative means.

### 7.3 Modeling results

Based on the previous model of the Brayton cycle using a LiH core and Xe working fluid to produce 25.44 kW for 720 s, the absorbers will need to capture 26.0 MJ of energy. For ammonia, this equates to an absorber mass of 78.24 kg. For the sake of symmetry, the absorbers will likely be split into two equal masses and positioned on opposite sides of the craft. Each unit will have a mass of 39.12 kg. The density of liquid ammonia near the freezing point is 732.9 kg/$m^3$, and like most materials it expands when transitioning from solid to liquid phase [55]. Because of this, the absorber canister must be as large as the volume the PCM will occupy while liquid, or at least .0534 $m^3$. With a core length of 1.58 m, the resulting radius would be .104 m, or 10.4 cm for each absorber.

The minimum length of each absorber should also be investigated to ensure the exhaust can cool to the proper temperature. This process is the same as in the flow analysis, but with the walls cooling the system instead of heating it. By inputting the state points for Xe, it can be found that the absorbers need only 7.6 cm to be cooled to the desired temperature with the same channel loading of the core (100 holes at 2mm diameter each). With the very small diameter of the absorbers, a much more forgiving design of 6-2cm diameter holes in each absorber would require a length of .84 m. This is still a shorter length than that of the core.

Adjusting the geometry of the absorbers to allow for six, 2 cm diameter flow channels increases the total volume to .0564 $m^3$, the radius to 10.7 cm, and the surface area to 1.06 $m^3$ each. Further addition of an aluminum housing to the absorbers adds a 1mm skin, increasing the radius to 10.8 cm, and the area to 1.07 $m^3$.

The surface area available for radiative heat transfer is equal to roughly 3/4 of the cylindrical area of the absorber, assuming a view factor of 1/4 between the absorber skin and the body of the main craft. The ends of the absorber are not counted because they are connected to piping or other components. In this case, the exposed surface area of each absorber is 0.804 $m^2$. Using equation 5 at an operating temperature of 195 K shows that the natural surface areas of the absorbers are able to reject 65.9 W of power each, or 131.8 W total. They need to remove a total of 26.0 MJ of energy, and so they will have to operate for $1.97*10^5$ s, or 2.28 days. This is longer than the recharge time of this core, and so additional radiator fins must be added.

The power level required to reject 26.0 MJ of energy over 86,400 seconds is 300.9 W. Again, using equation 5 the total area required can be found to be 3.37 $m^2$. The absorber housing covers 1.61 $m^2$, so 1.76 $m^2$ of exposed radiator area must be added. At 7.61 $kg/m^2$, this results in an extra 13.4 kg of radiator mass.

The resulting waste heat absorber/radiator configuration is two, 1.58 m long tubes of Ammonia with masses of 39.12 kg each, or 78.28 kg total. Added to that is the aluminum skin and flow channel cladding, which totals 4.68 kg each. Coupled with 13.4 kg of radiator mass, the heat rejection system has a mass of 101.0 kg. Each cylinder has a diameter of 21 cm, and each radiator fin has an edge length extending away from the craft of 55.7 cm. This adds 111.4 cm to the total diameter of the craft. The baseline diameter of the core with insulation for a 6 minute burn once per day is 80 cm, putting the total width of the craft at 191.4 cm. With the fairing of the Minotaur IV being just over 2 m at its widest point, the craft should still be able to fit inside.

This system can be compared to a system that did not use thermal capacitors or a duty cycle in order to better understand the changes in mass associated with it. A miniature Brayton cycle would have different state points, losses, and power generation profiles, so an existing technology is used for comparison instead. For a system powered by a properly scaled MMRTG for continuous power, the device would need to reject 1.125 kW of thermal power. This system would produce 75 W of electric power (a regular MMRTG produces 125 W of electric power from 2 kW of thermal,

the baseline core for pulsed power uses only 1.2 kW of thermal power, so the MMRTG is scaled accordingly). And at the same operating temperature of 195 K, the system would require 13.72 $m^2$ of radiator area, or 104.4 kg. Although this is very similar to the mass of the power cycle system, the benefit from this design comes from the very high power levels and high efficiency of the system.

A continuous 25 kWe system would require much larger radiators, and would be able to supply a much larger amount of total energy. A similar comparison shows that such a system would require nearly 5,570 kg of radiators to operate. Therefore, if a component required 25 kW of electrical power, it would need to be launched on a very large, very expensive mission, or used on a pulsed power system for a small fraction of the cost.

# CHAPTER 8: Switching Modes

## 8.1 Switch Vs Manifold

Switching between thermal propulsion mode and electrical propulsion mode presents challenges due to the high temperatures, long transit times, potential for leaks, and need for long term reliability. If the switch is warped or damage during operation it may render the entire craft inoperable. Magnets or levers may also suffer damage while exposed to high temperature exhaust and cease functioning. If the switch is not completely sealed for the duration of the mission, small amounts of propellant/working fluid may escape. Given that the mission may take years to decades to complete, even a small loss would be catastrophic.

The other option is to design a manifold that would simply keep the thermal system and electrical system in completely different loops. Each system would have access to separate flow channels, thus increasing the number of total channels and core length, but there would be no danger of broken seals or damaged components.

## 8.2 Switch Parameters

The maximum temperature the switch should see would be during the thermal propulsion mode. Using a LiH PCM core, this puts the maximum operating temperature at 965 K. Many materials will weaken at this temperature, especially elastic materials such as plastics. An effective switch would need to operate well within this temperature range. The mechanism may be comprised of tungsten, alumina, or zirconia to resist the high temperatures and provide structural strength. The seal may be comprised of softer materials such as tantalum or rhenium, which would deform to form the seal when closed.

The switch will definitely need to operate once when escaping earth's gravity well and changing to electric production mode. It may also need to switch at the destination in the event that it must rapidly decelerate. However, that option would include carrying a large mass of breaking propellant, and because the trajectory is predicted to be near circular the need for a large breaking maneuver will likely not be necessary. Due to this, it is assumed that the switch will operate only once; when transitioning from a terrestrial to heliocentric orbit. However, the seal will still need to hold for the entire lifetime of the system.

## 8.3 Switch types

A mechanical switching system would operate by using a physical arm or piston to close the exhaust aperture when desired. This method provides a strong, robust capability to the switching system because it can be designed with refractory metals, ceramics, or other high temperature materials. However, thermal expansion, corrosion, or contamination may prevent the moving parts from working as designed.

A magnetic switching system would allow for an electromagnet to penetrate into the rocket nozzle with a magnetic field and move the switch without exposing itself to the hot exhaust stream. This would allow the majority of the components to stay away from the dangerously high temperatures. Still, whatever components were left in the pathway of the exhaust would need to have very high operating temperatures. Even though joints or moving parts would not be as exposed to high temperatures, the actual valve itself may still fail due to thermal expansion or wear.

### 8.3.1 Option 1 – Closing plates

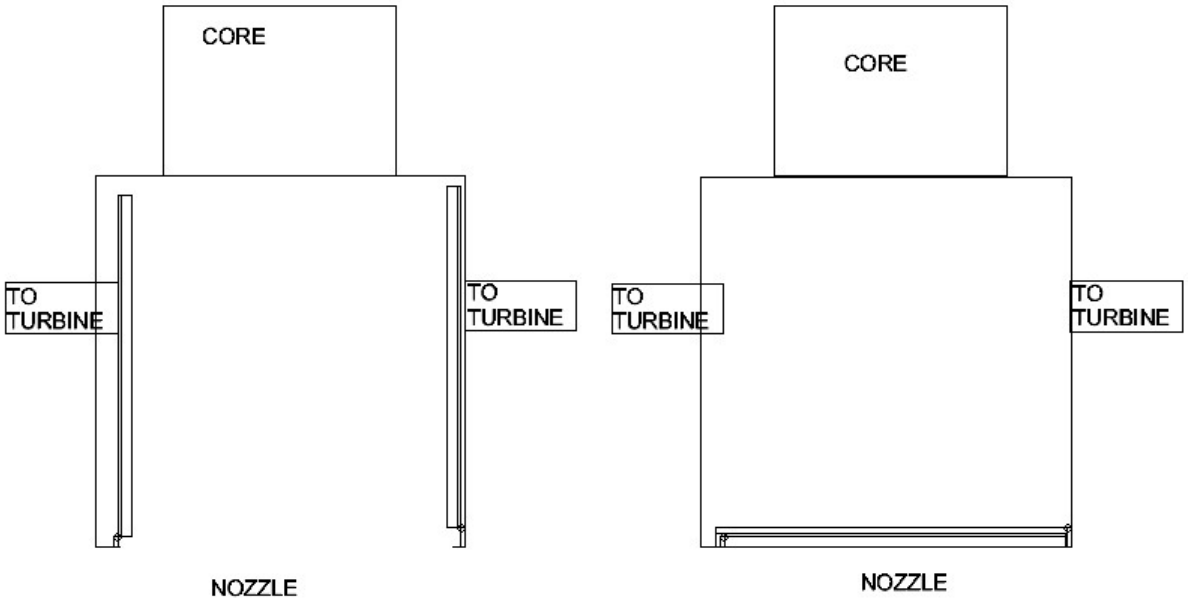


Figure 27: Thermal system (left) converted to electric system (right) by closing plates over the nozzle

The option of closing plates operates by having two hinged platforms initially stacked up against the wall of the exhaust chamber. They naturally cut off the flow to the turbines while in this initial position, and when it is time to convert to electric power mode they are pulled down and cover the exhaust aperture. This design is relatively simple and requires minimal moving parts. It also does not impede the flow of gas through the nozzle.

The downside of the method is the large seal that is formed between the plates and the walls of the craft. The large seal may be hard to maintain, and may easily leak if either plate is warped during thermal firing. Given the geometry it may be hard to apply enough force to keep a good seal. They also run the risk of being caught in the exhaust stream and prematurely closing the hatch if they are shaken loose during launch or from vibrations from firing.

### 8.3.2 Option 2 – rotating disc

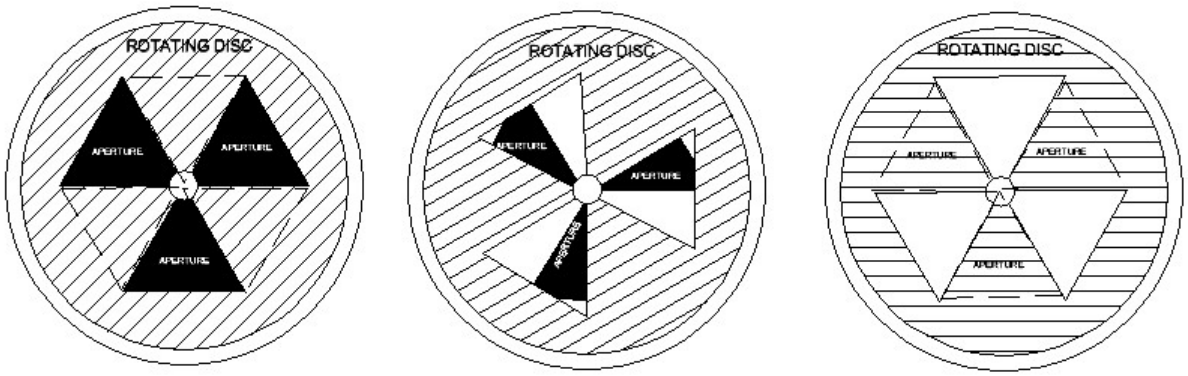


Figure 28: Switching option 2, a rotating disk similar to the flue on a grill

A rotating disc that is spun to close apertures provides another switching method that is less likely to fail during blow downs. It could also be switched back open if necessary. The main drawback to this method would be the fact that a physical arm would need to penetrate into the nozzle to turn the disc, or a magnetic component installed inside the nozzle on the disc. In contrast to the flat plate method, the turbine flow paths would not be automatically blocked, and separate rotating disc systems would be required to close of those channels as well. The disc would also

impede over half of the nozzle aperture even when open, reducing the mass flow and overall effectiveness of the propulsion system.

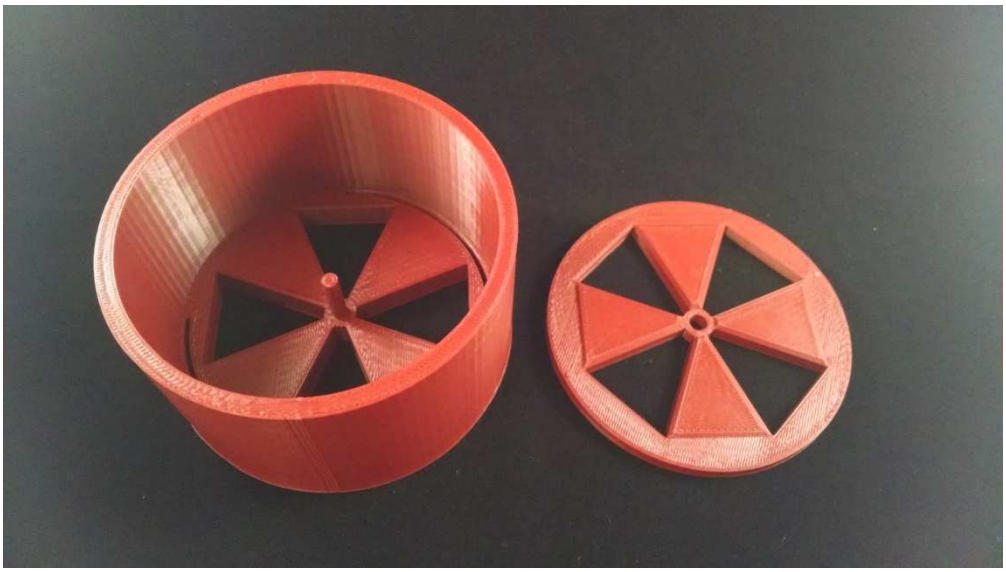

Figure 29: Rotating disc prototype

### 8.3.3 Option 3 – Closing Iris

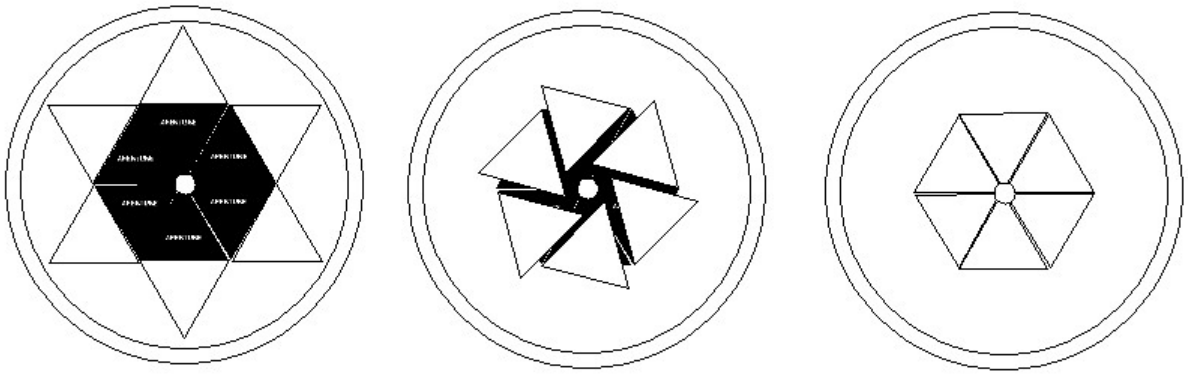

Figure 30: Iris using small, triangular plates to close off flow

Similar to the rotating disc, the closing iris would rotate an impedance in to place in order to seal the exit. This allows for slightly more of the aperture area to be exposed during firing than the rotating disc method, and can still be returned to the original state if desired. The potential for failure in this system is very large due to the small panels and high number of moving parts.

In all the aforementioned switching mechanisms the seals formed by the moving parts have the possibility of failing if the sealing action is not precisely performed. This is especially true for the rotating disc and closing iris methods, which introduce complex geometry and small pieces.

### 8.3.4 Option 4 - Manifold

One option that removes the dangers of moving parts and proper seal formation is a static manifold. This manifold would be able to keep the working fluids of the thermal and electrical modes separate, and run them each through their own sections of the core. A given mass flow rate of propellant will require a certain amount of contact with the hot walls of the core in order to reach the desired temperature. By introducing a manifold and essentially splitting up the flow channels between two separate systems, the contact area of each flow channel will need to be doubled. This would result in a core that was twice as long as necessary for a system with only one flow path. Although the total mass of the system may not change, the geometry would become much different. This may not be an issue if the launch envelope is not a limiting factor for the spacecraft.

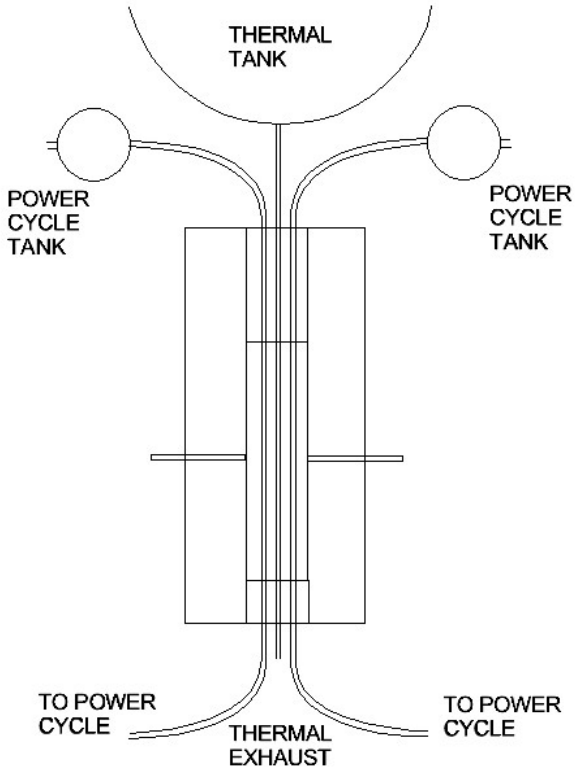


**Figure 31: Diagram of manifold channels re-directing flow through core**

The manifold would also require a system of automated valves that would allow or restrict flow based on which method would be used. These valves could safely operate under much more manageable temperatures than switching systems directly in the exhaust stream, and would require no specialized design or materials.

A complicated manifold may be difficult to manufacture, however. Tungsten is a favorite metal for high temperature operation due to its very high melting point. It is unfortunately quite brittle at lower temperatures and may crack when repeatedly headed and cooled. Tantalum is

another option that is much more malleable and still has a high melting temperature. It tends to oxidize rapidly, but because the system will be firing in space excess oxygen can be removed.

### 8.4 Down Selection

The negative aspects of the closing plates introduce too many risks to be considered for a project designed to be launched often. Particularly the doors bouncing and closing prematurely would not only compromise the mission but may result in explosions. The doors would also add a relatively large mass to the system, which is undesirable with such high costs for launch.

The spinning disc is more robust and adds much less mass to the system. Although it may reduce the efficiency of the nozzle, it would likely stand up to the temperatures and pressures to which it was exposed.

The closing iris is not robust enough to ensure that the system closes effectively and forms a strong seal. The iris shutters would be primarily attached to each other instead of the surrounding housing, which would be a much weaker seal than the spinning disc design.

The manifold removes many of the operational uncertainties involved with a switching mechanism by only using switches in manageable locations, and adds very little mass. Although the geometry of the core would change, the driving factor is the reduction in mass. Without the possibility of a failed seal, the system does not have such an obvious mode of failure and can operate for decades without forming a leak. Therefore, the manifold appears to be the best choice for a dual mode system.

In order to find the mass of the manifold, the flow channel cladding was simply doubled to allow for adequate length to redirect the flow from separate tanks to the core. This allows a tank to be placed anywhere along the length of the core. For the case of the baseline system, the manifold adds 14.5 kg of mass.

# CHAPTER 9: Propulsion System/Mission Trajectory

## 9.1 Propulsion System Overview

The parameters of the mission are designed to facilitate a mission from LEO to any target in the solar system without changing major components. The minimum value to be considered in orbit is roughly 300 km above the earth's surface. Most satellites, however, are significantly above this level, but for the sake of making the system universal that minimum value is used for this project. The craft must be less than or equal to 1000 kg in mass, and fit inside the faring of a Minotaur IV launch vehicle. While remaining within these constraints, the craft must exit earth's orbit, enter a heliocentric orbit, and spiral its way out through the solar system until matching the orbit of its destination.

Exiting the orbit of earth is considered a different problem than the heliocentric phase because many of the constants used are based on the body around which the craft orbits. The craft will start orbiting earth, where it will be primarily influenced by earth's gravitational pull. These orbital paths will be much smaller than those of an object around the sun, the forces the craft sees will occasionally be much stronger, and the accelerations involved may be higher. For these reason, it is important to consider the earth and heliocentric paths as separate trajectories.

Once reaching the destination, interacting with it will depend on what kind of object it is. For small objects without a gravitational pull, the craft will simply remain in a circular heliocentric orbit. For large bodies, such as planets, the gravitational pull of the object will attempt to pull the spacecraft in. Electric thrusters can be used to create an initial elliptic orbit as to avoid colliding with the body, and orbital phasing maneuvers can be used to circularize the orbit over time. Because the mission may require immediate capture, payload deployment, no capture at all, or some other parameter once the craft is at its destination, the method of entering orbit will not be explored further than acknowledging the possibility of capture exists with the existing capabilities of the craft. More specific actions than matching orbit will be considered part of the payload.

## 9.2 Earth escape Method 1 - Thermal

Using a thermal rocket blow down through the core has the benefit of providing a reasonable $\Delta V$ for each burst of power. The method of escape using the thermal rocket mode is an orbital phasing maneuver referred to as "perigee pumping." In this method, the rocket burns at a

specific point during its circular orbit tangential to the path of the orbit. This point is called the perigee of the orbit, and is the closest point between the craft and the planet. Diametrically opposite of the perigee is the apogee, and this is the farthest point between the craft and the planet. Burning at the perigee results the apogee distance increasing, and creating a more and more elliptical orbit. The perigee point stays at the same distance, but every burn pushes the apogee farther away until the craft can break free.

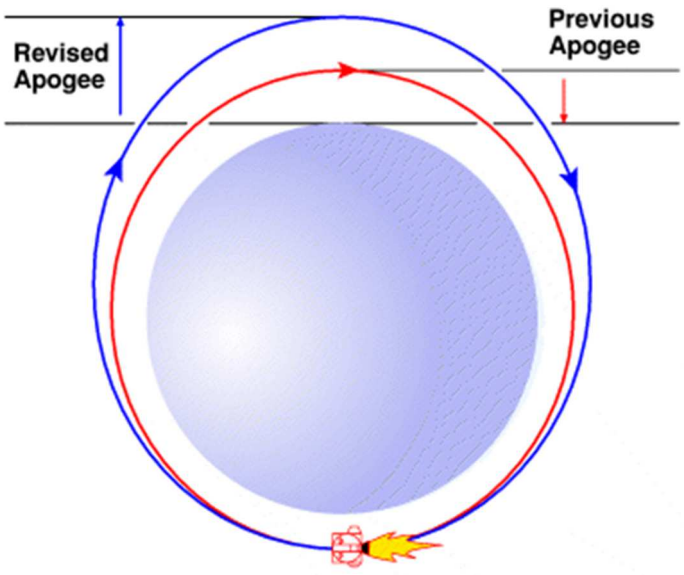


Figure 32: Effects of perigee pumping [90]

Depending on the ΔV provided per burn, the final orbits of the craft can take weeks or months. This is due to the apogee being so far from the planet that an orbit takes an incredible amount of time, but the craft cannot quite escape the gravitational field. In order to combat this, a different propellant may be used for the final burn. Xenon, for example, can provide a much higher ΔV value at the cost of a severely reduced ISP. This adds significantly to the mass of the propellant, but can reduce the time for earth escape by a considerable amount.

The fuel for the majority of the thermal mode will be hydrogen, to take advantage of the small atomic mass and high ISP values. This minimizes the total mass of the craft, and maximizes ΔV per unit volume of fuel.

The results for escape from earth using thermal propulsion are as follows. The craft will begin in LEO at a minimum altitude of 300 km, and with a rotational velocity of 7.73 km/s. This will be provided by the launch vehicle depositing the craft in orbit. From there, it will utilize one burn

for 12 minutes per day using a LiH core and PuO2 loaded fuel. The nozzle efficiency is assumed to be 50%. The periapsis of the orbit is equal to the altitude of the orbit added to the radius of the earth, resulting in a periapsis value of 6671 km.

In order to escape from earth, the orbital energy of the craft must be greater than 0 in equation 21 [18].

$$E = \frac{(V+\Delta V)^2}{2} - \frac{U_{earth}}{R} \tag{21}$$

Where E = Orbital energy, V = Craft velocity, ΔV = Change in craft velocity during burn, $U_{earth}$ = Standard gravitational parameter (398600 $km^3/s^2$), and R = Periapsis radius.

The value of E in this equation is normally negative, and once becomes positive it signifies that the orbiting body has escaped the object it orbits.

The Eccentricity of the orbit is given by equation 22 [18].

$$e = \sqrt{\frac{1-R}{a}} \tag{22}$$

Where e = Eccentricity, R = Periapsis radius, and a = Semi major axis.

When the eccentricity is equal to 0 the orbit is circular. When it is equal to 1, it is very elongated into an ellipse, and when it is greater than 1 the craft is no longer in orbit. The semi major axis is a parameter of the orbit that can be found by equation 23 [18] below.

$$a = \frac{-U_{earth}}{2*E} \tag{23}$$

Where a = Semi major axis, $U_{earth}$ = Standard Gravitational Parameter (398600 $km^3/s^2$), and E = Orbital energy.

While the periapsis distance stays constant as the craft makes multiple passes and elongates its orbit, the apoapsis, or point farthest from the planet, keeps increasing. The apoapsis distance can be found by equation 24 [18] below.

$$R_a = a(1+e) \tag{24}$$

Where $R_a$ = Apoapsis radius, a = Semi major axis, and e = Eccentricity.

This value is useful for understanding the path of the craft and how far it has to travel for its orbit. In order to find the total time for the orbit, equation 25 [18] is used.

$$t = \sqrt{\frac{2\pi * a^3}{U_{earth}}} \tag{25}$$

Where t = Time (in s), a = Semi major axis, and $U_{earth}$ = Standard Gravitational Parameter (398600 $km^3/s^2$).

With these equations for orbit, a model for periapsis pumping can be built, driven by the amount of ΔV gained per burn. However, when using $H_2$ as a propellant, the final orbital time before escape ends up being ~3639.6 days. For smaller ΔV values, the final orbits increase in duration as the craft gradually increases its apoapsis distance. Therefore, near the end of the earth escape trajectory it will save great amounts of time to use system that can provide a larger ΔV value for the final burn.

**Figure 33: Concept drawing of system with thermal propellant tank**

While still maintaining the use of the thermal rocket mode, a separate propellant can be used to increase the ΔV gained. Xenon, for example, has an atomic mass of 131; much larger than that of $H_2$. Using Xe for the final burn would result in a possible ΔV gain of 125 m/s, as opposed to the 11 m/s gained from an $H_2$ burn. However, the propellant mass for just that burn of Xe would be 120.4 kg, while $H_2$ uses 1.31 kg. It can be seen that using Xe as a propellant is quite costly from a mass point of view, but can save huge amounts of time if used correctly.

Another option for the final burn is to use a separate chemical thruster. This option may be mandatory for an all electric system, but can also be considered for use in the thermal system. The Aerojet Star 13B is capable of providing enough ΔV for the craft using thermal escape modes or electric

modes. At only 47 kg, this method is preferable to the xenon gas blow down. The Star 13B is explored in more detail below in the electrical escape section.

With a 12 minute burn once per day, using $H_2$ as the primary propellant and one Star 13B, the final escape time for a 1000kg craft from earth orbit would be ~120 days. The mass of the fuel and structure used to escape earth would be 496 kg, not including the core or power plant. The fuel tanks would take 6.37 $m^3$ of volume, well below the 23$m^3$ available for the Minotaur IV fairing, but still a significant amount volume.

### 9.3 Escape Method 2 - Electric

If electric thrust is used to escape the earth instead of a thermal mode, the system is quite similar. However, the need for switching between the two modes is removed, saving roughly 14kg of piping. Electric propulsion also has the added benefit of very high ISP values at the expense of very low ΔV gains per burst. If Two major contenders for electric propulsion are the NASA NEXT ion thruster and the Aerojet BPT thruster. The NEXT thruster has a higher ISP at 4190 s than the BPT's ISP of 1765, but can only provide a thrust of .60 N per 25 kW burn. The BPT can provide .84 N per burn. These values equate to a ΔV/burn of 1.28 m/s for the NEXT thruster, and 2.45 m/s for the BPT.

Similarly to the thermal escape method, the final burn will need to be something with a larger ΔV value. Because the thermal propulsion method will likely be excluded if the system uses electric propulsion for earth escape, a small chemical thruster could be used instead. The ATK Star13B is properly sized to provide 127 m/s of ΔV to a craft using the fuel efficient NEXT thruster, and 141 m/s ΔV to the craft using the BPT thruster, as it will have spent more mass on propellant to achieve the same orbit. The Star13B has a mass of 47 kg, and costs roughly $2,000[91]. When the craft requires 125 m/s to finally escape orbit, it will be on a very elliptical path with an orbital period of 6.33 days. The chemical thruster will then be ignited to leave orbit.

A comparison between the NEXT ion thruster and the BPT thruster can be seen in table 4 below. Both systems will use the ATK booster for the final escape burn, and have a total craft mass of 1000kg.

Table 4. Electric thrusters

| | NASA NEXT Thruster | Aerojet BPT2000 Thruster |
|---|---|---|
| Power per unit | 6.9 kW | 2.2 kW |
| Mass per unit | 25 kg | 5 kg |
| # of units* | 2.5 | 6.8 |
| Total thruster mass | 63.4 kg | 34.1 kg |
| Total propellant mass | 72.1 kg | 162.9 kg |
| Total system mass | 149.1 kg | 216.7 kg |
| Escape time (1 burn/day) | 2.78 yr | 1.11 yr |

* Fractions of thruster units used to achieve an accurate comparison.

As the table shows, the higher ISP of the NEXT thruster does in fact allow for a lighter system. However, the escape time is much longer with the NEXT thruster.

### 9.4 Earth Escape Method 3 - Chemical Rocket

As an alternative, the craft can use only chemical rockets to escape earth. This would remove the need for the thermal propulsion system and greatly reduce the time taken by the electrical propulsion system to leave earth. However, the payload would be greatly reduced due to the high propellant mass needed. The ATK Star27H rocket carries 337.84 kg of propellant and has an ISP of 291.4 s. Two of these rockets would be able to impart the necessary 3200 m/s of $\Delta V$ to escape earth. However, they each have a mass of 367.8 kg, or 735.6 kg together. This only leaves 264.4 kg available for the rest of the craft, including power plant, deep space thrusters, and payload. In special cases when a launch must be done immediately, this could be a viable alternative to using the power plant to escape, but the overall system mass would likely exceed the 1000kg limit set for this project.

### 9.5 Heliocentric Propulsion

In Heliocentric orbit, the spacecraft orbits the sun and gradually increases its orbital radius. The craft begins at a distance equal to that of earth's orbital radius, and every burn increases the

distance slightly. The method by which most spacecraft increase their orbit from one radius to another is called a Hohmann transfer. This method takes the least amount of energy to change the radius without taking advantage of gravity assists or other more complex maneuvers. To perform a Hohmann transfer, the spacecraft burns at the periapsis of the orbit, which elongates the orbital path and pushes the apoapsis to a larger distance. The craft then burns again at the apoapsis, which pushes the periapsis away from the original position. With the proper ΔV gained, the orbit becomes circular.

The equations for the ΔV required for the first and second Hohmann burns are provided below.

$$\Delta V_1 = \sqrt{\frac{\mu}{r_1}} * \left(\sqrt{\frac{2r_2}{r_1+r_2}} - 1\right) \quad (26)$$

$$\Delta V_2 = \sqrt{\frac{\mu}{r_2}} * \left(1 - \sqrt{\frac{2r_1}{r_1+r_2}}\right) \quad (27)$$

Where $\Delta V_1$ = ΔV value for the first burn, at the periapsis, $\Delta V_2$ = ΔV value for the second burn, at the apoapsis, μ = Gravitational parameter of the body around which the craft orbits (the sun has a gravitational parameter value of 1.327*10^11 $km^3/s^2$), $r_1$ = Periapsis radius, and $r_2$ = Apoapsis radius.

For every case where the radius increases, it can be seen that the value of the second burn will be smaller than that of the first burn. As the difference in radii gets smaller and smaller, the burns become closer and closer to being equal. Because this spacecraft is using a large number of very small burns, it can be assumed that the second burn approaches the same ΔV value as the first burn. Therefore, the ΔV required to create a circular orbit at any periapsis radius is equal to two times the value of the first burn of the Hohmann transfer. This approximation will provide an excess of fuel, but never result in a lack of fuel. Without going further in depth into the trajectory, this method should provide adequate fuel for any heliocentric destination.

In contrast to normal rocketry, the craft will follow an almost circular orbit as it spirals out into the solar system. Usually, a rocket follows the much more elliptic orbit induced by the Hohmann transfer, and thus a large amount of fuel is carried over the duration of the craft in order to perform the secondary burn. When the craft reaches its destination, it is at the same position as the target, but not in the same orbit, so it must make another burn to catch up with the orbiting

body. With the spiraling orbit, the craft will naturally match the speed of the planet once it matches the planet's orbital radius. If timed properly to meet the planet, it should be captured by the planet's gravity well without the use of hard burns or breaking systems.

## CHAPTER 10: Enabled Missions/Objectives

Understanding the missions enabled by this technology illustrates the capabilities that it allows for that would previously be too costly or too massive. Although these missions may not be often considered, with the ability to perform missions at low cost new and innovative missions can be performed in conjunction with currently planned missions such as rovers, orbiters, and flybys. Some of the possible missions are explained in more detail below.

The simplest example of a new mission enabled by this technology is a small, inexpensive method of transporting small satellites to distant planets. In this case, a Cubesat of roughly 1kg could travel out to its destination to collect data for decades. This would allow for universities or private investors to perform scientific research on other planets, without the aid of NASA or government intervention.

However, the propulsion system does carry a certain level of cost and mass that does not scale down to small missions. The power generation components will need to be large enough to avoid major losses, and even small amounts of radioisotope material can be expensive. Medium to large sized missions may see even more benefit from the pulsed power system, as it can save great amounts of cost on propellant and launch mass.

Small satellite constellations are a way to do multiple small scale missions at one time. If dozens of small satellites were transported to the destination as one medium sized payload, a swarm of them could gather data from multiple places along the orbital path at once. This could greatly reduce the time it would take to map a planet's surface. They could also be used on planets such as Enceladus, which sometimes eject plumes of matter in to space. A constellation of satellites in orbit would allow for these plumes to be analyzed no matter where on the surface they formed, as opposed to a single satellite that may have to traverse great distances to be in the right place at the right time.

Another major option is a mobile power plant for other satellites. With the ability to generate electrical power for very long periods of time, the pulsed power system can maintain an orbit around a planet and provide power and station keeping to itself and other satellites at the same destination. Station keeping is a term that refers to orbital maintenance; the ability to stay in an orbit that would naturally degrade over time. Station keeping is necessary for many orbits, and is usually done in terrestrial orbits through the use of electric thrusters and solar power. The

produced 25 kWe could also be used to power a laser that could charge the PV cells of a small satellite at distant planets, to replace the lack of solar power. This would allow the same satellites currently in earth orbit to perform tasks at other planets, while charging from the orbiting power source instead of the sun. A payload of 100 kg could provide 100's of watts of laser power to a constellation of satellites to reduce their individual mass and keep them in orbit for extended durations [92].

The small size of the system allows it to transport to the surface of a planet along with a rover if necessary. Although it may have to be further modified to withstand landing and/or environmental conditions, it could then be used to power drills or other high powered equipment. A rover that used it as a primary power source would be able to drive for a period of time during the day at high speeds, and would be able to explore a whole new area each day.

Very large scale missions may also be able to utilize the pulsed power and propulsion system, although manned missions or very heavy payloads are not explored in this project. The ability to provide high power levels would be relevant to high power electric thrusters, and possibly even help to expand the technological level of electric thrusters by providing power levels that were previously not thought to be possible.

Carrying satellites or acting as a power source allows the system to dramatically fluctuate between payloads of 1-100 kg, and so the performance and cost estimates will attempt to encapsulate a variety of options.

## CHAPTER 11: Performance Predictions and Cost Estimates

With all major components of the craft identified and explored, a few select configurations can be used to demonstrate the performance of the pulsed power spacecraft. The two major factors in most designs will be the total monetary cost for the mission, and the time it takes to get to the destination. With this in mind, a chart of cost VS time can be constructed for different missions.

Other missions may have different requirements, such as time, cost, mass, volume, or materials. Because the introduction of a duty cycle can have numerous and complex effects on any or all of these aspects, it is difficult to create a comprehensive list of all the different possibilities. Because of this, the systems looked at in this project are some of those with the lowest cost and longest transit times. This project shows the magnitudes of changes that can be done with this new method. If, in fact, time is more of an issue, the system can be designed in such a way to reduce transit times but increase the radiator masses or fuel costs.

The costs for components are described in table 5 below. Based on the different components used in a given configuration, the costs are summed and plotted to make clear the cost of the mission. For the performance estimates, some of the components will have a fixed mass and can be held constant for all missions. For example, each system will have the same power plant/core in order to get an accurate comparison. Table 5 shows the constant values calculated and variable values marked.

Table 5. Masses and costs

| Component | Cost/unit mass | Mass (kg) | Total Cost |
|---|---|---|---|
| PuO2 | $7.05 M/kg | 3 | $21.15 M |
| Tungsten Cermet | $19,730/kg [93] [94] | 3.44 | $67,900 |
| LiH | $732$/kg [96] | 11.96 | $17,700 |
| Tantalum Canister | $3,970/kg [95] | 7.45 | $65,800 |
| Pyrolytic Graphite Insulation | $3,360/kg [97] | 22.12 | $150,000 |
| Silica Aerogel Insulation | $667/kg [98] | 15.40 | $9,940 |
| Steel Frame/Radiators | ~$10/kg [100] | 26.96 | $404 |
| Tungsten pins | $374/kg [93] | 0.44 | $165 |
| Power Plant Plumbing | ~$10/kg [100] | 10.0 | $100 |
| Turbine/Compressor/Generator | ~$250,000 [102] | 72.2 [112] | $250,000 |
| Absorber | $3,270/kg [94] | 44.74 | $256,000 |
| Star 13B Motor | $2,000/unit | 47 | $2,000 |
| Electric Thruster Fuel | $120/kg [104] | Varies | Varies |
| Thermal Thruster Fuel | $120/kg [105] | Varies | Varies |
| Steel Structure | ~$10/kg [100] | Varies | Varies |
| Launch Costs | $29,000/kg [40] | Varies | Varies |
| Extra $PuO_2$ to account for decay | $7.05 M/kg | Varies | Varies |
| Totals | - | 264.71 | $21.97M |

In the graph below, a mission to Mars is performed with various differing goals. The craft will begin in LEO, exit earth's gravitational well, and spiral out towards Mars until it is captured and enters orbit. Different propulsion methods are used, as well as different payloads. Each pulsed

power system maintains a 1.2 kWt power source using $PuO_2$ as the fuel and the same LiH core capable of storing 60 MJ of thermal energy.

Other recent space missions are also included in the chart, such as the Mars Science Lab/Curiosity mission to Mars, the Opportunity rover mission, and the Indian Space Research Organization Mars Orbiter Mission.

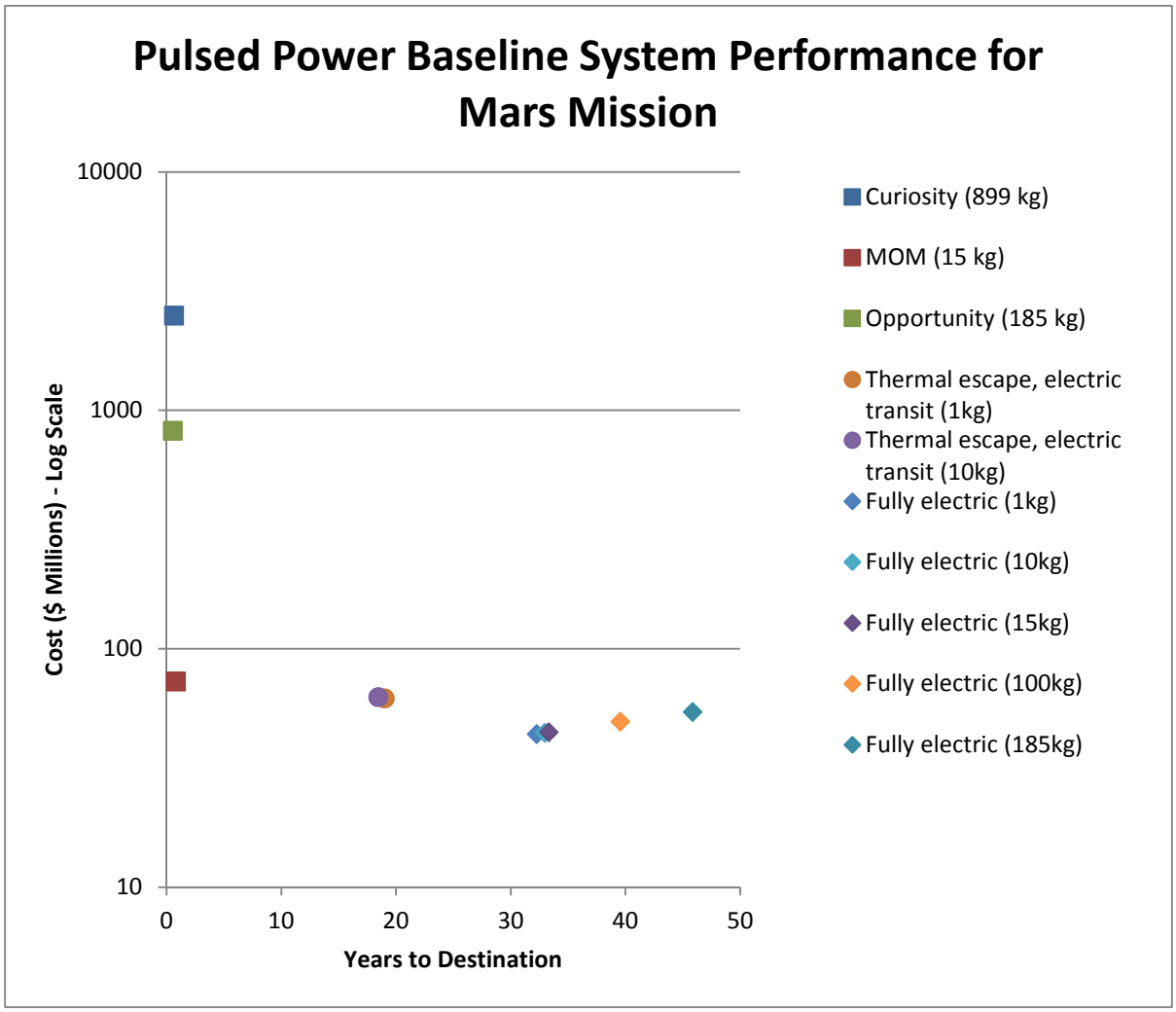


Figure 34: Mars mission comparison of pulsed power systems to past missions

The graph shows the cost of the missions decreases for the pulsed power system as the time to the destination increases. It is worth noting that the dual mode (thermal/electric) systems have masses in excess of the desired 1000kg. This may vary their cost predictions if they must use a different launch vehicle. Because of the large scales of the Curiosity and Opportunity missions, the

vertical axis on plotted on a logarithmic scale. In order to clarify the cost differences, the tabulated values are given below in table 6.

Table 6. Mission costs and times

| **Mission** | **Cost ($M)** | **Time (Y)** |
|---|---|---|
| Curiosity (899 kg) | 2500.0 | 0.66 |
| MOM (15 kg) | 73.0 | 0.816 |
| Opportunity (185 kg) | 820.0 | 0.54 |
| Thermal escape, electric transit (1kg) | 62.1 | 19.01 |
| Thermal escape, electric transit (10kg) | 62.7 | 18.446 |
| Fully electric (1kg) | 43.9 | 32.27 |
| Fully electric (10kg) | 44.4 | 32.95 |
| Fully electric (15kg) | 44.7 | 33.31 |
| Fully electric (100kg) | 49.5 | 39.56 |
| Fully electric (185kg) | 54.4 | 45.86 |

The value for the lowest cost mission to Mars so far was $73 million. Performed by the Indian Space Research Organization, it delivered a 15 kg payload into the Martian orbit. For the same payload, the pulsed power system would cost only $44.7 M. However, it would use electric thrusters only, and take over 33 years to reach its destination. It may or may not be worthwhile to save the extra ~$30 M at the expense of time.

It does, however, show the major benefit in very heavy payloads. The cost to deliver 100kg into Mars orbit only costs $49.5 M. Larger systems, like the opportunity, cost on the order of 100s of millions of dollars. A quick calculation for a pulsed power system delivering a similar payload of 185 kg results in a cost of $54.4 M, but a transit time of 43.8 years.

It can be seen that the trend in this data is to decrease the cost of missions while increasing the transit time. Deploying 10-100 Cubesats around Mars may be worthwhile to future generations for the cost of less than any other mission to Mars so far.

## 11.1 Modifications

The absorber and core masses are large portions of what make the craft heavy, and thus expensive. Reducing the size of the core will naturally reduce the size of the absorber and decrease radiator mass. For a 10 kg payload, permutations on core size are shown below.

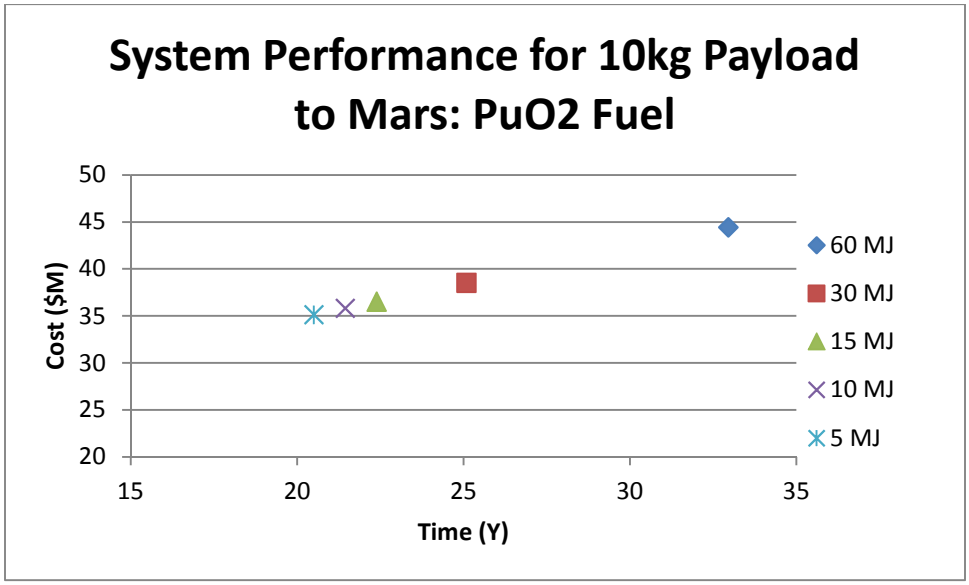


Figure 35: System performance for differing core sizes

From this chart, it can be seen that the cost and transit time decrease greatly with a decreasing core size. This is due to the fact that the same amount of total input power is present, but the device increases in mass with a larger core size. It is also very important to note that the firing rate changes as well; a smaller core requires less time to heat up with the same amount of thermal power in. The 5 MJ core, for example, fires every 2 hours. It is also so small that there is not enough area for flow channels through the core. It may be possible to redesign the system geometry in order to better accommodate the smaller core, but for the existing geometry a 30 MJ core is the smallest size that can handle the flow channel geometry.

If the cheapest fuel source, sr90, was used instead of PuO2, the cost for fuel would decrease but the time and launch costs would increase. Costing only $100,000/kg, only a little over 0.5kg would be required to match the power output of the Pu238 core. This would reduce the fuel costs from $21.15M to $0.05M. It would, however add a large shielding mass.

Because smaller diameter cores reduce the radius of the shield, smaller cores again benefit the performance of a Sr90 fueled system. A craft using Sr90 fuel with a 30MJ capacitor on a mission to carry 10kg to Mars would have a transit time of 29.5 years, but cost only $17.6 M.

Until this point, the main focus has been on exploring Mars. Other missions have entered Martian orbit and provide adequate information for comparison. However, missions to other planets may also be viable. In considering these missions, americium as a fuel source may yet prove itself viable thanks to its long half-life. The figure below shows the performance of spacecraft carrying a 10kg payload to different planets using a 30 MJ capacitor, but varying in fuel types.

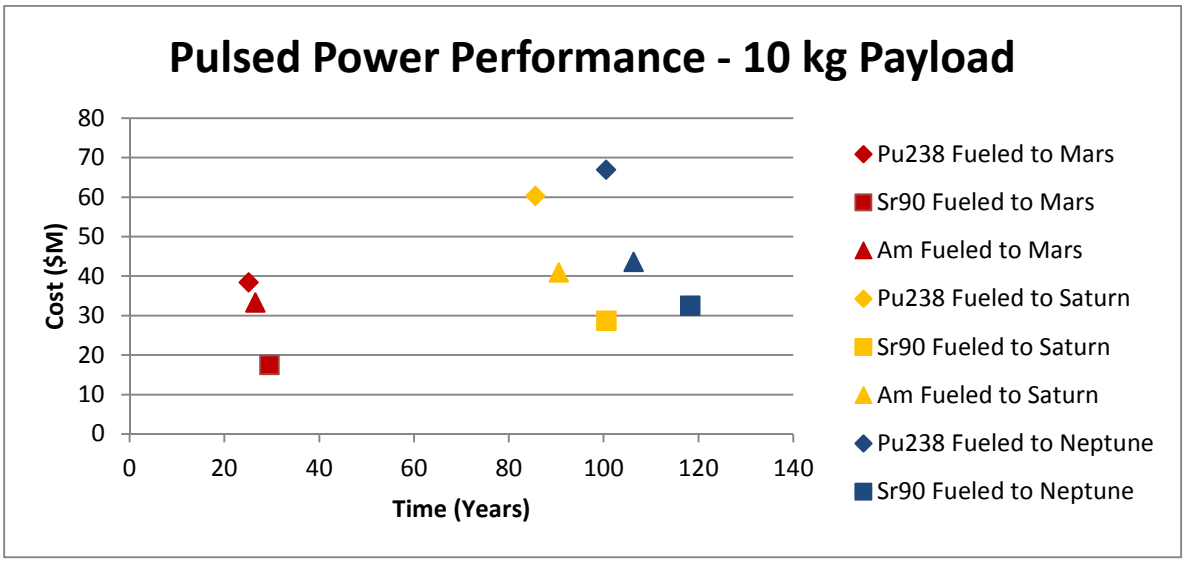


Figure 36: Cost and Transit time for different destinations and fuels

With these results in mind it is important to compare to alternative methods that may be more near-term. The first of which would be a continuously electrically propelled system powered by existing technologies such as an MMRTG. As seen above, the MMRTG produces 125 W of electric power on 4.8 kg of Pu238. To have enough electrical power to run a 6.9kw NEXT ion thruster, over 55 units would be needed. This would equate to a craft with a mass greater than 3,000 kg, and have a total cost of over $2 billion. The transit time may be significantly shorter due to the constant firing, but the cost of this mission would easily put this method in a different classification.

Another alternative is a smaller, lower power system with different thrusters. The Busek BHT-200 thruster operates at 200 We, and could be powered by ~1.6 MMRTGs [106]. In the case of delivering a 10kg payload to mars, this system would cost slightly over $61M. Although this price

tag is in the same range as the pulsed power system, it is still ~$20-30M more expensive. The estimated transit time for this mission would be only 3.3 years, however. In the case where the extra money was available this is definitely a viable option, but the pulsed system could cut the price in half.

# CHAPTER 12: PCM Heating Experiment

## 12.1 Overview

It is important to show experimentally the concept of the PCM core and its ability to influence the working fluid. However, high power systems involving high temperatures and large amounts of compressed xenon are outside the bounds of this project. Instead of building an exact replica of the core, a different PCM was used, and an open Brayton cycle was constructed around it to show feasibility. The final configuration used sulfur as a PCM and air as a working fluid, instead of lithium hydride and xenon, respectively. The cycle should show that the performance of the cycle increased with increasing temperature, and experienced a plateau in the region where the PCM was in a two phase state.

## 12.2 Safety Issues

Sulfur was used as the surrogate PCM material, and some safety concerns needed to be addressed because it can be a somewhat dangerous material to work with if not handled correctly. Sulfur melts at 115°C and has an auto ignition temperature of 248°C [107] [108]. This allowed for a operating margin of 133°C above the desired temperature. Naturally, the material was kept well below that value. If handled near an open flame, it can easily combust, or it can auto combust at high enough temperatures. To avoid this, the heating tape was tested without any sulfur present to determine what temperatures it could reach at specific power levels. Thermocouples were placed at the end of the tape closest to the power source and one at the point farthest from the source.

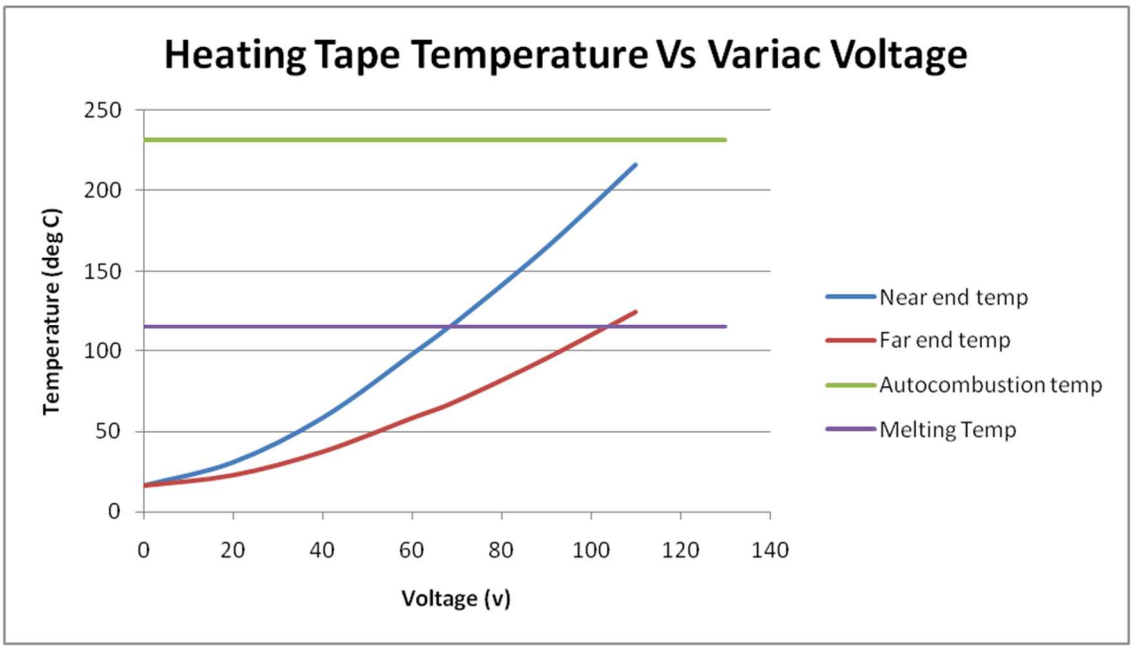


Figure 37: Temperatures of heating tape

Additionally, there was a danger of the compressed gas rupturing a component and spraying molten material out of the heat exchanger. Due to this, heat resistant gloves were worn, as well as a lab coat and eye protection.

During some tests, turbine shafts were rotating at high speeds. It was important to not wear loose clothing or anything that could become caught in the shaft. It was also important to make sure no pressure buildups in the air line were present, which could potentially explode. The experimental system was inspected for changes or possible dangers before each use.

The final safety issue addressed was the fact that molten sulfur tended to emit a small amount of vapor after transitioning to liquid phase. Do combat this, the laboratory was well ventilated and anyone in the lab during operation was wearing a filtration mask.

### 12.3 Experiment Design

The goal of the experiment was to show that the output of a power cycle would stay constant over the course of the phase change of the PCM core. To demonstrate this, compressed air was flowed through a tube in shell heat exchanger containing molten sulfur. As the air was heated by the sulfur, it expanded and was directed through a small turbine. This turbine then

turned a generator in order to provide a voltage. The output voltage was recorded by an Arduino controller and relayed to a computer system for recording.

Selection of components for the experiment was done by analyzing which off the shelf components were available and able to withstand the desired temperatures. Glass heat exchangers, such as condensing units used in chemistry, were considered due to their high operating temperatures of over 200°C [109], but they were not able to withstand the pressures. Instead, steel piping was used to create a tube in shell heat exchanger. Silicon tubing was used to direct the flow between components due to its high melting temperature of 260°C [110]. The system contained 275 g of sulfur contained in an outer heat exchanger pipe measuring 2" O.D. by 6" length. The steel flow tube in the exchanger had an outer diameter of 1/2". The heating tape used was a 120V Omegalux heating tape, 1/2" wide by 72" long. The turbine used was a TS-315 radial turbine built by Wolfgang Engineering. The generator used was a motor taken from a 12V brushless fan, which produced a voltage proportional to the shaft rotational speed when turned. Thermocouples were inserted into the heat exchanger to monitor temperature.

A diagram of the final system can be seen below.

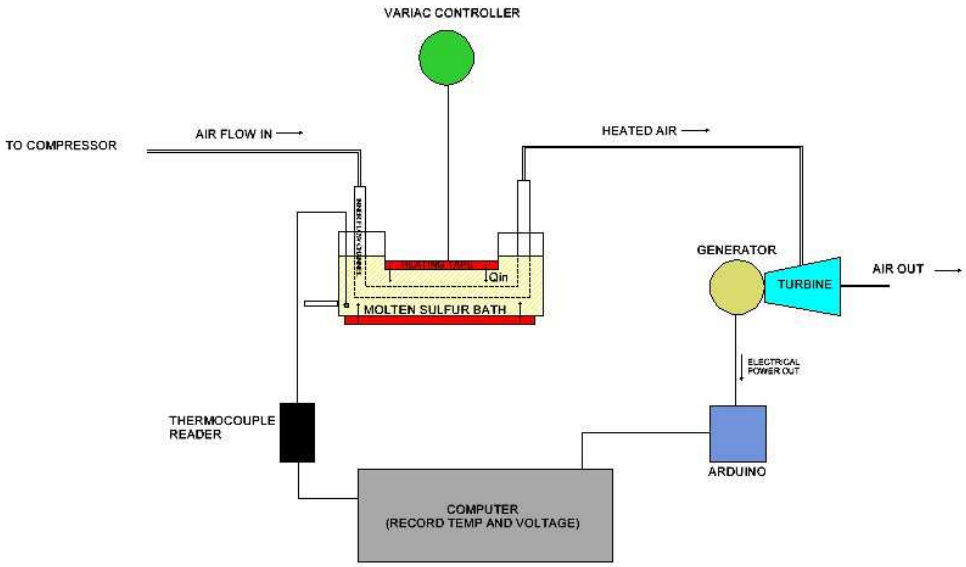


Figure 38: Flow diagram of power cycle

The air flow enters from the compressor (not pictured) on the left side of the diagram. It then flows through the heat exchanger, which is comprised of a large outer shell and a thin inner tube. In between the two is a bath of molten sulfur. The outside of the outer shell is wrapped in a heating tape capable of providing 310 W of thermal power to the system, and is controlled by a Variac controller in order to vary the power level. The hot gas then flows through the turbine, which turns the generator. That voltage that the generator produces is sent to the Arduino system and recorded by the computer. The thermocouple embedded in the sulfur bath monitors the system to ensure the sulfur does not approach the auto ignition temperature. The voltage was recorded as a performance metric instead of a rotational speed due to difficulties encountered with accurate measurements of the speed. Because the voltage is directly related to the rotational speed, the nature of the system could be accurately represented by the voltage measurements.

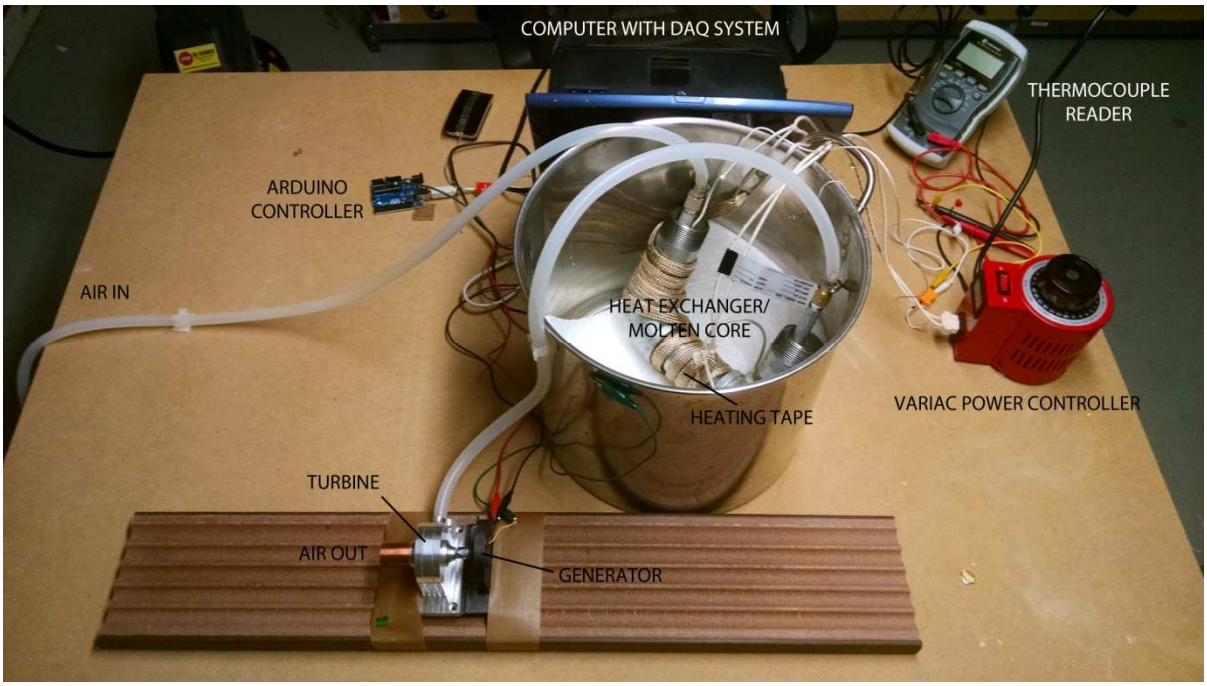


Figure 39: Image of actual power cycle

## 12.4 Results/Discussion

The results from this setup were quite an improvement on the results from the previous setup. A single blow down was performed to show the formation of a plateau in the power output. The sulfur bath was heated until melted, as measured by the thermocouple. The Variac controller was turned on and set to 258 W and the system allowed to heat. A temperature plateau was seen at 107 °C, and then slightly over-heated as seen below.

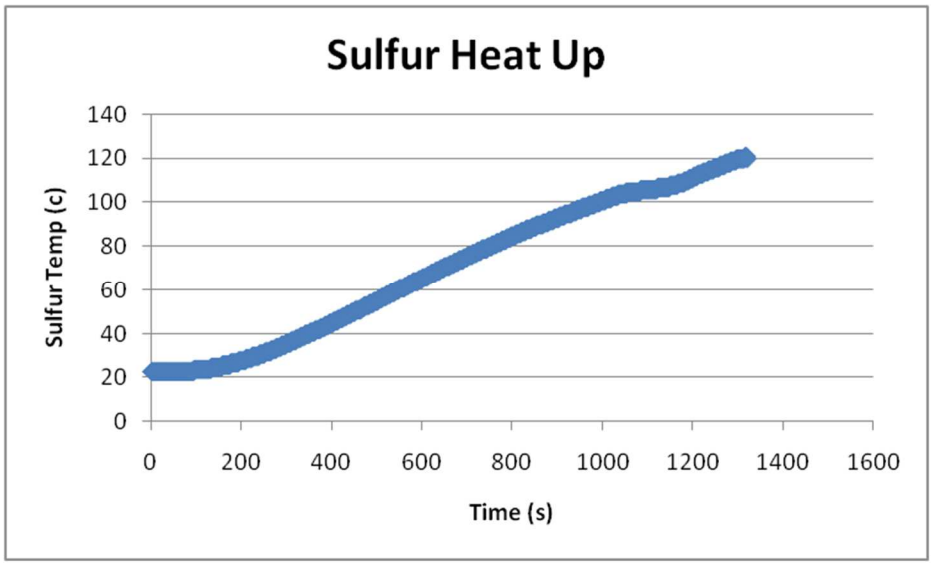


Figure 40: Temperature of sulfur bath during heat up

Sulfur has a reported melting temperature of 115°C [108], so the offset may have been due to changes in altitude or calibration of the thermocouple system. However, it was relatively close to the reported temperature and it could be seen upon inspection to be melted.

The compressor was then opened and the release valve set to 15 PSIG. Upon activation of the compressor, the turbine began to spin and produce a recordable voltage. The output of that voltage can be seen below.

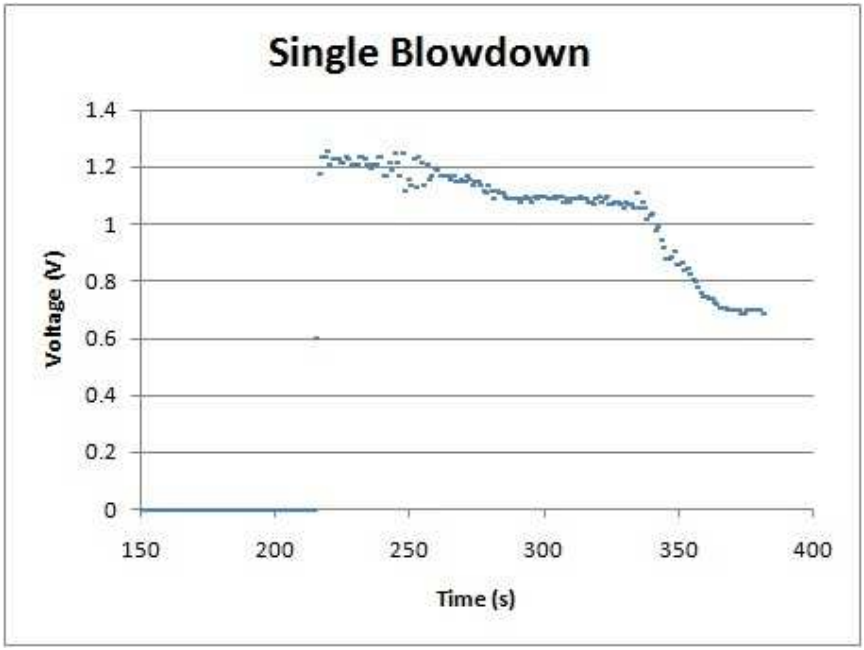


Figure 41: Results of single blow down experiment

These results show a clear plateau in the range of 1.1 V, which coincides with the idea that the power output will remain constant during the freezing process. Even though the voltage does not correspond directly to a power output, it is a viable measuring system in regards to other open circuit voltages recorded by the same device. To maximize power output, the system would need a load attached an a current flowing through the circuit. Without this, the total electrical power cannot be found, but the overall performance of the system can be understood by simply measuring the open circuit voltage.

One of the major aspects of the PCM core for the purpose of pulsed power generation is the ability to recharge and re-fire intermittently. To demonstrate this, the input power to the system was held at a constant 207 W and the compressor turned on for a blow down. After the voltage output had dropped to below the plateau area, the system was allowed to reheat at that same, constant power level. The electrical heating system was then more representative of a radioisotope that would provide constant thermal power to the system. This resulted in the periodic power profile below.

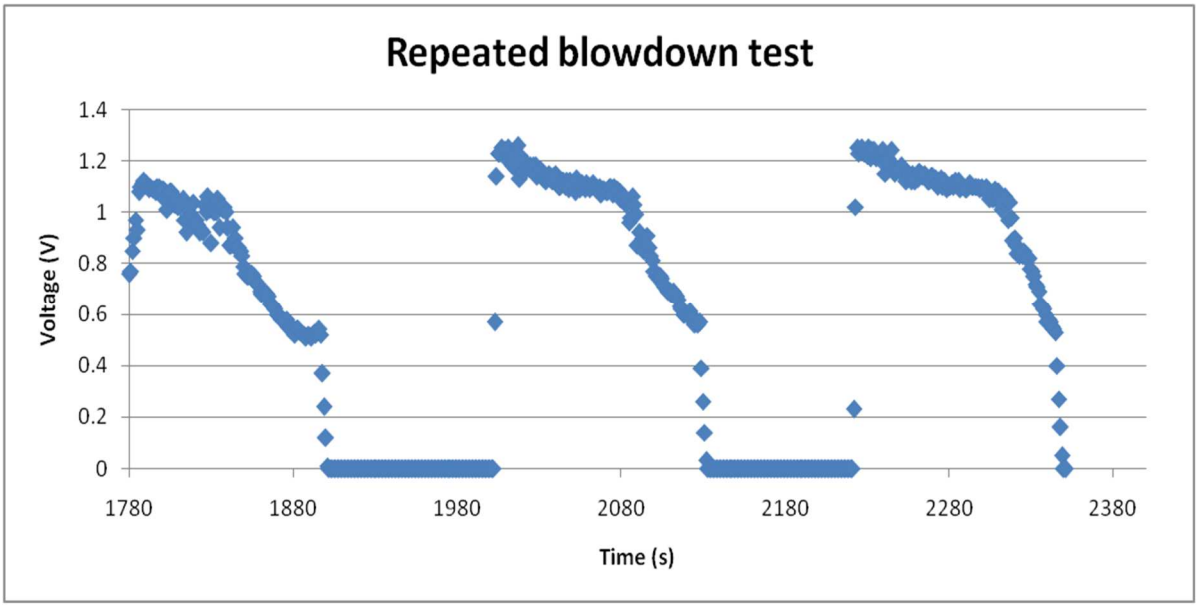


Figure 42: Results of the repeating blow down test

With the exception of the first blow down, very clear plateaus can be seen near the value of 1.1V, and even the first test shows some degree of leveling out during freezing. This shows that the system can repeat the blow down process repetitively in order to produce power using a PCM core.

**12.5 Computational Analysis of Experiment**

By understanding the results of the experiment and comparing them to the predicted results, the computational model of the larger system can be verified. One Important aspect of the experimental model includes the flow channel analysis, just like in the design of the full system. To achieve this, a number of material properties from the design are replaced with experimental properties, and the design steps rerun.

The relevant input data of the experimental setup are listed below in table 7.

Table 7. Experimental input data

| Property | Value |
|---|---|
| Sulfur thermal conductivity | 0.205 W/m*K |
| Flow channel Diameter | 0.00635 m |
| Inlet Pressure | 0.200 Mpa |
| Outlet Pressure | 0.101 Mpa |
| PCM temperature | 388 K |
| Cold Temperature | 291 K |
| Flow Channel Length | 0.1524 m |

According to this information, the Biot number should be 0.56, which is low enough for the lumped sum capacitance assumptions to hold true. Furthermore, the Reynolds and Prandtl numbers are 159.4 and 0.0007, respectively. This suggests laminar flow. Although the flow characteristics and materials are different, the analysis can still be performed on the experimental system and its performance predicted. Differences that may differ in the performance of the theoretical system are addressed later in this chapter.

Based on calculations for the exit temperature, the air should have exited the system at 357.0 $^{o}$K. This was found by using the values of the dimensionless numbers to find the convective heat transfer coefficient in the same method as described in the flow channel analysis, and assuming a linear temperature profile. Other parameters were solved for using the same method as the flow channel analysis. The calculated results of modeling the system are seen below in table 8.

Table 8. Calculated experimental results

| Property | Value |
|---|---|
| Exit Temperature | 332 K |
| Flow Velocity | 0.6 m/s |
| Nusselt Number | 3.66 |
| Prandtl Number | $7.0x10^{-4}$ |
| Reynolds Number | 159.4 |
| Mass Flow Rate | 0.1725 kg/s |
| Convective Heat Transfer Coefficient | 18.08 $w/m^2*K$ |

It is also important to identify the differences between the experimental demonstration and the actual power system design of the spacecraft. For example, the PCM used was obviously a different material for the experimental demonstration, but still illustrated the capabilities of a PCM core. This has the effect of changing the heat transfer properties and the Biot number. Fortunately, the properties are similar enough to maintain the same assumptions about the lumped sum capacitance model. Additionally, the experimental system exhibits laminar flow instead of turbulent. Laminar flow is often easier to predict than turbulent, so the system design should take in to account the possible need for longer channel lengths or changes in performance. Due to this, the laminar flow experiment should act as a "best case scenario" when dealing with experimental predictions.

The experimental system does not incorporate absorbers or heat rejection systems, and is not a closed cycle. This means none of the masses or efficiencies are taken in to account. However, the purpose of the experiment is to demonstrate the PCM core concept, not necessarily to demonstrate a functioning pulsed power prototype.

The results of the experimental Brayton cycle show the ability of a PCM core to level the power generation profile of the cycle over time, but there are certain aspects that introduce errors. Data gathering devices such as thermocouples can introduce errors, and so it was necessary to calibrate them before testing. To do this, they were submerged in an ice bath and found to read 3.3 $^{o}$K warmer than expected. Temperature readings were adjusted accordingly, and the experimental and computational results compared.

The expected temperature of the exiting gas was 357.0 $^{o}$K, found by computational analysis. However, the recorded temperature was 332.0 $^{o}$K. With the thermocouple bias adjusted for, the exit temperature was only 329.7 $^{o}$K, corresponding to an error of 7%.

**12.6 Error Analysis**

This error in temperature difference is likely due to the geometry of the system introducing curves in the flow channel. If the system was designed in such a way to allow for longer channels with better developed flow the error is expected to decrease. This should be the case with the long flow channels in the actual PCM core system. Other possible contributions to error may include effects of air pressure and humidity, as the experiment was not performed at sea level.

The single blow down test results displays a very clear plateau where the PCM is undergoing a phase change and keeping the exit temperature and pressure constant. However, the repeated test has less well defined plateaus, and the first test has a number of data points outside of the expected range. Whenever the system was started for the first time, the data points became erratic. Yet for the repeated test, the 2nd and 3rd heat up did not exhibit this behavior to such a degree. Therefore, it can be concluded that a "cold" start, one which takes place after a significantly long resting period, may experience a slight drop in overall performance. This should be taken in to account when designing systems that are intended to function intermittently, but is difficult to predict without extensive testing on an actual prototype. For the purposes of this project, it will be assumed that a small priming blow down will be sufficient to remove any buildup of stray particles or other issues that contribute to the erratic behavior.

**CHAPTER 13: Results and Conclusions**

From the systems designed in this project, a few major conclusions can be drawn. Smaller power plant masses and more rapid firing times can increase the performance of pulsed power spacecraft, radioisotope fuels can be very expensive, and with a sufficient level of patience the solar system can be explored by independent researchers with limited budgets. This allows for a wide variety of missions to be considered for use with this technology

Nuclear, chemical, and electric propulsion methods are all viable and effective methods of depositing spacecraft throughout the solar system, but their high costs are often restrictive for private entities and smaller institutions. With a pulsed system, a new venue of space exploration is opened to a large variety of patrons. With the ability to generate electrical power as well the pulsed power system can not only aid in propulsion, but continue to provide an important use for the duration of the mission.

The concept of a PCM core has been demonstrated to work in a laboratory setting and shown to function admirably. Although further testing and prototyping should be explored before launch, the standard Brayton cycle has been in use for decades and has been explored in depth, so models can be accurately constructed with the hot core as the source of heat for the cycle.

Variations on the spacecraft also allow for high levels of customization based on the requirements of the mission. Higher budgets may allow for larger payloads or faster transit times, or longer term missions may allow for low cost, large scale missions. Varying fuel types, materials, and geometries can all be done to cater to individual needs.

A mission to deliver a 10kg satellite to Mars can be accomplished with a budget below $18 million, allowing for the fact that the transit time is around 30 years. Long term missions to the outer planets can be done for ~$30-80 million, if the mission can endure a hundred year voyage.

Some possible missions enabled by this technology include solar system wide communications arrays, inexpensive satellites, and efficient propulsion devices. It also allows for power stations to be placed in orbit around planets to provide energy to satellite constellations through laser or RF power transmission. Drilling, mining, and research can all be performed on the surface of planets without large power plants weighing down the craft and adding to high launch costs.

Reducing the cost of space travel is an achievement all of humanity can benefit from. Using a duty cycle is one way to significantly decrease the cost of space exploration in a method not previously considered by the space community, but one that has definite advantages. For the cost of the Curiosity mission to Mars, roughly 50 missions to deep space could be performed to gather important scientific information about the universe. Were these missions undertook at the beginning of the space age in the 1950's, the researchers of today would now have access to a wealth of satellites in orbit around Mars, and in ~15 years, Jupiter.

**References**

[1] Chemicool.com, "Plutonium," http://www.chemicool.com/elements/plutonium.html 02/26/2015

[2] Oregon State University College of Engineering, "Rebuilding the supply of Pu238," http://ne.oregonstate.edu/rebuilding-supply-pu-238, 02/26/2015

[3] American Nuclear Society (ANS) “MMRTG” http://anstd.ans.org

[4] NASA, Advanced space transportation program, http://www.nasa.gov/centers/marshall/news/background/facts/astp.html 07/15/2014

[5] Spaceflightnow.com "Space Flight Now | Minotaur Launch Report," (2010) http://spaceflightnow.com/minotaur/stps26/101118preview 02/24/2015

[6] Sunpower Corp. “E-series solar panels” Document # 504860 April 2013

[7] NASA “Where are the Voyagers” http://voyager.jpl.nasa.gov/where/index.html 01/30/2015

[8] European Space Agency “ESA Science & technology: Rosetta” http://sci.esa.int/rosetta/ 01/28/2015

[9] NASA “Juno spacecraft and instruments” http://www.nasa.gov/mission_pages/juno/spacecraft/index.html 01/28/2015

[10] NASA “Advanced Space Transportation Program Fact Sheet,” http://www.nasa.gov/centers/marshall/news/background/facts/astp.html 02/09/2015

[11] Space.com “Derelict Booster to Beat Probe to Jupiter,” http://www.space.com/1991-derelict-booster-beat-pluto-probe-jupiter.html 02/17/2015

[12] ATK “ATK Motor Catalog 2012” Company Approved Document OSR no. 12-S-10-2

[13] NASA Ames “NASA Astrobiology: Life in the Universe,” https://astrobiology.nasa.gov/calendar/europa-plume-workshop/ 02/17/2015

[14] NASA “Small Spacecraft Technology Program Overview,” http://www.nasa.gov/directorates/spacetech/small_spacecraft/smallsat_overview.html 02/09/2015

[15] NASA “NASA Successfully Launches Three Smartphone Satellites” http://www.nasa.gov/home/hqnews/2013/apr/HQ_13-107_Phonesat.html 02/09/2015

[16] Phonesat “PhoneSat – home,” http://www.phonesat.org/index.php 02/09/2015

[17] From NASA.gov, "Ideal Rocket Equation," NASA, http://exploration.grc.nasa.gov/education/rocket/rktpow.html 04/29/2015

[18] From Bate, R. R., et. al., "Fundamentals of Astrodynamics," Dover Publications Inc., 1971

[19] From NASA.gov, "Specific Impulse," NASA, http://www.grc.nasa.gov/WWW/k-12/airplane/specimp.html 04/29/2015

[20] Los Alamos National Lab “NUCLEAR ROCKETS: To Mars and Beyond,” http://www.lanl.gov/science/NSS/issue1_2011/story4full.shtml 01/31/2015

[21] From Esselman, W. H., "The NERVA Nuclear Rocket Reactor Program," Westinghouse ENGINEER, May 1965

[22] Vacco Space Products " http://www.vacco.com/images/uploads/pdfs/cold_gas_thrusters.pdf," http://www.vacco.com/images/uploads/pdfs/cold_gas_thrusters.pdf 03/30/2015

[23] Busek Space Propulsion Systems “Busek Hall Effect Thrusters,” http://www.busek.com/technologies__hall.htm 02/09/2015

[24] NASAfacts "Multi-Mission Radioisotope Thermoelectric Generator," NASA information sheet 8/2013

[25] NASA “Advanced Stirling Radioisotope Generator (ASRG)” NASA Document NF-2013-07-568-HQ, 2015

[26] Chubb, D., "Fundamentals of Thermophotovoltaic Energy Conversion", Elsevier Science, 2007

[27] Shultis, J. K., Faw, R. E., "Fundamentals of Nuclear Science and Engineering," Marcel Dekker, 2002

[28] JPL “NASA Rover Finds Active and Ancient Organic Chemistry on Mars,” http://www.jpl.nasa.gov/news/news.php?feature=4413

[29] Howell, J. R., et. al., "Thermal Radiation Heat Transfer, 5th Edition," CRC Press, 2010

[30] Quarta, A. A., Mengali, G., " Minimum-time space missions with solar electric propulsion," Aerospace Science and Technology 15, 2011

[31] Squire, J. P., et. al. " VASIMR® Spaceflight Engine System Mass Study and Scaling with Power," International Electric Propulsion Conference 33, 2013

[32] Woellert, K., et. al., "Cubesats: Cost-effective science and technology platforms for emerging and developing nations," Advances in Space Research 47,2011

[33] Wood, D., Weigel, A., " THE EVOLUTION OF SATELLITE PROGRAMS IN DEVELOPING COUNTRIES," International Astronautical Congress presentation, 2009

[34] Swartwout, M., et. al., " Mission results for Sapphire, a student-built satellite," Acta Astronautica 62, 2008

[35] Santioni, et. al., " An innovative deployable solar panel system for Cubesats," Acta Astronautica 95, 2014

[36] Santioni, et. al., " An orientable solar panel system for nanospacecraft," Acta Astronautica 101, 2014

[37] Lappas, V., et. al., " CubeSail: A low cost CubeSat based solar sail demonstration mission," Advances in Space Research 48, 2011

[38] Forsberg, C. W., et. al., "An Advanced Molten Salt Reactor Using High-Temperature Reactor Technology," International Congress on Advances in Nuclear Power Plants, 2004

[39] Tournier, P. J., El-Genk, M., "Properties of noble gases and binary mixtures for closed Brayton Cycle applications," Energy Conversion and Management 49, 2008

[40] Sifner, O., et. al., “Thermodynamic Properties of Xenon from the Triple Point to 800K with Pressures up to 350 MPa,” Institute of Thermomechanics, 11/25/1992

[41] Aadmi, et. al., "Heat Transfer Characteristics of Thermal Energy Storage for PCM (Phase Change Material) Melting in Horizontal Tube: Numerical and Experimental Investigations," Energy, 2015

[42] Sahan, N., et. al., "Improving thermal conductivity phase change materials—A study of paraffin nano magnetite composites," Solar Energy Materials & Solar Cells 137, 2015

[43] Saihpush, A., O'Brien, J., Crepeau, J., " Phase Change Heat Transfer Enhancement Using Copper Porous Foam," Journal of Heat Transfer, 2008

[44] Chen, F., Walcott, M., "Polyethylene/paraffin binary composites for phase change material energy storage in building: A morphology, thermal properties, and paraffin leakage study," Solar Energy Materials & Solar Cells 137, 2015

[45] Liu, M., et. al., " Determination of thermo-physical properties and stability testing of high-temperature phase-change materials for CSP applications," Solar Energy Materials & Solar Cells 139, 2015

[46] Su, W., et. al., " Review of solid–liquid phase change materials and their encapsulation technologies," Renewable and Sustainable Energy Reviews 48, 2015

[47] Bruno, F., et. al., " Using solid-liquid phase change materials (PCMs) in thermal energy storage systems," University of South Australia

[48] Orbital ATK "Minotaur IV Space Launch Vehicle" Company approved document ID BR06005_2998, 2014 http://www.orbitalatk.com/flight-systems/space-launch-vehicles/minotaur/docs/2B3_MinotaurIV.pdf"

[49] Szatkowski, J "ULA Rideshare with Cubesat Missions for Lunar and Inter-Planetary Exploration," Presentation, 2nd Interplanetary Cubesate Workshop, 2013

[50] Spaceflight Inc. "Hosted Payloads | Spaceflight Services," http://spaceflightservices.com/launch/hosted-payloads/ 02/24/2015

[51] Atkinson, Nancy, “Launch Your Own Personal Satellite for $8,000 USD.” Universe Today, 08/09/2011

[52] Jerred, N. et. al., "Dual-Mode Propulsion System Enabling Cubesat Exploration of the Solar System," NASA Innovative and Advanced Concepts Final Report, 2014

[53] Schmidt, G. et.al., "THE NASA EVOLUTIONARY XENON THRUSTER (NEXT): THE NEXT STEP FOR U.S. DEEP SPACE PROPULSION," NASA Glenn Research Center, Document IAC-08-C4.4.2

[54] Aerojet Corp. "BPT-2000 HALL EFFECT THRUSTER," Company approved datasheet, 2003

[55] NIST “NIST Standard Reference Database 12” U.S Secretary of Commerce, 2005

[56] English, Robert "Technology for Brayton-Cycle Space Powerplants using Solar and Nuclear Energy," NASA Technical Paper 2558, Feb, 1986

[57] MatWeb “Silicon, Si,” http://www.matweb.com/search/DataSheet.aspx?MatGUID=7d1b56e9e0c54ac5bb9cd433a0991e27, 07/08/2014

[58] Engineering toolbox "Metals and Latent Heat of Fusion," http://www.engineeringtoolbox.com/fusion-heat-metals-d_1266.html 02/23/2015

[59] Goodfellow.com, “Boron – online catalog source…,” http://www.goodfellow.com/E/Boron.html 03/30/2015

[60] Goodfellow.com, “Germanium – online catalog source…,” http://www.goodfellow.com/E/Germanium.html 03/30/2015

[61] Dostal, Vaclav; et. al., “THE SUPERCRITICAL CARBON DIOXIDE POWER CYCLE: COMPARISON TO OTHER ADVANCED POWER CYCLES,” Journal of Nuclear Technology 154, 2006

[62] Breedlove, J., personal interview. CREARE Engineering, 4/25/2014

[63] Goodfellow.com “Beryllium – online catalog source…,” http://www.goodfellow.com/E/Beryllium.html 03/30/2015

[64] Howe, S.D., et.al., "Economical Production of Pu-238," NASA NIAC phase 1 final report, 2013

[65] Hore-Lacy, I., "Can americium replace plutonium in space missions?" World Nuclear News, 2014

[66] Radioisotope Power Systems Committee, "Radioisotope Power Systems," National Research Council, 2001

[67] Lide, David R., "CRC Handbook of Chemistry and Physics, 84th Edition," CRC Press, 2004

[68] Sure, L., et.al., "SURVEY OF ELECTRIC POWER PLANTS FOR SPACE APPLICATIONS," NASA document N66-14775, 1965

[69] Chemicool.com "Strontium," http://www.chemicool.com/elements/strontium.html 02/26/2015

[70] US Department of Energy, "DOE Handbook Radiological Worker Training," DOE-HDBK-1130-2007 December, 2007

[71] MIT.edu “3.7 Brayton Cycle,” http://web.mit.edu/16.unified/www/FALL/thermodynamics/notes/node28.html (12/12/14)

[72] Compressorworld.com “7 horsepower, 13 CFM Reciprocating (Piston) Compressor Booster, Max 500 PSIG,” http://www.compressorworld.com/piston-air-compressors/high-pressure-compressors/7-horsepower-13-cfm-reciprocating-piston-compressor-booster-max-500-psig.html#.VIcVCDHF8uA 12/16/14

[73] Emerson Climate Technologies “HVAC compression ratios,” http://www.ac-heatingconnect.com/hvac-compression-ratios/ 12/16/2014

[74] Mastovsky, J., “High-Temperature Conduction of Helium-Xenon Mixtures,” Journal of Engineering Physics, Oct 1977 (12/12/14)

[75] NASA “Voyager – The Interstellar Mission,” http://voyager.jpl.nasa.gov/ 12/16/14

[76] You, E., et. al., “Thermodynamics Properties of Binary Gas Mixtures for Brayton Space Nuclear Power System,” High Temperature Reactor Conference 2014 (12/12/14)

[77] CORE Materials, "http://core.materials.ac.uk/repository/doitpoms/tlp/swf/ellingham6b.swf," http://core.materials.ac.uk/repository/doitpoms/tlp/swf/ellingham6b.swf 07/08/2014

[78] Sifner, O., et. al., “Thermodynamic Properties of Xenon from the Triple Point to 800K with Pressures up to 350 MPa,” Institute of Thermomechanics, 11/25/1992 (12/12/14)

[79] Turns, S., "Thermal-Fluid Sciences: An Integrated Approach," Cambridge University Press, 2006

[80] Messer, Charles E., "A Survey Report on Lithium Hydride," United States Atomic Energy Commission, 12/7/1966

[81] MatWeb “Tantalum, Ta; Annealed,” http://www.matweb.com/search/DataSheet.aspx?MatGUID=638e0acc45ad481788d5ff142b1a7e0a&ckck=1, 07/08/2014

[82] MatWeb “Tungsten, W,” http://www.matweb.com/search/DataSheet.aspx?MatGUID=41e0851d2f3c417ba69ea0188fa570e3, 07/08/2014

[83] Incropera, F. P., DeWitt, D. P., "Introduction to Heat Transfer, 3rd Edition" Wiley, 1996

[84] Bich, E., et. al. “The viscosity and thermal conductivity of pure monatomic gasses from their normal boiling point up to 5000K in the limit of zero density and at .101325 MPa.” NIST Database, 10/18/1989 (12/12/14)

[85] Lien, K., et. al., "The Entrance Length for Fully Developed Turbulent Channel Flow," 15th Australasian Fluid Mechanics Conference, 2004

[86] Patel, R., "A note on fully developed turbulent flow down a circular pipe," Aeronautical Journal 78, 1974

[87] White, F. M., "Viscous Fluid Flow," McGraw Hill, 2006

[88] Lockheed Martin Corp, "Heat Rejection Radiators (HRS)," http://www.lockheedmartin.com/us/products/HeatRejectionRadiators.html 03/11/2015

[89] MatWeb, "Ammonia, NH3," http://www.matweb.com/search/DataSheet.aspx?MatGUID=98ce8c40d6524337933c9b278e3d0b1b 03/11/2015

[90] O'Brien, Frank "Apollo Flight Journal," NASA History Division, http://history.nasa.gov/afj/loressay.htm 04/01/2015

[91] Delft University of Technology, "Comparison of liquid, solid, and hybrid chemical rockets," http://www.lr.tudelft.nl/en/organisation/departments/space-engineering/space-systems-engineering/expertise-areas/space-propulsion/system-design/generate-candidates/comparison-of-rockets/ 04/01/2015

[92] NuFern Corp, "NuQ Operator's Manual," G025DOC Rev. Q, January 2014

[93] Sigma Aldrich, "Tungsten Powder," http://www.sigmaaldrich.com/catalog/product/aldrich/267511?lang=en&region=US 03/21/2015

[94] Sigma Aldrich, "Rhenium Powder,"
http://www.sigmaaldrich.com/catalog/product/aldrich/267279?lang=en&region=US 03/21/2015

[95] Sigma Aldrich, "Tantalum Powder,"
http://www.sigmaaldrich.com/catalog/product/aldrich/262846?lang=en&region=US 03/21/2015

[96] Sigma Aldrich "Lithium Hydride Powder,"
http://www.sigmaaldrich.com/catalog/product/aldrich/201049?lang=en&region=US 03/21/2015

[97] Graphitestore.com "Graphite Store: Pyrolytic Graphite,"
http://www.graphitestore.com/itemDetails.asp?item_id=3462&prd_id=483&cat_id=46&curPage=1 03/21/2015

[98] BuyAerogel.com, "BuyAerogel.com | Classic Silica Block,"
http://www.buyaerogel.com/product/block/ 03/21/2015

[99] Cabot Corporation "Lumira Translucent Aerogel," Datasheet, Cabot.com 03/23/2015

[100] OnlineMetals.com, ”Order Stainless 304 Sheet...,"
http://www.onlinemetals.com/merchant.cfm?pid=719&step=4&showunits=inches&id=30&top_cat=1 03/21/2015

[101] Electricmotorsport.com, "MotoEnergy ME1115..."
http://www.electricmotorsport.com/catalogsearch/result/?q=me1115 03/21/2015

[102] Log, H. P., et. al "Process Equipment Cost Estimation Final Report," National Energy Technology Center, DOE/NETL-2002/1169

[103] Sigma Aldrich, "Ammonia Anhydrous,"
http://www.sigmaaldrich.com/catalog/product/aldrich/294993?lang=en&region=US 03/21/2015

[104] Chemicool, "Xenon," http://www.chemicool.com/elements/xenon.html 03/21/2015

[105] Chemicool, "Hydrogen," http://www.chemicool.com/elements/hydrogen.html 03/21/2015

[106] Busek Co. Inc “Busek Low Power Hall Effect Thrusters,” Busek Space Propulsion Systems, Datasheet 70008510B

[107] MatWeb.com, “Sulfur, S, beta (elevated temperature),” http://www.matweb.com/search/DataSheet.aspx?MatGUID=92648adca5b04c8199e52bd9b44a0bb9 01/22/2015

[108] Georgia Gulf Sulfur Corporation, “Sulfur Properties,” http://www.georgiagulfsulfur.com/properties.htm 01/22/2015

[109] Friedrich & Dimmock, INC. “SIMAX GLASS PROPERTIES,” http://www.fdglass.com/pdf/simax.pdf 01/22/2015

[110] NewAge Industries, “Silcon Silicone Tubing,” http://www.newageindustries.com/silcon-silicone-tubing.asp 01/22/2015

[111] Borowski, S., et. al., "Nuclear Thermal Rocket (NTR) Propulsion: A Proven Game-Changing Technology for Future Human Exploration Missions," Paper, Global Space Exploration Conference, 2012

[112] Mason, L. S., Schreiber, J. G., "A Historical Review of Brayton and Stirling Power Conversion Technologies for Space Applications," NASA Glenn Research Center NASA/TM—2007-214976